HELICOPTER FLIGHT DYNAMICS

including a treatment of **TILTROTOR AIRCRAFT**

THIRD EDITION

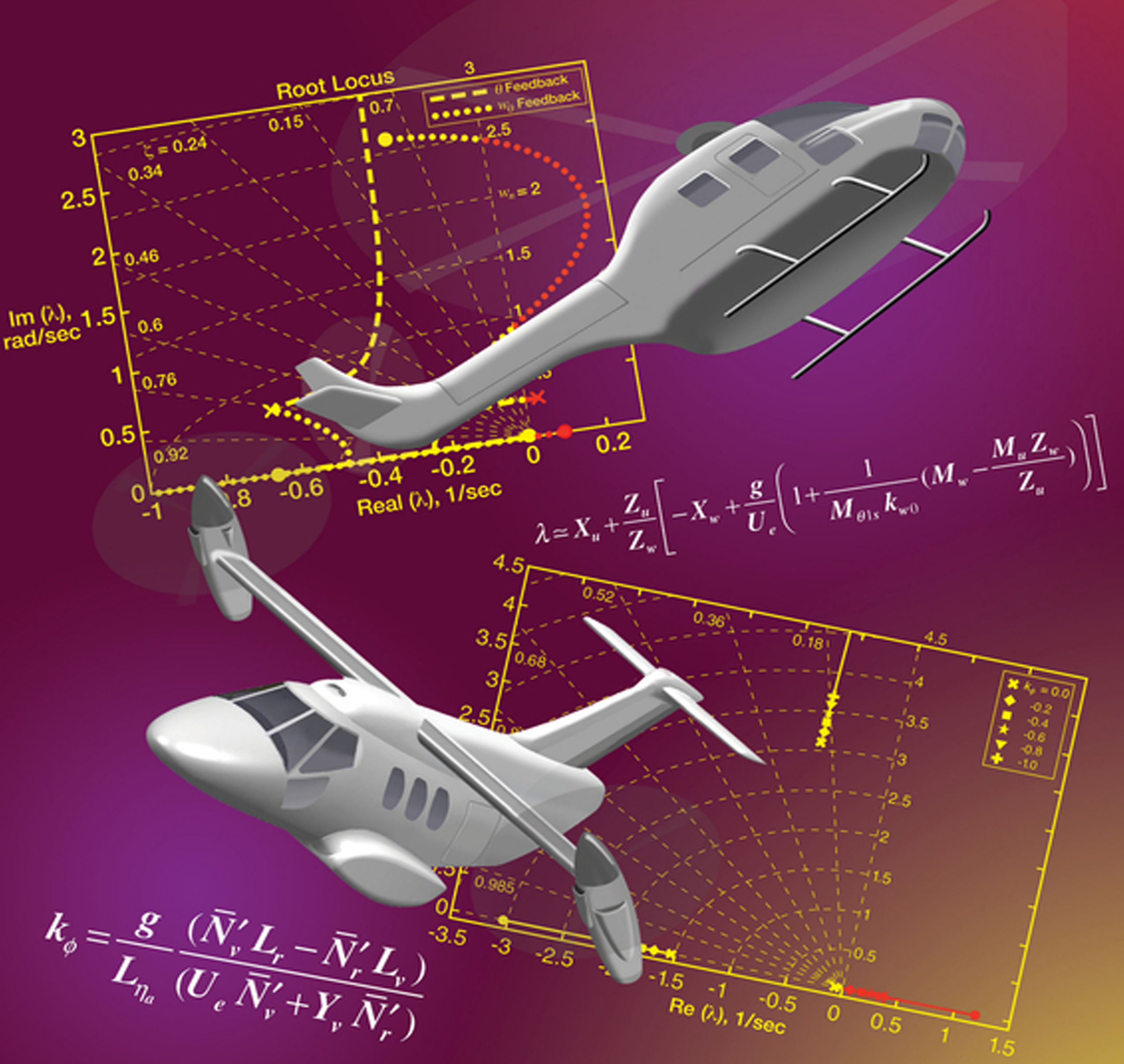

Gareth D. Padfield

WILEY

HELICOPTER FLIGHT DYNAMICS

HELICOPTER FLIGHT DYNAMICS

Including a Treatment of Tiltrotor Aircraft

Third Edition

Gareth D. Padfield

WILEY

This edition first published 2018

Edition History
American Institute of Aeronautics and Astronautics. (2e, 2007); American Institute of Aeronautics and Astronautics. (1e, 1996)

Registered Offices
John Wiley & Sons, Inc., 111 River Street, Hoboken, NJ 07030, USA
John Wiley & Sons Ltd, The Atrium, Southern Gate, Chichester, West Sussex, PO19 8SQ, UK

Editorial Office
The Atrium, Southern Gate, Chichester, West Sussex, PO19 8SQ, UK

For details of our global editorial offices, customer services, and more information about Wiley products visit us at www.wiley.com.

Wiley also publishes its books in a variety of electronic formats and by print-on-demand. Some content that appears in standard print versions of this book may not be available in other formats.

Library of Congress Cataloging-in-Publication Data

Names: Padfield, G. D., author.
Title: Helicopter flight dynamics : including a treatment of tiltrotor
aircraft / Gareth D. Padfield, University of Liverpool.
Description: Third edition. | Hoboken, NJ : John Wiley & Sons, Inc., [2018] |
Includes bibliographical references and index. |
Identifiers: LCCN 2018032337 (print) | LCCN 2018033453 (ebook) | ISBN
9781119401025 (Adobe PDF) | ISBN 9781119401070 (ePub) | ISBN 9781119401056
(hardcover)
Subjects: LCSH: Helicopters–Handling characteristics. |
Helicopters–Aerodynamics. | Tiltrotor aircraft.
Classification: LCC TL716.5 (ebook) | LCC TL716.5 .P33 2018 (print) | DDC
629.132/3–dc23
LC record available at https://lccn.loc.gov/2018032337

Cover design: Courtesy of Gareth D. Padfield and Mark Straker
Cover image: Gareth D. Padfield and Mark Straker

Set in 9.5/11.5pt TimesLTStd by SPi Global, Chennai, India.

Printed and bound by CPI Group (UK) Ltd, Croydon, CR0 4YY

10 9 8 7 6 5 4 3 2 1

To my family

Joey, Jude, and George

For this third (and final) edition, I add a dedication to rotorcraft engineers who practice their skills with respect for their colleagues, with care for the environment, with a passion for quality, and with openness to discovery and innovation.

Contents

Series Preface

The field of aerospace is multidisciplinary and wide ranging, covering a large variety of disciplines and domains, not only in engineering but in many related supporting activities. These combine to enable the aerospace industry to produce innovative and technologically advanced products. The wealth of knowledge and experience that has been gained by expert practitioners in the aerospace field needs to be passed on to others working in the industry and to researchers, teachers, and the student body in universities.

The *Aerospace Series* aims to be a practical, topical, and relevant series of books for people working in the aerospace industry, including engineering professionals and operators, academics, and allied professions such as commercial and legal executives. The range of topics is intended to be wide ranging, covering design and development, manufacture, operation, and support of aircraft, as well as topics such as infrastructure operations and advances in research and technology.

Flight dynamics, stability, and control are scientific disciplines of key importance for the design and operation of all flight vehicles. While there are many textbooks dealing with these topics for fixed-wing aircraft, there are relatively few covering the more complex topic of rotorcraft flight dynamics.

This book, *Helicopter Flight Dynamics,* is the third edition of the important textbook covering the flight dynamics and flying qualities of helicopters and tiltrotor aircraft. New material covering the modelling, simulation, and flying qualities of tiltrotors, the historical development of the flying qualities of rotorcraft, and coupled system theory applied to rotorcraft has significantly strengthened the content and scope. The book is aimed at practising engineers but is also highly relevant for undergraduate and graduate courses in rotorcraft flight dynamics and flying qualities.

Peter Belobaba, Jonathan Cooper and Allan Seabridge

Preface to Third Edition

Long ago, in the late 1960s, the author was introduced to a clever mathematical method for explaining and predicting the loss of stability that can occur when pilots increase their control gain to reduce the excursions in aircraft flight path, attitude, or speed. The clever part of the approximation came from a recognition that, although both pilot and aircraft dynamics might be complex – multidimensional and nonlinear – in combination, a new dynamic emerged that could be represented by a relatively simple, linear, model of low order. Effectively, the pilot action separated the combined system dynamics into two or more subsystems. In the extreme case of very high pilot gain, the controlled states become fully constrained while the uncontrolled states form into new modes with the potential risk of instability. The author's understanding of flight dynamics was in its infancy in 1968, but this technique enabled physical interpretations that became one of the foundations on which his continued learning would be based – a foundation of analytic approximations that provide insight into why and how things happen the way they do.

The publication on this research (Ref. 4A.6), titled *The Strongly Controlled Aircraft*, applied Ronald Milne's theory of weakly-coupled systems; Ronald was the author's supervisor for his final-year undergraduate project. Many engineers have influenced the author's thinking and career journey but none so significantly as Ronald Milne, following the fortuitous choice of final year project. A great feeling of sadness, but also honour, arose when the author was asked by Ronald's family to write his obituary for the Royal Aeronautical Society in 2014.

In earlier editions of this book, the author applied this theory to helicopters, developing low-order approximations to the natural modes and revealing instabilities resulting from strong flight-path and attitude control. In this third edition, the author takes the opportunity to examine aircraft accidents through the 'lens' of strongly-controlled-aircraft theory. In the case of speed instability on the approach for fixed-wing aircraft, the aeronautical science underpinning the causal factors has been understood for decades. In a new appendix to Chapter 5, the author describes the roots of this understanding and applies this to recent accidents; one on a commercial fixed-wing transport, the other on a commercial rotorcraft for comparison. In the case of directional instability due to adverse yaw, the author has applied the theory to a simulation of the XV-15 to explore the possible contributing factors in a recent accident on a tiltrotor; this analysis is contained in an appendix to Chapter 10.

Chapter 10 is one of two new chapters in the third edition and presents an integrated treatment of modelling, simulation, and flying qualities of tiltrotor aircraft. The author has drawn on publications from research and operational tiltrotors and the extensive risk-reduction work conducted under several projects, part-funded by the European Union, in preparation for a future civil tiltrotor. Bringing the content of this chapter together has been a major task and could not have been accomplished without the support of several colleagues who deserve mention. Understanding the functioning of gimbal rotors, with constant-velocity or universal joints connecting the rotor to the drive shaft, was especially challenging. Most of the literature associated with modelling of tiltrotors treat the rotor as a combination of articulated blades, modelled like the rotors described in Chapter 3. The author broke free of this misrepresentation based on the understanding that, with either type of joint, out-of-plane cyclic flapping did not lead to a resisting centrifugal force. David Miller, of Boeing Rotorcraft, gave the author guidance and his patience as this revelation emerged; to be obvious once understood. David had been involved in many aspects of the V-22 design and development and provided the author with insight into many aspects of tiltrotors that are to be found in Chapter 10. Other engineers who the author consulted on the material in Chapter 10 include Phil Dunford (ex-Boeing), Wayne Johnson (NASA), Al Brand (Bell Helicopters), Andrea Ragazzi (Leonardo Helicopters), Pierangelo Masarati (Politecnico di Milano), Chengjian He (ART), and Roy Bradley. All were positive and supportive and helped to shape the material herein.

Special thanks to Binoy Manimala (now with Leonardo Helicopters), who worked with the author as a post-doc researcher at Liverpool and developed the FLIGHTLAB models of the XV-15, EUROTILT, and ERICA tiltrotor configurations. Binoy also contributed to much of the research on tiltrotor structural load alleviation (SLA), along with Daniel Walker, and the author has drawn examples from our papers in Chapter 10. Colleagues across Europe in the RHILP, ACT-TILT, and NICETRIP projects are acknowledged for their contributions to the tiltrotor research undertaken at Liverpool. The early work in RHILP was particularly significant, under the leadership of Philippe Rollet (Airbus Helicopters), in laying the foundations for the research on tiltrotor flying qualities, modelling and SLA in these projects. Thanks to co-authors on the flying qualities papers from these projects, Michael Meyer, Victoria Brookes, and Neil Cameron. Thanks to Fabio Nannoni and Luca Medici (Leonardo Helicopters) for the use of images of their aircraft, ERICA, the AW609, and NGCTR.

Chapter 9 is also new in this third edition and draws significantly on the author's 2012 American Helicopter Society (AHS) Nikolsky Lecture and subsequent written paper. The chapter discusses the 'story of an idea' that quality can be quantified. This was an important aspect of the development of flying qualities standards, test procedures, and technologies. The author takes the reader back to the mid-1940s to find the starting point in the story. Since then, operational requirements, innovative technologies and regulatory standards have evolved together as the narrative continued. The author acknowledges the contributions from numerous engineers and pilots to this evolution throughout the chapter and, of course, the AHS for allowing the reproduction of material.

Chapter 5 has been augmented with extensions to the theory of weakly-coupled-systems and applications to rotorcraft. The new appendix in this chapter examines and compares the low-speed speed instability problem for fixed and rotary-wing aircraft. The author draws material from accident investigations but shows analysis for one of the case aircraft described in Chapter 4, rather than the accident aircraft.

The author originally intended to expand Chapter 3 significantly but decided that the Chapter 10 material on Level 2, multibody-dynamic modelling of tiltrotors would suffice. Chapter 3 has, however, been augmented with material from recent research at Liverpool on simulation fidelity, where we refer to the predictive fidelity of the flight model and perceptive fidelity of the simulation experienced by the pilot. The author is grateful to the team at Liverpool for the strong collaboration on this theme, particularly Mark White, Linghai Lu, Philip Perfect (now with Blue Bear Systems), Emma Timson (now with Airbus Helicopters), and our colleagues at the Institute for Aerospace Research in Ottawa – Bill Gubbels and pilots Rob Erdos and the late Stephan Carignan.

Special gratitude is owed to Dr. Linghai Lu (post-doc researcher with the author and now a senior lecturer at Liverpool John Moores University) for his constant and untiring support to the author in the preparation of this third edition. Creating and re-creating simulation results for helicopters and tiltrotors, reviewing and commenting on the author's analysis and textural descriptions, and producing charts of data, Linghai has been an immense help to the author.

The author's continuing collaboration with creative artist Mark Straker has resulted in a set of new technical figures and sketches that can be found throughout the book. Mark also worked with the author to create the cover design for this third edition. Mark's consistent quality and willingness to work from the author's rough sketches deserves very special thanks.

Thanks to staff at Wiley publishing for working with me on the production of this book.

Thanks again to you, the reader, and I do hope my book helps you develop a good understanding of helicopter and tiltrotor flight dynamics; above all else, that is my intention.

Gareth D. Padfield

Caldy, United Kingdom

January 2018

Preface to Second Edition

In the preface to the first edition of my book, I talked about flight dynamics as a '*living and mature subject, to which many contributions are yet to be made*'; I believe this statement is still true and every new generation of engineers has something new to add to the store of knowledge. During the 10 years since its publication, the disciplines of flight dynamics and handling/flying qualities engineering have matured into a systems approach to the design and development of those functions and technologies required to support the piloting task. At the same time, as pilot-centred operational attributes, flying qualities are recognised as the product of a continual tension between performance and safety. These two descriptions and the interplay between them highlight the importance of the subject to continuing helicopter development. The most obvious contributors to flying qualities are the air vehicle dynamics – the stability and control characteristics – and these aspects were treated in some depth in the first edition. Flying qualities are much more, however, and this has also been emphasized. They are a product of the four elements: the aircraft, the pilot, the task, and the environment, and it is this broader, holistic view of the subject, which is both a technical discipline and an operational attribute, which emphasizes the importance to flight safety and operational effectiveness. I have tried to draw out this emphasis in the new material presented in Chapter 8, Degraded Flying Qualities, which constitutes the bulk of the new content in this second edition.

During the preparation of the first edition, ADS-33C was being used extensively in a range of military aircraft programmes. The handling qualities (HQs) criteria represented key performance drivers for the RAH-66 Comanche, and although this aircraft programme would eventually be cancelled, industry and the surrounding helicopter 'community' would learn about the technology required to deliver Level 1 HQs across a range of operational requirements. The last decade has seen ADS-33 applied to aircraft such as NH-90 and the United Kingdom's attack helicopter, and also to new operations including maritime rotorcraft and helicopters carrying external loads, and used as a design guide for civil tilt rotor aircraft. It is now common at annual European and American Helicopter Fora to hear presentations on new applications of ADS-33 or extensions to its theoretical basis. The Standard has also been refined over this period and currently exists in the ADS-33E-PRF (performance) version, emphasizing its status as a performance requirement. A brief resume of developments is added to Chapter 6.

Significant advances have also been made on the modelling and simulation front, and it is very satisfying to see the considerable pace at which the modelling of complex helicopter aerodynamics is moving. It surely will not be very long before the results of accurate physical flow modelling will be fully embodied into efficient, whole aircraft design codes and real-time simulation. A combination of high-quality computer tools for comprehensive synthesis and analysis and robust design criteria pave the way for massive reductions in timescales and costs for design, development, and certification. The modelling and simulation material in Chapters 3–5 is largely unchanged in this second edition. This is simply a result of the author needing to put limits on what is achievable within the timescale available.

In August 1999, I left government 'service' to join The University of Liverpool with a mandate to lead the aerospace activity, both on the research and the learning and teaching (L&T) axes. I was confident that my 30 years of experience would enable me to transition naturally into academia on the research axis. I had very little experience on the L&T axis however, but have developed undergraduate modules in rotorcraft flight, aircraft performance and flight handling qualities. I confirm the adage – to learn something properly, you need to teach it – and it has been very satisfying to 'plough' some of my experience back into the formative 'soil' of future careers.

As with the first edition, while this work is a consolidation of my knowledge and understanding, much has been drawn from the efforts and results of others, and not only is acknowledging this fact appropriate but it also feels satisfying to record these thanks, particularly to the very special and highly motivated group of individuals in the Flight Science and Technology Research Group at the University of Liverpool. This group has formed and grown organically, as any university research group might, over the period since 2000 and, hopefully, will continue to develop capabilities and contribute to the universal pool of knowledge and understanding. Those, in academe who have had the pleasure and privilege to 'lead' a group of young post-graduate students and post-doctoral researchers will perhaps understand the sense in which I derive satisfaction from witnessing the development of independent researchers, and adding my mite to the process.

Thanks to Ben Lawrence and Binoy Manimala, who have become experts in FLIGHTLAB and other computational flight dynamics analyses and helped me in numerous ways, but particularly related to investigating the effects of trailing wake vortices on helicopters. Neil Cameron derived the results presented in Chapter 8 on the effects of control system failures on the handing qualities of tiltrotor aircraft. Gary Clark worked closely with me to produce the results in Chapter 8 relating to terrain-following flight in degraded visibility. Immeasurable gratitude to Mark White, the simulation laboratory manager in FS&T, who has worked with me on most of the research projects initiated over the last five years. The support of Advanced Rotorcraft Technology, particularly Ronald Du Val and Chengjian He, with various FLIGHTLAB issues and the development of the HELIFLIGHT simulator, has been extensive and is gratefully acknowledged.

Those involved in flight dynamics and handling qualities research will understand the significant contribution that test pilots make to the subject, and at Liverpool we have been very fortunate indeed to have the sustained and consistently excellent support from several ex-military test pilots, and this is the place to acknowledge their contribution to my developing knowledge captured in this book. Sincere thanks to Andy Berryman, Nigel Talbot, Martin Mayer, Steve Cheyne, and Charlie Brown; they should hopefully know how important I consider their contributions to be.

Thanks to Roger Hoh and colleagues at Hoh Aeronautics, whose continuous commitment to handling qualities excellence has been inspirational to me. Roger has also made contributions to the research activities in FS&T, particularly related to the development of handling criteria in degraded conditions and the attendant design of displays for flight in degraded visual environments. The whole subject of visual perception in flight control has been illuminated to me through close collaboration with David Lee, Professor of Perception in Action at The University of Edinburgh. David's contributions to my understanding of the role of optical flow and optical tau in the control of motion has been significant and is gratefully acknowledged.

Over the last 10 years I have received paper and electronic communications from colleagues and readers of the first edition worldwide who have been complementary and have politely identified various errors or misprints, which have been corrected. These communications have been rather too numerous to identify and mention individually here, but it is hoped that a collective thank you will be appreciated.

Mark Straker produced the figures in the form they appear in this book to his usual very high standard; thanks again, Mark, for your creative support.

Finally, grateful thanks to Julia Burden at Blackwell Publishing, who has been unrelenting in her encouragement, dare I say persistence, with me to produce material for this second edition. Any Head of a large academic department (at Liverpool I am currently Head of Engineering with 900 students and 250 staff) will know what a challenging and rather absorbing business it can be, especially when one takes it on to direct and increase the pace of change. So, I was reluctant to commit to this second edition until I felt that I had sufficient new research completed to justify a new edition; the reader will now find a consolidation of much of that new work in the new Chapter 8. Only the authors who have worked under the pressures of a tight schedule, whilst at the same time having a busy day job, will know how and where I found the time.

So, this book is offered to both a new and old readership, who might also find some light-hearted relief in a 'refreshed' version of one of my poems, or sky-songs as I call them, *Helicopter Blues*, which can be sung in a 12-bar blues arrangement like Robert Johnson's 'When You Got a Good Friend' (*normally in EM but in Am if you're feeling cool*).

I got the helicopter blues
They're going 'round in my head
I got the helicopter blues
They're still going 'round in my head
brother please tell me what to do about these helicopter blues

My engine she's failing
Gotta reduce my torque
My engine she keeps failing
Gotta pull back on my power
seems like I'm autorotating from all these helicopter blues

My tail rotor ain't working
Ain't got no place to go
My tail rotor she ain't working
Ain't got no place to turn
These helicopter blues brother, they're driving me insane

My humms are a humming
Feel all fatigued, used and abused
My humms are humming
I'm worn out from all this aerofoil toil
If I don't get some maintenance sister, I've had it with these helicopter blues

My gearbox is whining
Must need more lubrication
I said I can't stand this whining
please ease my pain with boiling oil
If I don't get that stuff right now
I'm gonna lock up with those helicopter blues

Dark blue or light
The blues got a strong hold on me
It really don't matter which it is
The blues got no respect for me
Well, if only I could change to green
Maybe I could shake off these helicopter blues

I've designed a new helicopter
It'll be free of the blues
I've used special techniques and powerful computers
I'm sure I know what I'm doing
now I gotta find someone to help me chase away these helicopter blues

I went to see Boeing
Said I got this new blues-free design
I went up to see Boeing, told them my story and it sounded fine
But they said why, blue's our favourite colour
Besides which, you're European

So I took my design to Eurocopter
I should have thought of them first
If I'd only gone to Eurocopter
I wouldn't be sitting here dying of thirst
They said 'c'est la vie mon ami', vous ne pouvez pas faire un hélicoptère sans bleu

I went to see Sikorsky
I thought – They'll fix the blues
They sent for Nick Lappos to fix the helicopter blues
Nick said don't be such a baby, Gareth
Just enjoy those helicopter blues

Now what would Ray Prouty do?
People say, Ray – he ain't got no blues
Please help me Ray – how much more aerodynamics do I need
Maybe Ray would say, wake up and smell the coffee
Learn how to hide those helicopter blues

I've learned to live with them now
I'm talking about the helicopter blues
Even got to enjoy them
Those sweet, soothing helicopter blues
I'm as weary as hell but please don't take away my helicopter blues

Gareth D. Padfield
Caldy, England

Preface to First Edition

In this preface, I want to communicate three things. First, I would like to share with the reader my motivation for taking on this project. Second, I want to try to identify my intended audience and, third, I want to record some special acknowledgements to colleagues who have helped me.

When I decided to pursue a career as an aeronautical engineer, my motivation stemmed from an aesthetic delight in flight and things that flew, combined with an uncanny interest in tackling, and sometimes solving, difficult technical problems. Both held a mystery for me and together, unbeknown to me at the time, helped me to 'escape' the Welsh mining community in which I had been sculptured, on to the roads of learning and earning. Long before that, in the late 1940s, when I was taking my first gasps of Welsh air, the Royal Aircraft Establishment (RAE) had been conducting the first research flight trials to understand helicopter stability and control. It should be remembered that at that time, practical helicopters had been around for less than a decade. From reading the technical reports and talking with engineers who worked in those days, I have an image of an exciting and productive era, with test and theory continuously wrestling to provide first-time answers to the many puzzles of helicopter flight dynamics.

Although there have been quiet periods since then, the RAE sustained its helicopter research programme through the 1950s, 1960s, and 1970s, and by the time I took charge of the activities at Bedford in the mid-1980s, it had established itself at the leading edge of research into rotor aerodynamics and helicopter flight dynamics. My own helicopter journey began in the Research Department at Westland Helicopters in the early 1970s. At that time, Westland was engaged with the flight testing of the prototype Lynx, a helicopter full of innovation for a 1960s design. This was also an exciting era, when the foundations of my understanding of helicopter flight dynamics were laid down. Working with a small and enthusiastic group of research engineers, the mysteries began to unfold, but at times it felt as if the more I learned, the less I understood. I do not want to use the word *enthusiastic* lightly in this context; a great number of helicopter engineers that I have known have a degree of enthusiasm that goes way beyond the call of duty, so to speak, and I do believe that this is a special characteristic of people in this relatively small community. While it is inevitable that our endeavours are fuelled by the needs of others – the ubiquitous customer, for example – enthusiasm for the helicopter and all of the attendant technologies is a powerful and dynamic force. In writing this book I have tried to share some of my enthusiasm and knowledge of helicopter flight dynamics with as large an audience as possible, and that was probably sufficient personal motivation to undertake the task. This motivation is augmented by a feeling that my own experience in theory and test has given me insight into, and a somewhat unique way of looking at, the subject of flight dynamics that I hope will appeal to the reader in search of understanding.

There are, however, more pragmatic reasons for writing this book. While fixed-wing flight dynamics, stability, and control have been covered from a number of perspectives in more than a dozen treatises over the years, there has never been a helicopter textbook dedicated to the subject; so there is, at least, a perceived gap in the available literature, and, perhaps more importantly, the time is ripe to fill that gap. The last 10–20 years has seen a significant amount of research in flight simulation and flying qualities for helicopters, much of which has appeared in the open literature but is scattered in scores of individual references. This book attempts to capture the essence of this work from the author's perspective, as a practitioner involved in the RAE (Defence Research Agency DRA) research in national and international programmes. It has been a busy and productive period – indeed it is still continuing – and I hope that this book conveys the impression of a living and mature subject, to which many contributions are yet to be made.

The book is written mainly for practising flight dynamics engineers. In some organizations, such a person might be described as a flying qualities engineer, a flight simulation engineer, or even a flight controls engineer, but my personal view is that these titles reflect sub-disciplines within the larger field of flight dynamics. Key activities of the flight dynamics engineer are simulation modelling, flying qualities, and flight control. Simulation brings the engineer into a special and intimate relationship with the system he or she is modelling, and the helicopter is a classic example.

The present era appears to be characterized by fast-disappearing computational constraints on our ability to model and simulate the complex aeroelastic interactions involved in helicopter flight. Keeping step with these advances, the flight dynamics engineer must, at the same time, preserve an understanding of the link between cause and effect. After all, the very objectives of modelling and simulation are to gain an understanding of the effects of various design features and insight into the sensitivity of flight behaviour to changes in configuration and flight condition. In the modelling task, the flight dynamics engineer will need to address all the underlying assumptions, and test them against experimental data, in a way that provides as complete a calibration as possible. The flight dynamics engineer will also have a good understanding of flying qualities and the piloting task, and he or she will appreciate the importance of the external and internal influences on these qualities and the need for mission-oriented criteria. Good flying qualities underpin safe flight, and this book attempts to make the essence of the theoretical developments and test database, assembled over the period from the early 1980s through to the present time, accessible to practising engineers. Flight testing is an important part of flight dynamics, supporting both simulation validation and the development of flying qualities criteria. In this book, I have attempted to provide the tools for building and analysing simulation models of helicopter flight, and to present an up-to-date treatment of flying qualities criteria and flight test techniques.

While this is primarily a specialist's book, it is also written for those with empathy for the broader vision, within which flight dynamics plays its part. It is hoped that the book, or parts of the book, will appeal to test pilots and flight test engineers and offer something useful to engineers without aeronautical backgrounds, or those who have specialized in the aerodynamic or controls disciplines and wish to gain a broader perspective of the functionality of the total aircraft.

In writing Chapters 2, 6, and 7, I have tried to avoid a dependence on 'difficult' mathematics. Chapters 3–5, on the other hand, require a reasonable grasp of analytical and vectorial mechanics as would, for example, be taught in the more extensive engineering courses at first and higher degree levels. With regard to education programmes, I have had in mind that different parts of the book could well form the subject of one or two term courses at post-graduate or even advanced undergraduate level. I would strongly recommend Chapter 2 to all who have embarked on a learning programme with this book. Taught well, I have always considered that flight dynamics is inspirational and, hence, a motivating subject at university level, dealing with whole aircraft and the way they fly, and, at the same time, the integration of the parts that make the whole. I have personally gained much from the subject and this book also serves as an attempt to return my own personal understandings into the well of knowledge.

In the sense that this book is an offering, it also reflects the great deal of gratitude I feel towards many colleagues over the years, who have helped to make the business enjoyable, challenging, and stimulating for me. I have been fortunate to be part of several endeavours, both nationally and internationally, that have achieved significant progress, compared with the sometimes more limited progress possible by individuals working on their own. International collaboration has always held a special interest for me and I am grateful to Advisory Report on Rotorcraft System Identification (AGARD), Garteur, Technical Cooperation Program (TTCP) and other, less formal, ties with European and North American agencies, for providing the auspices for collaboration. Once again, this book is full of the fruits of these activities. I genuinely consider that helicopters of the future will perform better, be safer, and be easier to fly because of the efforts of the various research groups working together in the field of flight dynamics, feeding the results into the acquisition processes in the form of the requirements specifications, and into the manufacturing process, through improved tools and technologies.

In the preparation of this book, several colleagues have given me specific support, which I would like to acknowledge. For assistance in the generation and presentation of key results, I would like to acknowledge the Rotorcraft Group at DRA Bedford. But my gratitude to the Bedford team goes far beyond the specific support activities, and I resist identifying individual contributions for that reason. As a team, we have pushed forward in many directions over the last 10 years, sometimes at the exciting but lonely leading edge, at other times filling in the gaps left by others pushing forward with greater pace and urgency. I want to record that this book very much reflects these team efforts, as indicated by the many cited references. I was anxious to have the book reviewed in a critical light before signing it off for publication, and my thanks go to colleagues and friends Ronald Milne, Ronald DuVal, Alan Simpson, Ian Simons, and David Key for being kind enough to read individual chapters and for providing me with important critical reviews. A special thanks to Roy Bradley for reviewing the book in its entirety and for offering many valuable ideas that have been implemented to make the book better.

I first had the serious idea of writing this book about four years ago. I was familiar with the Blackwell Science series and I liked their productions, so I approached them first. From the beginning, my publisher at Blackwell, Julia Burden, was helpful and encouraging. Later, during the preparation, the support from Julia and her team was sustained and all negotiations have been both positive and constructive; I would like to express my gratitude for this important contribution. I would like also to acknowledge the vital support of my employer, the DRA, for allowing me to use material from my research activities at RAE and DRA over the past 18 years. My particular thanks to my boss, Peter England, manager, Flight Dynamics and Simulation Department at DRA Bedford, who has been continually supportive with a positive attitude that has freed me from any feelings of conflict of interest. Acknowledgements for DRA material used and figures or quotes from other sources are included elsewhere in this book. The figures in this book were produced by two artists, those in Chapter 2 by Peter Wells and the rest by Mark Straker. Both worked from often very rough drafts and have, I believe, done an excellent job – thank you both.

All these people have helped me along the road in a variety of different ways, as I have tried to indicate, but I am fully accountable for what is written in this book. I am responsible for the variations in style and 'colour', inevitable and perhaps even desirable in a book of this scope and size. There have been moments when I have been guided by inspiration and others where I have had to be more concerned with making sure the mathematics was correct. I have done my best in this second area and apologise in advance for the inevitable errors that will have crept in. My final thanks go to you, the reader, for at least starting the journey through this work. I hope that you enjoy the learning and I wish you good fortune with the application of your own ideas, some of which may germinate from reading this book. It might help to know that this book will continue to be my guide to flight dynamics and I will be looking for ways in which the presentation can be improved.

Gareth D. Padfield

Sharnbrook, England

Acknowledgements

The following people and organisations are gratefully acknowledged for granting permission for the use of copyright material.

The UK MoD and Defence Research Agency for Figures 2.31, 2.43, 2.44, 2.50, 3.15, 3.28, 3.29, 3.35, 3.37, 3.38, 5.7–5.9, 5.28–5.31, 5.34, 6.7, 6.8, 6.9, 6.10, 6.18, 6.19, 6.35, 6.36, 6.38, 6.39, 6.47–6.52, 6.59, 7.10–7.24, 7.38, 7.44, 7.45, and 7.46.[1] The US Army for Figs 6.15, 6.17, 6.20, 6.25, 6.30, 6.33, 6.40–6.45, 6.56, 6.61, 6.64, 6.65, 6.70, and 7.28 and Table 7.4. The American Helicopter Society (AHS) for Figures 3.16 and 7.5 (with the US Army). Bob Heffley for Figures 6.6 and 6.11. Cambridge University Press for the quote from Duncan's book at the beginning of Chapter 3. Chengjian He and the AHS for Figure 5.27. Chris Blanken, the US Army and the AHS for Figures 7.29 and 7.30. Courtland Bivens, the AHS and the US Army for Figure 6.63. David Key and the Royal Aeronautical Society for Figures 6.3 and 6.31. David Key for the quote at the beginning of Chapter 7. DLR Braunschweig for Figures 6.21 and 6.23 (with RAeS), 6.32, 6.37, 6.58 (with the AHS), 6.68 (with the US Army), and 7.4 (with AGARD). Eurocopter Deutschland for Figures 6.46 and 6.66. Ian Cheeseman and MoD for Figures 3.28 and 3.29. Jeff Schroeder and the AHS for Figures 7.32–7.36. Jeremy Howitt and the DRA for Figures 7.39, 7.40, and 7.41. Knute Hanson and the Royal Aeronautical Society for Figure 6.69. Lt. Cdr. Sandy Ellin and the DRA for Figures 2.7, 3.44, and 3.45. Mark Tischler and AGARD for Figures 5.25, 5.26, 6.34, and 6.57. McDonnell Douglas Helicopters, AGARD and the US Army for Figure 6.71. NASA for Figures 4.12 and 6.2. Institute for Aerospace Research, Ottawa, for Figures 6.54 and 7.7 (with the AHS). Pat Curtiss for Figures 3.46, 3.47, and 5.4. Roger Hoh for Figures 6.24, 6.26 (with the AHS), 6.29 (with the RAeS), and 7.27 (with the AHS). Sikorsky Aircraft, the US Army and the AHS for Figure 6.72. Stewart Houston and the DRA for Figures 5.10–5.13. Tom Beddoes for Figure 3.42. Jan Drees for Figure 2.8. AGARD for selected text from References 6.72 and 7.25. Westland Helicopters for granting permission to use configuration data and flight test data for the Lynx helicopter. Eurocopter Deutschland for granting permission to use configuration data and flight test data for the Bo105 helicopter. Eurocopter France for granting permission to use configuration data and flight test data for the SA330 Puma helicopter.

In the second edition, once again the author drew from the vast store of knowledge and understanding gained and documented by others and the following people and organizations are gratefully acknowledged for the use of copyright material.

Philippe Rollet and Eurocopter for the use of Table 8.9. John Perrone at the University of Waikato for Figures 8.4, 8.6, and 8.11. James Cutting at Cornell University and MIT Press for Figures 8.7, 8.8, and the basis of Figure 8.10. NASA for Figure 8.14. David Lee for Figures 8.18 and 8.19. The US Army Aviation Engineering Directorate for the use of Table 6.6 and Figures 6.74, 6.75, and 6.77 and general reference to ADS33. AgustaWestland Helicopters for the use of the photographs of the EH101 at the start of Chapter 8 and also on the book cover. Roger Hoh and the American Helicopter Society for Figure 8.2. The American Helicopter Society for a variety of the author's own figures published in Ref 8.31, 8.33, and 8.55. The Institution of Mechanical Engineers for Figure 8.45 from the author's own paper. The Royal Aeronautical Society for the use of the author's own figures from Ref 8.53. J. Weakly and the American Helicopter Society for Figure 8.43. Franklin Harris for Figure 8.62.

For the third edition of this book, the author acknowledges the following people and organizations for the use of material.

In Chapter 3, to the Royal Aeronautical Society (RAeS) for use of material presented by the author as chairman of the Rotorcraft Virtual Engineering Conference held in Liverpool in November 2016; to the Canadian NRC for use of material on the ASRA Bell 412; to the RAeS for various figures from References in the appendix to Chapter 3.

In Chapter 5, to the US National Transportation Safety Board for use of material relating to the accident on Asiana Airlines Flight 214. To the UK Air Accident Investigation Branch for use of material relating to the accident on G-WNSB.

In Chapter 8, material has been drawn from the author's papers on time-to-contact published by the RAeS and the AHS; permission to use the material is acknowledged.

Chapter 9 is derived largely from the author's Nikolsky lecture to the American Helicopter Society (AHS) annual forum in 2012; the author acknowledges permission from Mike Hirschberg and the AHS to reproduce this.

Contributions to Chapter 10 on tiltrotor flight dynamics come from many sources, which are acknowledged. To Phil Dunford, Boeing Rotorcraft, and the AHS, for material in Refs. 10.1 and 10.9; to NASA and the US Army for various images of the XV-15 and the large civil tiltrotor; to Leonardo Helicopters and Jay Miller/AHS for images of the AW609; to Airbus Helicopters and Leonardo Helicopters for the image of the DART rotor; to Bob Fortenbaugh (author), Bell Helicopters, and Leonardo Helicopters, and the RAeS for the use of Figure 10.6; to Jay Miller for the use of the image of the V-22 Osprey; to ART for the use of the image of the FLIGHTLAB model editor (Figure 10.2); to Pierangelo Masarati and Springer for the use of Figure 10.13; to Troy Gaffey, Bell Helicopters and the AHS for quoted text on gimbal flap-lag coupling and Figure 10.30 from Ref 10.4; to the AHS and authors of Ref. 10.29 for Figure 10.18; to Mark Potsdam, NASA and the AHS, for material from Refs 10.31 and 10.32; to Wayne Johnson and NASA for material from Ref. 10.33; to Albert Brand and Ron Kisor, Bell Helicopters, and the AHS for the use of material from Refs. 10.39 and 10.40; to the RHILP and ACT-TILT project teams for use of material from the University of Liverpool's research publications from these projects and to the RAeS and AHS for use of material from the author's related publications; to Dwayne Kimbal and the AHS for Figures 10.71–10.73 from Ref. 10.72; to David Miller and Boeing Rotorcraft for the use of material from Refs. 10.75 and 10.76; to Chuck Dabundo and co-authors, and the AHS, for material from Ref. 10.93; to Leonardo Helicopters for the use of Figure 10.92 depicting the NGCTR; to Jay Miller/AHS and Bell Helicopters for the use of Figure 10.93 showing the first flight of the V-280; to the Italian ANSV for use of material from Ref. 10.99.

Notation

a_0	main rotor blade lift curve slope (1/rad)
a_1, b_1	cosine, sine components of left rotor gimbal tilt angle
a_2, b_2	cosine, sine components of right rotor gimbal tilt angle
a_g	constant acceleration of the τ guide
a_{0T}	tail rotor blade lift curve slope (1/rad)
$a_{n-1}, a_{n-2}, \ldots$	coefficients of characteristic (eigenvalue) equation
$\mathbf{a}_p$	acceleration of P relative to fixed earth (components a_x, a_y, a_z) (m/s^2, ft/s^2)
$\mathbf{a}_{p/g}$	acceleration vector of P relative to G (m/s^2, ft/s^2)
a_{xb}, a_{yb}, a_{zb}	acceleration components of a blade element in rotating blade axes system (m/s^2, ft/s^2)
a_{zpk}	peak normal acceleration (m/s^2, ft/s^2)
c	rotor blade chord (m, ft)
c	constant τ motion
$d(\psi, r_b)$	local drag force per unit span acting on blade element (N/m, lbf/ft)
eR	flap hinge offset (m, ft)
$e_\zeta R$	lag hinge offset (m, ft)
$\mathbf{f}(t)$	forcing function vector
$f_\beta(\psi), f_\lambda(\psi)$	coefficients in blade flapping equation
$f_y(r_b), f_z(r_b)$	in-plane and out-of-plane aerodynamic loads on rotor blade at radial station r_b
g	acceleration due to gravity (m/s^2, ft/s^2)
g_{1c0}, g_{1c1}	lateral cyclic stick–blade angle gearing constants
g_{1s0}, g_{1s1}	longitudinal cyclic stick–blade angle gearing constants
g_{cc0}, g_{cc1}	collective lever–lateral cyclic blade angle gearing constants
g_{cT0}	pedal/collective lever–tail rotor control run gearing constant
g_θ, g_ϕ	nonlinear trim functions
g_{sc0}, g_{sc1}	collective lever–longitudinal cyclic blade angle gearing constants
g_{T0}, g_{T1}	pedal–tail rotor collective blade angle gearing constant
g_T	tail rotor gearing
h	height above ground (m, ft)
h_e	eye-height
$h, \dot{h}$	height (m, ft), height rate (m/s, ft/s)
h_{fn}	height of fin centre of pressure above fuselage reference point along negative z-axis (m, ft)
h_R	height of main rotor hub above fuselage reference point (m, ft)
h_T	height of tail rotor hub above fuselage reference point (m, ft)
i, j, k	unit vectors along x-, y- and z-axes
k	τ-coupling constant
k	lift dependent drag parameter
k_I	interlink gearing between differential collective pitch and aileron
k_1, k_2, k_3	inertia coupling parameters
k_{1s}, k_{1c}	feedforward gains (rad/unit stick movement)
k_3	= tan tail rotor delta 3 angle
k_ϕ, k_p	gains in roll axis control system (rad/rad, rad/(rad/s))

$k_{\phi c}$	critical value of k_ϕ for fuselage-rotor coupling
k_g	feedback gain in collective – normal acceleration loop (rad/m^2)
k_r	gain for yaw rate feedback
k_{w0}	gain for vertical velocity feedback
$k_{\lambda f}$	main rotor downwash factor at fuselage
$k_{\lambda fn}$	main rotor downwash factor at fin
$k_{\lambda T}$	main rotor downwash factor at tail rotor
$k_{\lambda tp}$	main rotor downwash factor at tailplane
k_0, k_q	feedback gains in pitch axis control system (rad/rad, rad/(rad/s))
$k_{\theta i}$, $k_{\phi i}$	trim damping factors
$\ell(\psi, r)$	lift per unit span (N/m, lbf/ft)
l_{1L}, l_{1R}	lift on blade element on left (blade 2) and right (blade 1) sides of blade pair 1
l_f	fuselage reference length (m, ft)
l_{fn}	distance of fin centre of pressure aft of fuselage reference point along negative x-axis (m, ft)
l_T	distance of tail rotor hub aft of fuselage reference point (m, ft)
l_{tp}	distance of tailplane centre of pressure aft of fuselage reference point (m, ft)
$m(r)$	blade mass distribution
m_{am}	apparent mass of air displaced by rotor in vertical motion
n, n_{zpk}	load factor (g)
p, q, r	angular velocity components of helicopter about fuselage x-, y- and z-axes (rad/s)
$p_{pk}/\Delta\phi$	attitude quickness parameter (1/s)
p_{ss}, p_s	steady state roll rate (rad/s)
r, r_b ($^-$)	blade radial distance (with overbar – normalized by radius R) (m, ft)
r, r_c	radial distance from vortex core and vortex core radius
$\mathbf{r}_{p/g}$	position vector of P relative to G (components x, y, z) (m, ft)
q_{ss}	steady-state pitch rate
s	Laplace transform variable
s	rotor solidity $= N_b c/\pi R$
s_T	tail rotor solidity
t	time (s)
$\bar{t}$	normalized time (t/T)
t_r	time in a manoeuvre when the reversal occurs (s)
t_w	heave time constant $(-1/Z_w)$ (s)
$\bar{t}_w$	t_w normalized by T
t_1	manoeuvre time (s)
$t_{r10,\,50,\,90}$	time constants – time to 10%, 50%, 90% of steady-state response (s)
$\mathbf{u}\,(t)$	control vector
u, v, w	translational velocity components of helicopter along fuselage x-, y- and z-axes ($\delta w \equiv w$, etc.) (m/s, ft/s)
u^{bl}, v^{bl}, w^{bl}	translational velocities in blade axes (Appendix 10D)
v_i	induced velocity at disc (m/s, ft/s)
v_{ihover}	induced velocity at disc in hover (m/s, ft/s)
$v_{i\infty}$	induced velocity in the far field below rotor (m/s, ft/s)
$\mathbf{v}_j$	eigenvectors of $\mathbf{A}^T$
$\mathbf{v}_g$, $\mathbf{v}_p$	velocity vector of G, P relative to fixed Earth
$\mathbf{v}_{p/g}$	velocity vector of P relative to G (components $u_{p/g}$, $v_{p/g}$, $w_{p/g}$)
v_g	velocity of motion guide (m/s, ft/s)
v_{g0}	initial velocity of motion guide (m/s, ft/s)
w	velocity along aircraft z-axis (m/s, ft/s)
w_{ss}	steady-state velocity along aircraft z-axis (m/s, ft/s)
$w\,(r, t)$	blade out-of-plane bending displacement (m, ft)
w_0	vertical velocity (m/s, ft/s)

$w_g\ (t)$	gust velocity component along z-axis (m/s, ft/s)
w_{gm}	maximum value of velocity in ramp gust (m/s, ft/s)
$\mathbf{w}_i$	eigenvectors of $\mathbf{A}$
w_λ	$w - k_{\lambda f}\,\Omega R \lambda_0$ total downwash over fuselage (m/s, ft/s)
w_{ss}	steady-state normal velocity (m/s, ft/s)
w_{ss}	steady-state velocity along aircraft z axis (m/s, ft/s)
$\mathbf{x}(t)$	state vector
$x,\ x_{cmd}$	position and position command in pilot/vehicle system
$x,\ z$	distance along x- and z-directions
$x,\ \bar{x}$	distance (normalised distance (with hat)) to go in manoeuvre (m, ft)
$\bar{x}', \bar{x}''$	normalised velocity and acceleration in manoeuvre
$x,\ y,\ z$	mutually orthogonal directions of fuselage axes – x forward, y to starboard, z down; centred at the helicopter's centre of mass
$\mathbf{x}_0$	initial condition vector $\mathbf{x}(0)$
$x_{bl},\ y_{bl},\ z_{bl}$	blade axes system (proprotor)
x_{cg}	centre of gravity (centre of mass) location forward of fuselage reference point (m, ft)
$\mathbf{x}_e$	equilibrium value of state vector
x_e	distance in eye-height/s
$\dot{x}_e$	velocity in eye-heights
x_{g0}	initial displacement of motion guide (m, ft)
$x_g,\ y_g,\ z_g$	gimbal axes system (proprotor)
$x_h,\ y_h,\ z_h$	hub axes system (proprotor)
x_g	distance to go in motion guide (m, ft)
x_m	distance to go in manoeuvre (m, ft)
x_r	edge rate (1/s)
$\mathbf{x}_f,\ \mathbf{x}_r,\ \mathbf{x}_p,\ \mathbf{x}_c$	elemental state vectors (f – fuselage, r – rotor, p – powerplant, c – control)
z_g	distance of ground below rotor (m, ft)
$\mathbf{A},\ \mathbf{B}$	system and control matrices
$\mathbf{A}_{ff},\ \mathbf{A}_{fr}$, etc.	system matrices; *ff* – fuselage subsystem, *fr* – rotor to fuselage coupling
$\mathbf{A}_{11},\ \mathbf{A}_{12}\ \ldots$	submatrices in partitioned form of $\mathbf{A}$
A_b	blade area (m^2, ft^2)
A_d	rotor disc area (m^2, ft^2)
A_f	agility factor – ratio of ideal to actual manoeuvre time
$A_x,\ A_y$	x- and y-axes acceleration components of aircraft relative to Earth (m/s^2, ft/s^2)
$\mathbf{B}_{ff},\ \mathbf{B}_{fr}$, etc.	control matrices; *ff* fuselage subsystem, *fr* rotor to fuselage coupling
$C_D,\ C_{D0},\ C_L$	aircraft drag coefficient, zero lift drag coefficient and lift coefficient
C_1'	$= \frac{1}{1+a_0 s/16\lambda_0}$ lift deficiency factor
C_2'	$= \frac{a_0 s}{16\lambda_0}$
$\mathbf{C}_1\ (\psi)$	time–dependent damping matrix in individual blade flapping equations
C_{if}	normalized fuselage force and moment coefficients, $i = x,\ y,\ z,\ l,\ m,\ n$
C_{La}	aerodynamic flap moment coefficient about roll axis
$C_{l\alpha}$	slope of lift curve on wing or aerofoil vs. incidence
$C_{l\delta a}$	slope of lift curve on aileron/flaperon
$C_{Lmax}\ (C_{lmax})$	maximum aerofoil (wing) lift coefficient
$\mathbf{C}_M\ (\psi)$	time-dependent damping matrix in multiblade flapping equations
$\mathbf{C}_{M0}\ (\psi)$	constant damping matrix in multiblade flapping equations
C_{Ma}	aerodynamic flap moment about pitch axis
$C_{nfa},\ C_{nfb}$	fuselage aerodynamic yawing moment coefficients
C_Q	main rotor torque coefficient
$C_{Qi},\ C_{Qp}$	induced and profile torque coefficients
C_{QT}	tail rotor torque coefficient
C_T	rotor thrust coefficient

C_{T_T}	tail rotor thrust coefficient
C_W	weight coefficient
C_x, C_y, C_z	main rotor force coefficients
$C_{yf\eta}$	normalized sideforce on fin
C_ζ	lag damping
C_{ztp}	normalized tailplane force
D	aircraft drag (N, lbf)
$D(s)$	denominator of closed-loop transfer function
$\mathbf{D}_\mathrm{I}(\psi)$	time-dependent stiffness matrix in individual blade flapping equations
$\mathbf{D}_M(\psi)$	time-dependent stiffness matrix in multiblade flapping equations
$\mathbf{D}_{M0}(\psi)$	constant stiffness matrix in multi-blade flapping equations
$E(r)I(r)$	distributed blade stiffness
$F^{(1)}$	out-of-plane rotor blade force
$F^{(2)}$	in-plane rotor blade force
$F(r, t)$	distributed aerodynamic load normal to blade surface
$\mathbf{F}(\mathbf{x}, \mathbf{u}, t)$	nonlinear vector function of aircraft motion
$F_0^{(1)}$	main rotor force component
$F_{1c}^{(1)}$	one-per-rev cosine component of $F^{(1)}$
$F_{1s}^{(1)}$	one-per-rev sine component of $F^{(1)}$
$F_{2c}^{(1)}$	two-per-rev cosine component of $F^{(1)}$
$F_{2s}^{(1)}$	two-per-rev sine component of $F^{(1)}$
$F_{1c}^{(2)}$	one-per-rev cosine component of $F^{(2)}$
$F_{1s}^{(2)}$	one-per-rev sine component of $F^{(2)}$
$\mathbf{F}_g$	vector of external forces acting at centre of mass (components X,Y, Z)
F_T	tail rotor-fin blockage factor
F_{vi}, F_w, etc.	flap derivatives in heave/coning/inflow rotor model
$G_e(s)$, $H_e(s)$	engine/rotorspeed governor transfer function
$G_{\eta 1cp}(\omega)$	cross-spectral density function between lateral cyclic and roll rate
$H_{\eta 1cp}(\omega)$	frequency response function between lateral cyclic and roll rate
$\mathbf{H}_I(\psi)$	time-dependent forcing function matrix in individual blade flapping equations
$\mathbf{H}_M(\psi)$	time-dependent forcing function matrix in multi-blade flapping equations
$\mathbf{H}_{M0}(\psi)$	forcing function matrix in multi-blade flapping equations
I_β	flap moment of inertia (kg m^2, slug ft^2)
I_n	moment of inertia of nth bending mode (kg m^2, slug ft^2)
I_R	moment of inertia of rotor and transmission system (kg m^2; slug ft^2)
I_s, I_{yaw}	moments of inertia of tiltrotor shaft and drive train associated with rotor rotation rate and aircraft yaw rate (kg m^2)
I_{vi}, I_w, etc.	inflow derivatives in heave/coning/inflow rotor model
I_{xx}, I_{yy}, I_{zz}	moments of inertia of the helicopter about the x-, y- and z-axes (kg m^2; slug ft^2)
I_{xz}	product of inertia of the helicopter about the x- and z-axes (kg m^2; slug ft^2)
K_3	rotorspeed droop factor
K_β	centre-spring rotor stiffness (Nm/rad, ft lb/rad)
$K_{\theta s}$, $K_{\theta p}$	attitude feedback gains for feedback to series and parallel actuators
K_{GF}, K_Q, K_E	gains in tiltrotor governor feedforward model (Fig. 10.71)
K_p, K_x	pilot and display scaling gains
L, M, N	external aerodynamic moments about the x-, y- and z-axes (N m, ft lb)
$\mathbf{L}_\beta$	transformation matrix from multi-blade to individual blade coordinates
L_f, M_f, N_f	fuselage aerodynamic moments about centre of gravity (N m, ft lb)
L_{fn}, N_{fn}	fin aerodynamic moments about centre of gravity (N m, ft lb)
L_{θ_0}, $M_{\theta_{1s}}$	control derivatives normalized by moments of inertia (1/s^2)

L_T, N_T, M_T	tail rotor moments about centre of gravity (N m, ft lb)
L_v, M_q, etc.	moment derivatives normalized by moments of inertia (see Appendix 4B.2 for various units)
L_w	turbulence scale for vertical velocity component (m, ft)
M, M_d	Mach number, drag divergence Mach number
M_a	mass of helicopter (kg, lb)
$M_{bA}\ M_{bI}\ M_{bS}$	blade hub moment due to aerodynamics (A), inertia (I) and spring (S) (Nm)
M_{bAc}, M_{bAs}	cosine and sine components of blade aerodynamic moment M_{bA} (Nm)
M_β	first moment of mass of rotor blade (kg m; slug ft)
M_β	hub moment about the centre of mass (Nm/rad)
$\mathbf{M}_g$	vector of external moments acting at centre of mass (components L, M, N)
$M_h^{(r)}(0, t)$	rotor hub moment (N m, ft lb)
M_h, L_h	main rotor hub pitch and roll moments (N m, ft lb)
M_R, L_R	main rotor pitch and roll moments (N m, ft lb)
M_{tp}	tail plane pitching moment (N m, ft lb)
M_{z0}, M_{zc}, M_{zs}	tiltrotor inplane loads in multiblade coordinates (Nm)
$M_{zb1}, M_{zb2}, M_{zb3}$	tiltrotor inplane loads in individual-blade coordinates (Nm)
$M_{\delta e}$	pitching moment due to longitudinal stick/elevator (rad/s^2 in.)
N_b	number of blades on main rotor
N_{bA}	tiltrotor blade inplane aerodynamic moment (Nm)
N_H	yawing moment due to rotor about rotor hub (N m, ft lb)
$N_{r_{effective}}$	effective yaw damping in Dutch roll motion (1/s)
P_e, Q_e, R_e	trim angular velocities in fuselage axes system (rad/s)
P_i	rotor induced power (kW, HP)
$P_n\ (t)$	blade generalized coordinate for out-of-plane bending
P_r	permutation matrix in trim algorithm
P_R	main rotor power (kW, HP)
P_T	tail rotor power (kW, HP)
P_x, P_y	position of aircraft from hover box (m, ft)
Q, R	weighting matrices in linear-quadratic-Gaussian approach to control
Q_{acc}	accessories torque (N m, ft lb)
Q_e, Q_{eng}	engine torque (N m, ft lb)
Q_{emax}	maximum continuous engine torque (N m, ft lb)
Q_R	main rotor torque, proprotor torque (N m, ft lb)
Q_s	tiltrotor interconnect drive shaft torque (Nm, ft lb)
Q_T	tail rotor torque (N m, ft lb)
Q_w	quickness for aircraft vertical gust response (1/s)
R	rotor radius (m, ft)
$R(s)$	numerator of closed-loop transfer function
R_T	tail rotor radius (m, ft)
S_β	Stiffness number $\frac{\lambda_\beta^2-1}{\gamma/8}$
S_{fn}	fin area (m^2, ft^2)
$S_n\ (r)$	blade mode shape for out-of-plane bending
S_p, S_s	fuselage plan and side areas (m^2, ft^2)
S_{tp}	tail plane area (m^2, ft^2)
$S_z\ (0, t)$	shear force at rotor hub (N, lbf)
T	main rotor thrust (N, Ibf)
T	manoeuvre duration (s)
T_{heq}	time constant in heave axis first-order equivalent system (s)
T_{htobl}	transformation matrix from hub to blade axes
T_{ige}	rotor thrust in-ground effect (N, lbf)
T_{oge}	rotor thrust out-of-ground effect (N, lbf)

T_x	distance between edges on surface (m, ft)
T_{prop}, X_{uprop}	thrust and drag derivative due to propeller
T_T	tail rotor thrust (N, lbf)
T_θ	lead time in pitch response (sec)
$T_{\theta 2}$	incidence lag (sec)
U_e, V_e, W_e	trim velocities in fuselage axes system (m/s, ft/s, knots)
U_P, U_T	normal and in-plane rotor velocities (m/s, ft/s)
u_p, u_t	normal and in-plane rotor velocities on tiltrotor in airplane mode (m/s, ft/s) (note u_p reverse sign to U_P)
V, V_x	aircraft forward velocity (m/s, ft/s)
V_c	rotor climb velocity (m/s, ft/s)
V_c	tangential velocity at the edge of the vortex core (m/s, ft/s)
V_d	rotor descent velocity (m/s, ft/s)
V_f	total velocity incident on fuselage (m/s, ft/s)
V_{fe}	total velocity in trim (m/s, ft/s, knots)
V_{fn}	total velocity incident on fin (m/s, ft/s)
$V_h^{(r)}(0, t)$	rotor hub shear force (N, lbf)
V_{res}	resultant velocity at rotor disc (m/s, ft/s)
V_{tp}	total velocity incident on tailplane (m/s, ft/s)
$V_T(r)$	tangential velocity in vortex as a function of distance from core r (m/s, ft/s)
V_x, V_y	velocity components of aircraft relative to Earth
W	aircraft weight (N, kgf, lbf)
$\mathbf{W}$	eigenvector matrix associated with $\mathbf{A}$
X, Y, Z	external aerodynamic forces acting along the x-, y- and z-axes (N, lbf)
X_a, X_b, X_p, X_c	pilot cockpit controls for tiltrotor aircraft (inches)
X_{th}	pilot throttle control (%)
X_f, Y_f, Z_f	components of X, Y, Z from fuselage (N, lbf)
X_{hw}, Y_{hw}	rotor forces in hub/wind axis system (N, lbf)
X_R, X_T	components of X from main and tail rotors (N, lbf)
X_{tp}, X_{fn}	components of X from empennage (*tp* – horizontal tailplane, *fn* – vertical fin) (N, lbf)
X_u, X_p, etc.	X force derivatives normalized by aircraft mass (see Appendix 4B.2 for various units)
X_{uprop}	X_u from propeller
$\mathbf{Y}(t)$	principal matrix solution of dynamic equations of motion in vector form
Y_{fn}	aerodynamic sideforce acting on fin (N, lbf)
Y_p, $Y_a(s)$	transfer function of pilot and aircraft
Y_T	component of Y force from tail rotor (N, lbf)
Y_v, Y_r, etc.	Y force derivatives normalized by aircraft mass (see Appendix 4B.2 for various units)
Z_w	heave damping derivative (1/s)
Z_{θ_0}	heave control sensitivity derivative (see Appendix 4B.2 for various units)
Z_{tp}	component of Z force from tailplane (N, lbf)
Z_w, Z_q, etc.	Z force derivatives normalized by aircraft mass (see Appendix 4B.2 for various units)
$\alpha\ (\psi, r, t)$	total incidence at local blade station (rad)
α	wing incidence (rad)
α_1, α_2	incidence break points in Beddoes theory (rad)
α_{1cw}	effective cosine component of one-per-rev rotor blade incidence (rad)
α_{1sw}	effective sine component of one-per-rev rotor blade incidence (rad)
α_d	disc incidence (rad)
α_f	incidence of resultant velocity to fuselage (rad)
α_{flap}, α_{wh}	components of local blade incidence (rad)
α_{inflow}	component of local blade incidence (rad)
α_{pitch}, α_{twist}	components of local blade incidence (rad)
α_{tp}	incidence of resultant velocity to tailplane
α_{tp0}	zero-lift incidence angle on tailplane (rad)

$\beta(t)$	rotor flap angle (positive up) (rad)
$\beta(t)$	sideslip velocity (rad)
$\beta_1, \beta_2, \beta_3, \beta_4$	flapping angles of individual blades on a tiltrotor
β_f	sideslip angle at fuselage (rad)
β_{fn}	sideslip angle at fin (rad)
$\beta_{1c_{\theta 1s}}$	$= \partial\beta_{1c}/\partial\theta_{1s}$, flapping derivative with respect to cyclic pitch
$\beta_0, \beta_{1c}, \beta_{1s}$	rotor blade coning, longitudinal and lateral flapping angles (subscript w denotes hub/wind axes) – in multi-blade coordinates (rad)
β_{0T}	tail rotor coning angle (rad)
β_{1cT}	tail rotor cyclic (fore – aft) flapping angle (rad)
β_{1cwT}	tail rotor cyclic (fore – aft) flapping angle in tail rotor hub/wind axes (rad)
β_d	differential coning multi-blade flap coordinate (rad)
β_{fn0}	zero-lift sideslip angle on fin (rad)
$\boldsymbol{\beta}_1$	vector of individual blade coordinates
$\beta_i(t)$	flap angle of i th blade (rad)
β_{jc}, β_{js}	cyclic multi-blade flap coordinates (rad)
$\boldsymbol{\beta}_M$	vector of multi-blade coordinates
β_m	proprotor nacelle angle (0 – helicopter, 90° – airplane)
β_R, β_L	flapping angles for blades on right and left proprotors
δ	ratio of instantaneous normal velocity to steady state value $\delta = \frac{w}{w_{ss}}$
δ_0	main rotor profile drag coefficient
δ_2	main rotor lift dependent profile drag coefficient
δ_3	tail rotor or tiltrotor delta 3 angle ($\tan^{-1} k_3$)
$\delta_a, \delta_e, \delta_r$	tiltrotor fixed wing control surface (flaperon, elevator, rudder) angles (rad)
$\delta_a, \delta_b, \delta_x, \delta_y$	pilot cyclic control displacements
δ_c	collective lever displacement
$\delta_f\,(\eta)$	tiltrotor flap deflection (flap effectiveness factor) (rad)
δ_{T0}	tail rotor profile drag coefficient
δ_{T2}	tail rotor lift dependent profile drag coefficient
$\delta u, \delta w$, etc.	perturbations in velocity components (m/s, ft/s)
δ_γ	inverse of determinant in rotor stability matrix
γ	flight path angle (rad or deg)
$\dot{\gamma}$	rate of change of γ with time (rad/s or deg/s)
γ_a	$\gamma - \gamma_f$ (rad or deg)
$\bar{\gamma}_a$	γ_a normalized by final value γ_f
$\bar{\gamma}'_a$	rate of change with normalized time $\bar{t}$
γ_f	final value of flight path angle (rad or deg)
γ	tuned aircraft response
γ	Lock number $= \frac{\rho c a_0 R^4}{I_\beta}$
γ^*	$= C'_1\gamma$; equivalent Lock number
γ_{fe}	flight path angle in trim (rad)
γ_s	shaft angle (positive forward, rad)
γ_T	tail rotor Lock number
$\gamma_{\eta 1cp}$	coherence function associated with frequency response fit between lateral cyclic and roll rate
$\eta_c, \eta_{1s}, \eta_{1c}$	pilot's collective lever and cyclic stick positions (positive up, aft, and to port)
η_{1s0}, η_{1c0}	cyclic gearing constants
η_{ct}	tail rotor control run variable
η_a, η_e, η_r	aileron, elevator and rudder angles (rad, deg)
η_p	pedal position (inch)
$\lambda_0, \lambda_{1c}, \lambda_{1s}$	rotor uniform and first harmonic inflow velocities in hub/shaft axes (normalized by ΩR)

λ_{0T}	tail rotor uniform inflow component
λ_{CT}	inflow gain
λ_i	eigenvalue
λ_i	main rotor inflow
λ_{ih}	hover inflow
λ_{fw}	a fixed-wing aircraft eigenvalue
λ_β	flap frequency ratio; $\lambda_\beta^2 = 1 + \frac{K_\beta}{I_\beta \Omega^2}$
χ	main rotor wake angle (rad)
χ_ε	track angle in equilibrium flight (rad)
χ_1, χ_2	wake angle limits for downwash on tail (rad)
$\lambda_{\beta T}$	tail rotor flap frequency ratio
λ_n	flap frequency ratio for *n*th bending mode
λ_θ	blade pitch frequency ratio
λ_p	phugoid mode eigenvalue
λ_r	roll subsidence eigenvalue
λ_s	spiral mode eigenvalue
λ_{sp}	short-period mode eigenvalue
λ_{tp}	normalized downwash at tailplane
λ_ζ	blade lag frequency ratio
μ	advance ratio $V/\Omega R$
μ	real part of eigenvalue or damping (1/s)
μ_c	normalized climb velocity
μ_d	normalized descent velocity
μ_T	normalized velocity at tail rotor
μ_{tp}	normalized velocity at tailplane
μ_x, μ_y, μ_z	velocities of the rotor hub in hub/shaft axes (normalized by ΩR)
μ_{zT}	total normalized tail rotor inflow velocity
v	lateral acceleration (normalized sideforce) on helicopter (m/s^2, ft/s^2)
v	turbulence component wavenumber = frequency/airspeed
θ	optical flow angle (rad)
θ_0	collective pitch angle (rad)
$\overline{\theta}_0$	collective pitch normalized by θ_{0f}
θ_{0f}	final value of collective (rad)
θ, ϕ, ψ	Euler angles defining the orientation of the aircraft relative to the Earth (rad)
θ_0, θ_{0T}	main and tail rotor collective pitch angles (rad)
θ_{0d}	differential collective pitch (rad)
θ_{1sd}	differential longitudinal cyclic pitch (rad)
θ_{0T}^*	tail rotor collective pitch angle after delta 3 correction (rad)
$\theta_{0.75\,R}$	blade pitch at 3/4 radius (rad)
θ_{1s}, θ_{1c}	longitudinal and lateral cyclic pitch (subscript w denotes hub/wind axes) (rad)
θ_{1sT}	tail rotor cyclic pitch applied through δ_3 angle (rad)
θ_{tw}	main rotor blade linear twist (rad)
ρ	air density (kg/m^3, slug/ft^3)
σ	rms turbulence intensity
σ	combination of roll angle and lateral flapping (rad)
τ	time to contact surface or object or time to close a gap in a state (s)
$\dot{\tau}$	rate of change of τ with time
τ_g	tau guide (constant accel or decel) (s)
$\tau_{surface}$	tau to the surface during climb manoeuvre (s)

τ_x	tau of the motion variable x, defined as $\frac{x}{\dot{x}}$ where x is the distance or gap to a surface, object or new state and $\dot{x}$ is the instantaneous velocity (s)
τ_{GF}, τ_Q, τ_E	Various time constants in tiltrotor governor feedforward model (secs)
τ_1, τ_2	time constants in Beddoes dynamic stall model (s)
τ_β	time constant of rotor flap motion (s)
$\tau_{c1} - \tau_{c4}$	actuator time constants (s)
τ_{e1}, τ_{e2}, τ_{e3}	engine time constants (s)
$\tau_{h_{eq}}$	time delay in heave axis equivalent system
τ_λ	inflow time constant (s)
τ_{lat}	estimated time delay between lateral cyclic input and aircraft response (s)
τ_p	roll time constant $(= -1/Lp)$ (s)
τ_p	phase delay between attitude response and control input at high frequency (s)
τ_{ped}	estimated time delay between pedal input and aircraft response (s)
$\boldsymbol{\omega}^{bl}$	angular velocity in blade axes (Appendix 10.D)
ω_{bw}	bandwidth frequency for attitude response (rad/s)
ω_m	natural frequency of low-order equivalent system for roll response (rad/s)
ω_c	crossover frequency defined by point of neutral stability (rad/s)
ω_d	Dutch roll frequency (rad/s)
ω_f	fuel flow variable
ω_ϕ	natural frequency of roll regressing flap mode (rad/s)
ω_{fmax}, ω_{fidle}	fuel flow variable at maximum contingency and flight idle
$\boldsymbol{\omega}_g$	angular velocity vector of aircraft with components p, q, r
ω_g	angular velocity of the tiltrotor gimbal (rad/s)
ω_p	phugoid frequency (rad/s)
ω_θ	frequency associated with control system stiffness (rad/s)
ω_{sp}, ζ_{sp}	pitch short-period frequency (rad/s) and relative damping
ω_t	task bandwidth (rad/s)
ω_x	angular velocity in blade axes $= p_{hw} \cos\psi - q_{hw} \sin\psi$ (rad/s)
ω_y	angular velocity in blade axes $= p_{hw} \sin\psi + q_{hw} \cos\psi$ (rad/s)
ω_{xb}, ω_{yb}, ω_{zb}	components of angular velocity of a tiltrotor blade in blade axes (rad/s)
ϕ_β	phase angle between cyclic pitch and cyclic flapping (rad)
ψ	heading angle, positive to starboard (rad)
ψ	rotor blade azimuth angle, positive in direction of rotor rotation (rad)
ψ_1,ψ_2	rotor azimuth angles on left and right rotors of a tiltrotor (rad)
ψ_w	rotor sideslip angle (rad)
ψ_i	azimuth angle of ith rotor blade (rad)
ζ	blade lag angle (rad)
ζ_d	Dutch roll damping factor
ζ_p	phugoid damping factor
ζ_{sp}	pitch short period damping factor
$\Delta\theta_{DB}$	pitch dropback (rad)
Φ_m	phase margin (degrees)
$\Phi_{wg}(\mathrm{v})$	power spectrum of w component of turbulence
Θ_e, Φ_e, Ψ_e	equilibrium or trim Euler angles (rad)
Ω or Ω_R	main rotor speed (rad/s)
Ω_s	tiltrotor interconnect drive shaft rotational speed (rad/s)
Ω_{ae}	aircraft angular velocity in trim flight (rad/s)
Ω_i	rotorspeed at flight idle (rad/s)
Ω_{mi}	ratio of Ω_m to Ω_i
Ω_m	rotorspeed at maximum continuous power
Ω_T	tail rotor speed (rad/s)

Subscripts

$1c$	first harmonic cosine component
$1s$	first harmonic sine component
bl	blade
d	Dutch roll
e	equilibrium or trim condition
g	gravity component or centre of mass G
h	hub axes
$htobl$	hub to blade (axis transformation)
hw	hub/wind axes
nf	no-feathering (plane/axes)
p	phugoid
p, a	in control system, relating to pilot and autostabiliser inputs
ph	phugoid
s	spiral
s, ss	steady state
sp	short period
tp	tip path (plane/axes)
R, T, f, fn, tp	main rotor, tail rotor, fuselage, fin, tailplane

Dressings

$\dot{u} = \frac{\mathrm{d}u}{\mathrm{d}t}$	differentiation with respect to time t
$\beta' = \frac{\mathrm{d}\beta}{\mathrm{d}\psi}$	differentiation with respect to azimuth angle ψ
–	Laplace transformed variable or normalised variable

List of Abbreviations

AC	attitude command
ACAH	attitude command attitude hold
ACP	aerodynamic computation point
ACS	active control system
ACT	active control technology
ACT-TILT	active control technology for tiltrotors
ACT-FHS	Active control technology – flying helicopter simulator
ACVH	attitude command velocity hold
AD	attentional demands
AD	acceleration-deceleration
ADFCS	advanced digital flight control system
ADOCS	advanced digital optical control system
ADS	Aeronautical Design Standard
AEO	air engineering officer
AFCS	automatic flight control system
AFS	advanced flight simulator
AGARD	Advisory Group for Aeronautical Research and Development
AH	attack helicopter
AHS	American Helicopter Society
AIAA	American Institute of Aeronautics and Astronautics
ALXW	approach and landing in cross-wind
APC	aircraft-pilot coupling
AR	aspect ratio (in MTE)
AS	Aerospatiale
ASE	automatic stabilisation equipment
ASRA	Advanced Systems Research Aircraft
ATA	air-to-air
AvP	Aviation Publication
BL	butt line
CA	collision avoidance
CAA	Civil Aviation Authority
CAP	control anticipation parameter
CAR	Civil Air Regulations
CC	conversion corridor
CF	CentriFugal (force)
CFD	computational fluid dynamics
CGI	computer-generated imagery
CH	cargo helicopter
CHR	Cooper–Harper Rating (as in HQR)
CPS	corridor protection system
CS	Certification Standards (EASA)
CSM	conceptual simulation model
CTP	Critical Technology Programme
CTR	civil tiltrotor

CV	constant velocity (joint)
DAFCS	Digital Automatic Flight Control System
DART	Development of Advanced Rotor for Tiltrotor
DCP	differential collective pitch
DERA	Defence Evaluation and Research Agency
DMP	differential motion parallax
DLR	Deutsche Forschungs- und Versuchsantalt fuer Luft- und Raumfahrt
DoF	degree of freedom
DRA	Defence Research Agency
DVE	degraded visual environment
EAS	estimated air speed
EASA	European Aviation Standards Agency
ECD	Eurocopter Deutschland
ECF	Eurocopter France
EHST	European Helicopter Safety Team
EPSRC	Engineering and Physical Science Research Council
ERICA	Enhanced Rotorcraft Innovative Concept Achievement
ERF	European Rotorcraft Forum
FAA	Federal Aviation Authority
FB-412	FLIGHTLAB Bell 412 simulation model
FDR	flight data recorder
FFS	force feel system
FLME	FLIGHTLAB Model Editor
FoV	field of view
FPVS	flight path vector system
FRL	Flight Research Laboratory (Canada)
FS	Fuselage Station
FSAA	flight simulator for advanced aircraft
FTM	flight test manoeuvre
FUMS	fatigue usage monitoring system
FXV-15	FLIGHTLAB model of XV-15 tiltrotor
GARTEUR	Group for Aeronautical Research and Technology in Europe
GSR	Glideslope re-capture
GTR	generic tiltrotor
GUI	graphical user interface
GVE	good visual environment
HM, CM, AM	helicopter mode, conversion mode, airplane mode
HMD	helmet-mounted display
HP	horse power
HQR	handling qualities rating
H-SE	Helicopter-Safety Enhancement
HT	Hover turn
HUMS	health and usage monitoring system
IADP	Innovative Aircraft Demonstrator Platforms
IAS	indicated air speed
IC	interconnecting shaft (tiltrotor)
IFR	instrument flight rules
IHST	International Helicopter Safety Team
IMC	instrument meteorological conditions
IP	integrated project
IPR	in-progress-review
KIAS	indicated air speed (knots)
LCTR	large civil tiltrotor

LHX	light helicopter experimental
LTM	lateral translation mode
LOES	low-order-equivalent system
MA/OA	missed approach/obstacle-avoid
MBB	Messerschmit–Bolkow–Blohm
MBC	multi-blade coordinates
MBD	multi-body dynamics
MSA	multi-segment approach
MDA	minimum descent altitude
MTE	mission task element
NACA	National Advisory Committee for Aeronautics
NAE	National Aeronautical Establishment
NASA	National Aeronautics and Space Administration
NGCTR	Next Generation Civil Tilt Rotor
NICETRIP	Novel, Innovative, Competitive, Effective, Tilt Rotor Integrated Project
NoE	nap of the earth
NRC	National Research Council (Canada)
NTSB	National Transportation Safety Board
OFE	operational flight envelope
OGP	oil and gas producers
OH	observation helicopter
OVC	outside visual cues
PAFCA	Partial Authority Flight Control Augmentation
PAPI	precision approach path indicator
PF	pilot flying
PM	pilot monitoring
PFCS	primary flight control system
PHC	precision hover capture
PI	proportional-integral
PIO	pilot-induced oscillation
PSD	power spectral density
RAE	Royal Aircraft Establishment
RAeS	Royal Aeronautical Society
RASCAL	Rotorcraft Aircrew Systems Concepts Airborne Laboratory
RC	rate command
RC/RCC	rapid conversion/rapid re-conversion
RCAH	rate command attitude hold
RHILP	rotorcraft handling, interference and loads prediction
ROD	rate of descent
(R)RPM/rpm	(rotor) revolutions per minute
RSS	rapid side-step
RT	response type
RTR	rapid vertical re-position
RVP	rapid teardrop reconversion
SA	situation awareness
SA	Sud Aviation
SAE	Society of Automotive Engineers
SAR	search and rescue (role)
SCAS	Stability and Control Augmentation System
SDG	statistical discrete gust
SFE	safe flight envelope
SFR	simulation fidelity rating
SHOL	ship-helicopter operating limits

SID	system identification
SLA	structural load alleviation
SNIOPs	simultaneous, non-interfering operations
SS	sea state
TAS	true air speed
TC	turn coordination
TCL	thrust control lever
TF	terrain following
TPP	tip path plane
TQM	total quality management
TRAN	transport (role)
TRC	translational rate command
TRCPH	translational rate command position hold
TTCP	The Technical Cooperation Programme (United Kingdom, United States, Canada, Australia, New Zealand)
T/W	thrust/weight ratio
UCE	usable cue environment
UH	utility helicopter
USHST	United States Helicopter Safety Team
V_{min}	lower edge of conversion corridor
V_{con}	upper edge of conversion corridor
VCR	visual cue ratings
VE	virtual engineering
VF	valley following
VMC	visual meteorological conditions
VMS	vertical motion simulator
VNE	never-exceed velocity
VP	virtual prototype
VRS	vortex ring state
V/S	vertical dpeed
VSTOL	vertical/short take-off and landing
VTOL	vertical take-off and landing
WG	working group (AGARD)
WL	water line
WW2	World War 2
agl	above ground level
cg	centre of gravity
IGE/ige	in-ground effect
OGE/oge	out-of-ground effect
rms	root mean square
rpm	revs per minute
rrpm	rotor revs per minute

The DRA research Lynx ALYCAT (Aeromechanics LYnx Control and Agility Testbed) shown flying by the large motion system of the DRA advanced flight simulator (Photograph courtesy of Simon Pighills)

1 Introduction

The underlying premise of this book is that flight dynamics and control is a central discipline, at the heart of aeronautics, linking the aerodynamic and structural sciences with the applied technologies of systems and avionics and, above all, with the pilot. Flight dynamics engineers need to have breadth and depth in their domain of interest, and often hold a special responsibility in design and research departments. It is asserted that more than any other aerospace discipline, flight dynamics offers a viewpoint on, and is connected to, the key rotorcraft attributes and technologies – from the detailed fluid dynamics associated with the interaction of the main rotor wake with the empennage, to the servo-aeroelastic couplings between the rotor and control system, through to the evaluation of enhanced safety, operational advantage, and mission effectiveness of good flying qualities. It is further asserted that the multidisciplinary nature of rotorcraft flight dynamics places it in a unique position to hold the key to concurrency in requirements capture and design, i.e. the ability to optimise under the influence of multiple constraints.

In the author's view, the role of the practising flight dynamics engineer is therefore an important one, and there is a need for guidebooks and practitioner's manuals on the subject to assist in the development of the required skills and knowledge. This book is an attempt at such a manual, and it discusses flight dynamics under two main headings – simulation modelling and flying qualities. The importance of good simulation fidelity and robust flying qualities criteria in the requirements capture and design phases of a new project cannot be overstated, and this theme will be expanded on later in this chapter and throughout the book. Together, these attributes underpin confidence in decision-making during the high-risk early design phase and are directed toward the twin goals of achieving super-safe flying qualities and getting designs right, first time. These goals have motivated much of the research conducted in government research laboratories, industry, and universities for several decades.

In this short general Introduction, the aim is to give the reader a qualitative appreciation of the two main subjects – simulation modelling and flying qualities. The topics that come within the scope of flight dynamics are also addressed briefly but are not covered in the book for various reasons. Finally, a brief roadmap to the nine technical chapters is presented.

1.1 Simulation Modelling

It is beyond dispute that the observed behaviour of aircraft is so complex and puzzling that, without a well-developed theory, the subject could not be treated intelligently.

We use this quotation from Duncan (Ref. 1.1) in expanded form as a guiding light at the beginning of Chapter 3, the discourse on building simulation models. Duncan wrote these words in relation to fixed-wing aircraft many decades ago and they still hold a profound truth today. However, while it may be 'beyond dispute' that well-developed theories of flight are vital, a measure of the development level at any one time can be gauged by the ability of Industry to predict behaviour correctly before first flight, and rotorcraft experience to date is not good. In the 1989 American Helicopter Society (AHS) Nikolsky Lecture (Ref. 1.2), Crawford promotes a back-to-basics approach to improving rotorcraft modelling to avoid major redesign effort resulting from poor predictive capability. Crawford cites examples of the redesign required to improve, or simply

Helicopter Flight Dynamics: Including a Treatment of Tiltrotor Aircraft, Third Edition. Gareth D. Padfield.

put right, flight performance, vibration levels, and flying qualities for several contemporary US military helicopters. A similar story could be told for European helicopters. In Ref. 1.3, the author presents data on the percentage of development test flying devoted to handling and control, with values between 25% and 50% being quite typical. The message is that helicopters take a considerable length of time to qualify to operational standard, usually much longer than originally planned, and a principal reason lies with the deficiencies in analytical design methods. Highlighting this aspect further, Dunford discusses the evolution of the V-22 Osprey in Ref. 1.4 citing the immaturity of aeromechanics prediction as a contributor to the 18-year-long development phase. In this third edition of the book, tiltrotor aircraft feature as a topic in Chapter 10.

Underlying the failure to model flight behaviour adequately are three aspects. First, there is no escaping that the rotorcraft is an extremely complex dynamic system and the modelling task requires extensive skill and effort. Second, such complexity needs significant investment in analytical methods and specialist modelling skills, and the recognition by programme managers that these are most effectively applied in the formative stages of design. The channelling of these investments towards the critically deficient areas is also clearly very important. Third, there is still a serious shortage of high-quality, validation test data, both at model scale and from full-scale flight test. There is an adage in the world of flight dynamics relating to the merits of test versus theory, which goes something like – 'everyone believes the test results, except the person who made the measurements, and nobody believes the theoretical results, except the person who calculated them'. This stems from the knowledge that it is easier, for example, to program the computer to output rotor blade incidence at 3/4 radius on the retreating side of the disc than it is to measure this incidence. What are required, in the author's opinion, are research and development programmes that integrate the test and modelling activities so that the requirements for the one drive the other.

There are some signs that the importance of modelling and modelling skills is recognised at the right levels, but the problem will require constant attention to guard against the attitude that 'big' resources should be reserved for production, when the user and manufacturer, in theory, receive their greatest rewards. Chapters 3–5 of this book are concerned with modelling conventional helicopters, but we shall not dwell on the deficiencies of the acquisition process, but rather on where the modelling deficiencies lie. Chapter 10 addresses modelling and simulation of tiltrotors. The author has taken the opportunity in this Introduction to reinforce the philosophy promoted in Crawford's Nikolsky Lecture with the thought that the reader may well be concerned as much with the engineering 'values' as with the technical detail.

No matter how good the modelling capability, without criteria as a guide, helicopter designers cannot even start on the optimization process; with respect to flying qualities, a completely new approach has been developed, and forms a significant content of this book.

1.2 Flying Qualities

> *Experience has shown that a large percentage, perhaps as much as 65%, of the lifecycle cost of an aircraft is committed during the early design and definition phases of a new development program. It is clear, furthermore, that the handling qualities of military helicopters are also largely committed in these early definition phases and, with them, much of the mission capability of the vehicle. For these reasons, sound design standards are of paramount importance both in achieving desired performance and avoiding unnecessary program cost.*

This quotation, extracted from Ref. 1.5, states the underlying motivation for the development of flying qualities criteria – they give the best chance of having mission performance designed in, whether through safety and economics with civil helicopters or through military effectiveness. But flying quality is an elusive topic and it has two equally important facets that can easily get mixed up – the objective and the subjective. Only recently has enough effort been directed towards establishing a valid set of flying qualities criteria and test techniques for rotorcraft that has enabled both the subjective and objective aspects to be addressed in a complementary way. That effort has been orchestrated under the auspices of several different collaborative programmes to harness the use of flight and ground-based simulation facilities and key skills in North America and Europe. The result was Aeronautical Design Standard (ADS)-33, which has changed the way the helicopter community thinks, discusses, and acts about flying quality. Although the primary target for ADS-33 was the Light Helicopter Experimental (LHX), and later the RAH-66 Comanche programme, other nations have used or developed the standard to meet their own needs for requirements capture and design. Chapters 6–8 of this book will refer extensively to ADS-33, with the aim of giving the reader some insight into its development. The reader should note, however, that these chapters, like ADS-33 itself, address how a helicopter with good flying qualities should behave, rather than how to construct a helicopter with good flying qualities. In this third edition, the author looks back before ADS-33 and, in the new Chapter 9, explores the origins of rotorcraft flying qualities, and builds on the 'story of an idea' that quality can be quantified.

In search of the meaning of *flying quality*, the author has come across many different interpretations, from Pirsig's somewhat abstract but appealing, 'at the moment of pure quality, subject and object are identical' (Ref. 1.6), to a point of view put forward by one flight dynamics engineer: 'flying qualities are what you get when you've done all the other things'. Unfortunately, the second interpretation has a certain ring of truth because, until ADS-33, there was very little coherent guidance on what constituted good flying qualities. The first breakthrough for the flying qualities discipline came with the recognition that criteria needed to be related to task. The subjective rating scale, developed by Cooper and Harper (Ref. 1.7) in the late 1960s, was already task and mission oriented. In the conduct of a handling qualities experiment, the Cooper–Harper approach forces the engineer to define a task with performance standards and to agree with the pilot on what constitutes minimal or extensive levels of compensation. But the objective criteria at that time were more oriented to the stability and control characteristics of aircraft than to their ability to perform tasks well. The relationship is clearly important but the lack of task-oriented test data meant that early attempts to define criteria boundaries involved a large degree of guesswork and hypothesis. Once the two ingredients essential for success in the development of new criteria, task-orientation and test data, were recognised and resources were channelled effectively, the combined expertise of several agencies focused their efforts, and during the 1980s and 1990s, a completely new approach was developed. With the advent of digital flight control systems, which provide the capability to confer different mission flying qualities in the same aircraft, this new approach can be exploited to the full.

One of the aspects of the new approach is the relationship between the internal attributes of the air-vehicle and the external influences. The same aircraft might have perfectly good handling qualities for nap-of-the-earth operations in the day environment, but degrade severely at night; obviously, the visual cues available to the pilot play a fundamental role in the perception of flying qualities. This is a fact of operational life, but the emphasis on the relationship between the internal attributes and the external influences encourages design teams to think more synergistically, e.g. the quality of the vision aids, and what the symbology should do, becomes part of the same flying qualities problem as what goes into the control system, and, more importantly, the issues need to be integrated in the same solution. We try to emphasise the importance of this synergy first in Chapter 2, then later in Chapters 6 and 7.

The point is made on several occasions in this book, for emphasis, that good flying qualities make for safe and effective operations; all else being equal, less accidents will occur with an aircraft with good handling qualities compared with an aircraft with merely acceptable handling, and operations will be more productive. This statement may be intuitive, but there is very little supporting data to quantify this, although the compelling evidence is growing. Later, in Chapter 7, the potential benefits of handling to flight safety and effectiveness through a probabilistic analysis are examined, considering the pilot as a component with failure characteristics like any other critical aircraft component. The results may appear controversial and they are certainly tentative, but they point to one way in which the question 'How valuable are flying qualities?' may be answered. This theme is continued in Chapter 8, where the author presents an analysis of the effects of degraded handling qualities on safety and operations, looking in detail at the impact of degraded visual conditions, flight system failures, and strong atmospheric disturbances. Chapter 10 addresses the flying qualities of tiltrotors.

1.3 Missing Topics

It seems to be a common feature of book writing that the end product turns out quite different than originally intended, and *Helicopter Flight Dynamics* is no exception. It was planned to be much shorter and to cover a wider range of subjects! In hindsight, the initial plan was perhaps too ambitious, although the extent of the final product, cut back considerably in scope, has surprised even the author.

There are three major topic areas, originally intended as separate chapters, that have virtually disappeared – stability and control augmentation (including active control), design for flying qualities, and simulation validation (including system identification tools). All three are referred to as required, usually briefly, throughout the book, but there have been such advances in recent years that to give these topics appropriate coverage would have extended the book considerably. They remain topics for future treatment, particularly the progress with digital flight control and the use of simulators in design, development, and certification. In the context of both these topics, we appear to be in an era of rapid development, suggesting that a better time to document the state of the art may well be some years from now. The absence of a chapter or section on simulation model validation techniques may appear to be particularly surprising, but is compensated for by the availability of the AGARD (Advisory Report on Rotorcraft System Identification), which gave a detailed coverage of the state of the art in this subject up to the early 1990s (Ref. 1.8).

Since the publication of the first and second editions, significant strides have been made in the development of simulation models for use in design and training simulators. Refs. 1.9 and 1.10 review some of these developments but we are somewhat in mid-stream with this new push to quantify and increase fidelity and the author has resisted the temptation to bring this topic into the second or third editions. Chapter 3 does briefly discuss some of the latest developments, however.

The book says very little about the internal hardware of flight dynamics – the pilot's controls and the mechanical components of the control system including the hydraulic actuators. The pilot's displays and instruments and their importance for flight in poor visibility are briefly treated in Chapter 7 and the associated perceptual issues are treated in some depth in Chapter 8, but the author is conscious of the many missing elements here. In Chapter 3, the emphasis has been on modelling the main rotor, and many other elements, such as the engine and transmission systems, are given limited coverage.

It is hoped that the book will be judged more on what it contains than on what it doesn't.

1.4 Simple Guide to the Book

Following this Introduction, the book contains nine technical chapters. For an overview of the subject of helicopter flight dynamics, the reader is referred to the Introductory Tour in Chapter 2. Engineers familiar with flight dynamics, but new to rotorcraft, may find this a useful starting point for developing an understanding of how and why helicopters work. Chapters 3–5 are a self-contained group concerned with modelling helicopter flight dynamics. To derive benefit from these chapters requires a working knowledge of the mathematical analysis tools of dynamic systems. Chapter 3 aims to provide sufficient knowledge and understanding to enable a basic flight simulation of a helicopter to be created.

Chapter 4 discusses the problems of trim and stability, providing a range of analytical tools necessary to work at these two facets of helicopter flight mechanics. Chapter 5 extends the analysis of stability to considerations of constrained motion and completes the 'working with models' theme of Chapters 4 and 5 with a discussion on helicopter response characteristics. In Chapters 4 and 5, flight test data from the Royal Aircraft Establishment's (RAE's) research Puma and Lynx and the Deutsche Forschungs- und Versuchsantalt fuer Luft- und Raumfahrt (DLR's) Bo105 are used extensively to provide a measure of validation to the modelling. In Chapter 5 of the third edition, the author has included a detailed analysis of two accidents using the approximation theory from Chapter 4. This piece shows how both rotary and fixed-wing aircraft can suffer the same adverse aircraft-pilot-coupling during low speed flight. Chapters 6 and 7 deal with helicopter flying qualities from objective and subjective standpoints respectively, although Chapter 7 also covers several 'other topics', including agility and flight in degraded visual conditions. Chapters 6 and 7 are also self-contained and do not require the same background mathematical knowledge as that required for the modelling chapters. A unified framework for discussing the response characteristics of flying qualities is laid out in Chapter 6, where each of the four 'control' axes are discussed in turn. Quality criteria are described, drawing heavily on ADS-33 and the associated publications in the open literature. Chapter 8 was new in the second edition and contains a detailed treatment of the sources of degraded flying qualities, particularly flight in degraded visual conditions, the effects of failures in flight system functions, and the impact of severe atmospheric disturbances. These subjects are also discussed within the framework of quantitative handling qualities engineering, linking with ADS-33, where appropriate. The idea here is that degraded flying qualities should be taken into consideration in design with appropriate mitigation technologies.

Two new chapters have been written for the third edition. Chapter 9 documents the historical developments of rotorcraft flying qualities, placing the advances reported in Chapters 6 and 7 in context. Chapter 10 presents an extensive coverage of the flight dynamics of tiltrotor aircraft.

Chapters 3 and 4 are complemented and supported by appendices. Herein lie the tables of configuration data and stability and control derivative charts and tables for the three case study aircraft. Chapter 10 is similarly complemented with its own appendices, featuring data on the tiltrotor case study aircraft, the Bell/NASA/Army XV-15.

The author has found it convenient to use both metric and British systems of units as appropriate throughout the book, although with a preference for metric where an option was available. Although the metric system is strictly the primary world system of units of measurements, many helicopters are designed to the older British system. Publications, particularly those from the United States, often contain data and charts using the British system, and it has seemed inappropriate to change units for the sake of unification. This does not apply, of course, to cases where data from different sources are compared. Helicopter engineers are used to working in mixed units; for example, it is not uncommon to find, in the same paper, references to height in feet, distance in metres and speed in knots – such is the rich variety of the world of the helicopter engineer.

A final point before launching into Chapter 2: The author discusses in Chapter 3 and elsewhere how mathematical models are useful for predicting behaviour and how they can help engineers understand behavioural causes and effects. Finding analytical approximations to complex behaviour is often the best pathway to understanding causal relationships, and the reader should find examples of this throughout the book. In Chapters 5 and 10, analytic models offer explanations for root causes of accidents and represent classic examples of the power of analytics. More generally, approximations to flying qualities parameters can build the bridge between design criteria and engineering configuration. It is hoped that the book will encourage the reader to develop skills in analytic modelling to strengthen this bridge and advance the knowledge base of rotorcraft flight dynamics.

An EH101 Merlin approaching a Type 23 Frigate during development flight trials (Photograph courtesy of Westland Helicopters)

2 Helicopter and Tiltrotor Flight Dynamics – An Introductory Tour

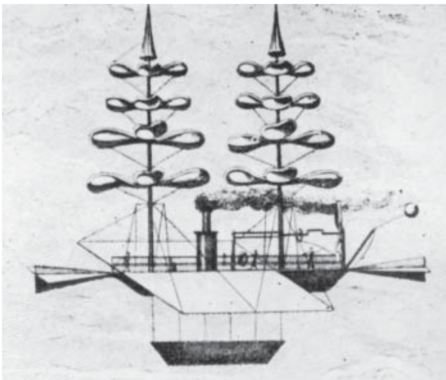

In aviation history, the nineteenth century is characterized by man's relentless search for a practical flying machine. The 1860s saw a peculiar burst of enthusiasm for helicopters in Europe *and the above picture, showing an 1863 design by* Gabrielle de la Landelle*, reflects the fascination with aerial tour-boats at that time. The present chapter takes the form of a "tour of flight dynamics" on which the innovative, and more practical, European designs from the 1960s – the Lynx, Puma, and Bo105 – will be introduced as the principal reference aircraft of this book. These splendid designs are significant in the evolution of the modern helicopter, and an understanding of their behaviour will provide important learning material on this tour and throughout the book.*

2.1 Introduction

This chapter is intended to guide the reader on a Tour of the subject of this book with the aim of instilling increased motivation by sampling and linking the wide range of subtopics that make the whole. The chapter is likely to raise more questions than it will answer. It will point to later chapters of the book where these are picked up and addressed in more detail. The Tour topics will range from relatively simple concepts such as how the helicopter's controls work, to more complex effects such as the influence of rotor design on dynamic stability, the conflict between stability and controllability, and the specialised handling qualities required for military and civil mission task elements (MTEs). All these topics lie within the domain of the flight dynamics engineer and within the scope of this book. This chapter is required reading for the reader who wishes to benefit most from the book. Many concepts are introduced and developed in fundamental form here in this chapter, and the material in later chapters will draw on the resulting understanding gained by the reader.

Helicopter Flight Dynamics: Including a Treatment of Tiltrotor Aircraft, Third Edition. Gareth D. Padfield.

One feature is re-emphasised here. This book is concerned with modelling flight dynamics and developing criteria for flying qualities, rather than how to design and build a helicopter or tiltrotor to achieve defined levels of quality. We cannot, nor do we wish to, ignore design issues; requirements can be credible only if they are achievable with the available hardware. However, largely because of the author's own background and experience, design will not be a central topic in this book and there will be no chapter dedicated to it. Design issues will be discussed in context throughout the later chapters and some of the principal considerations will be summarised on this Tour, in Section 2.5.

2.2 Four Reference Points

We begin by introducing four useful reference points for developing an appreciation of flying qualities and flight dynamics; these are summarised in Figure 2.1 and comprise the following:

(1) the mission and the associated piloting tasks;
(2) the operational environment;
(3) the vehicle configuration, dynamics, and the flight envelope;
(4) the pilot and pilot–vehicle interface (pvi).

With this perspective, the vehicle dynamics can be regarded as internal attributes, the mission and environment as the external influences and the pilot, and pvi as the connecting human factors. While these initially need to be discussed separately, it is their interaction and interdependence that widen the scope of the subject of flight dynamics to reveal its considerable scale. The influences of the mission task on the pilot's workload, in terms of precision and urgency, and the external environment, in terms of visibility and gustiness, and hence the scope for exploiting the aircraft's internal attributes, are profound, and in many ways, are key concerns and primary drivers in rotorcraft technology development. Flying qualities are determined at the confluence of these references.

2.2.1 The Mission and Piloting Tasks

Flying qualities change with the weather or, more generally, with the severity of the environment in which the rotorcraft operates; they also change with flight condition, mission type and phase, and individual mission tasks. This variability will be emphasised repeatedly and in many guises throughout this book to emphasise

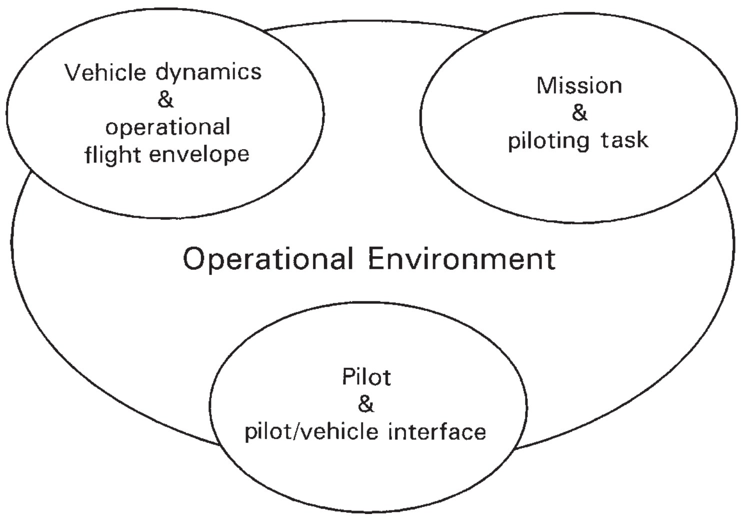

Fig. 2.1 The four reference points of rotorcraft flight dynamics

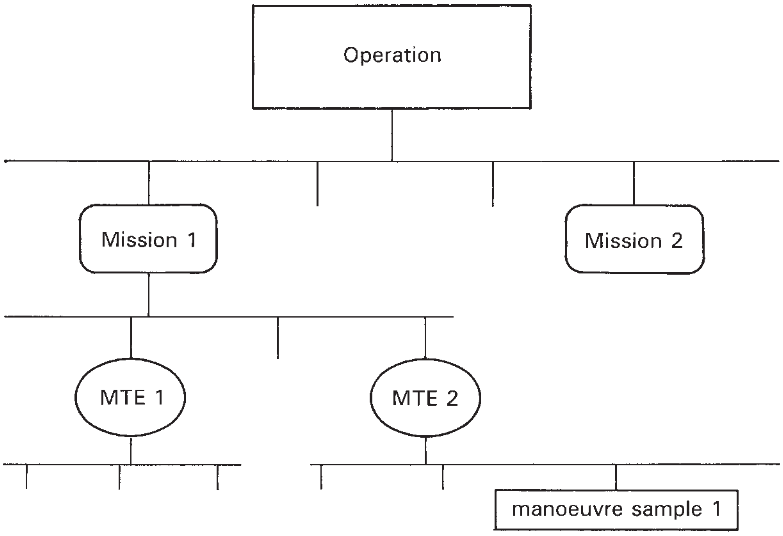

Fig. 2.2 Flying task hierarchy

that we are not just talking about an aircraft's stability and control characteristics, but more about the synergy between the internals and the externals referred to above. In later sections, the need for a systematic flying qualities structure that provides a framework for describing criteria will be addressed, but we need to do the same with the mission and the associated flying tasks.

For our purposes, it is convenient to describe the flying tasks within a hierarchy as shown in Figure 2.2. An operation is made up of many missions, which, in turn, are composed of a series of contiguous mission task elements (MTEs). An MTE is a collection of individual manoeuvres and will have a definite start and finish and prescribed temporal and spatial performance requirements. The manoeuvre sample is the smallest flying element, often relating to a single flying axis, e.g. change in pitch or roll attitude. Objective flying qualities criteria are normally defined for, and tested with, manoeuvre samples; subjective pilot assessments are normally conducted by flying MTEs.

The flying qualities requirements in the US Army's handling qualities requirements, Aeronautical Design Standard (ADS)-33C (Ref. 2.1), are related directly to the required MTEs. Hence, while missions, and correspondingly aircraft type, may be quite different, MTEs are often common and are a key discriminator of flying qualities. For example, both utility transports in the 30-ton weight category and anti-armour helicopters in the 10-ton weight category may need to fly slaloms and precision hovers in their nap-of-the-earth (NoE) missions. This is one of the many areas where ADS-33C departs significantly from its predecessor, Mil Spec 8501A (Ref. 2.2), where aircraft weight and size served as the key defining parameters. The MTE basis of ADS-33C also contrasts with the fixed-wing requirements, MIL-F-8785C (Ref. 2.3), where flight phases are defined as the discriminating mission elements. Thus, the nonterminal flight phases in Category A (distinguished by rapid manoeuvring and precision tracking) include air-to-air combat, in-flight refuelling (receiver), and terrain following, while Category B (gradual manoeuvres) includes climb, in-flight refuelling (tanker), and emergency deceleration. Terminal flight phases (accurate flight path control, gradual manoeuvres) are classified under Category C, including take-off, approach, and landing. Through the MTE and flight phase, current rotary and fixed-wing flying qualities requirements are described as mission-oriented criteria.

To understand better how this relates to helicopter and tiltrotor flight dynamics, we shall now briefly discuss two typical reference missions. Figure 2.3 illustrates a civil mission, described as the offshore supply mission; Figure 2.4 illustrates the military mission, described as the armed reconnaissance mission. On each figure a selected phase has been expanded and shown to comprise a sequence of MTEs (Figures 2.3b and 2.4b). A typical MTE is extracted and defined in more detail (Figures 2.3c and 2.4c). In the case of the civil mission, we have selected the landing onto the helideck; for the military mission, the 'mask–unmask–mask' sidestep is the selected MTE. It is difficult to break the MTEs down further; they are normally multi-axis

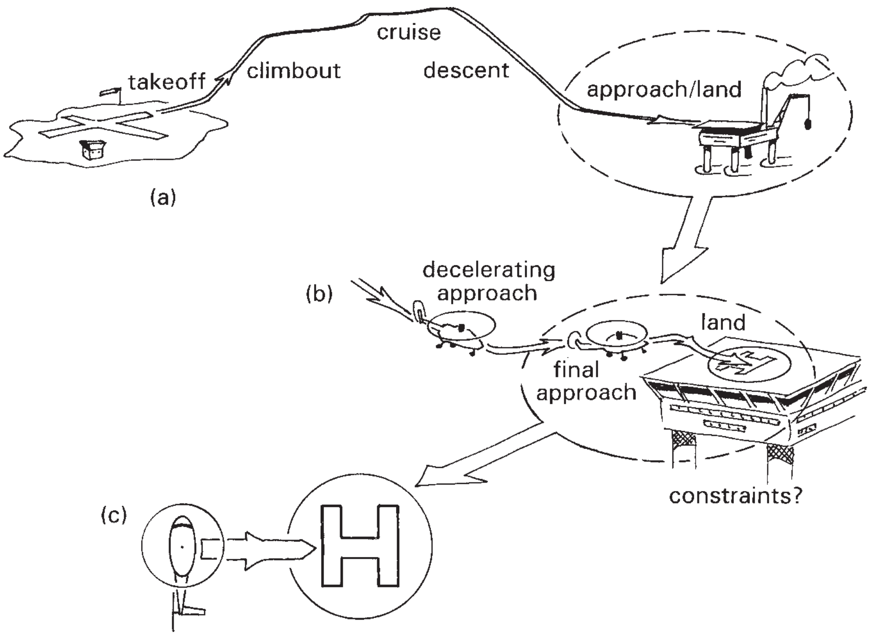

Fig. 2.3 Elements of a civil mission – offshore supply: (a) offshore supply mission; (b) mission phase: approach and land; (c) mission task element: landing

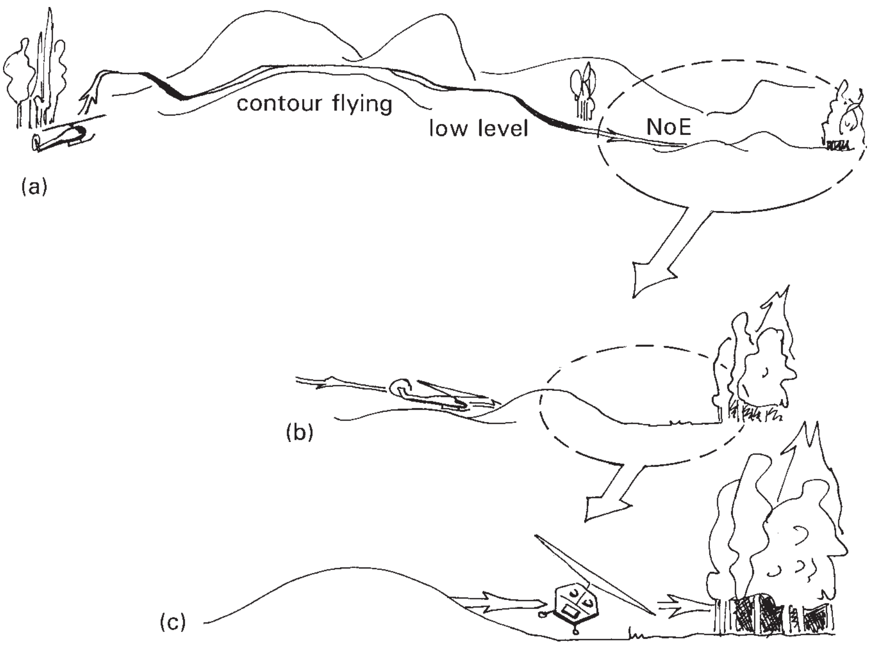

Fig. 2.4 Elements of a military mission – armed reconnaissance: (a) armed reconnaissance mission; (b) mission phase – NoE; (c) mission task element – sidestep

tasks and, as such, contain several concurrent manoeuvre samples. The accompanying MTE text defines the constraints and performance requirements, which are likely to be dependent on a range of factors. For the civil mission, for example, the spatial constraints will be dictated by the size of the helideck and the touchdown velocity by the strength of the undercarriage. The military MTE will be influenced by weapon performance characteristics and any spatial constraints imposed by the need to remain concealed from the radar systems of threats. Further discussion on the design of flight test manoeuvres as stylised MTEs for the evaluation of flying qualities is contained in Chapter 7 and later in Chapter 10 for tiltrotors.

Ultimately, the MTE performance will determine the flying qualities requirements of the rotorcraft. This is a fundamental point. If all that a rotorcraft had to do was to fly from one airport to another in daylight and good weather, it is unlikely that flying qualities would ever be a design challenge; taking what comes from meeting other performance requirements would probably be quite sufficient. But if a rotorcraft is required to land on the back of a ship in sea state 6 or to be used to fight at night, then conferring satisfactory flying qualities that minimise the probability of mission or even flight failure is a major design challenge. Criteria that adequately address the developing missions are the cornerstones of design, and the associated MTEs are the data source for the criteria.

The reference to weather and flying at night suggests that the purely *kinematic* definition of the MTE concept is insufficient for defining the full operating context; the environment – in terms of weather, temperature, and visibility – are equally important and bring us to the second reference point.

2.2.2 The Operational Environment

A typical operational requirement will include a definition of the environmental conditions in which the rotorcraft needs to work in terms of temperature, density altitude, wind strength, and visibility. These will then be reflected in an aircraft's flight manual. The requirement's wording may take the form: 'This helicopter must be able to operate (i.e. conduct its intended mission, including start-up and shut-down) in the following conditions – 5000 ft. altitude, 15 °C, wind speeds of 40 knots gusting to 50 knots, from any direction, in day or night'. This description defines the limits to the operational capability in the form of a multidimensional envelope.

Throughout the history of aviation, the need to extend operations into poor weather and at night has been a dominant driver for both economic and military effectiveness. Fifty years ago, helicopters were fair-weather machines with marginal performance; now they regularly operate in conditions from hot and dry to cold, wet, and windy, and in low visibility. One of the unique operational capabilities of the helicopter is its ability to operate in the NoE or, more generally, in near-earth conditions defined in Ref. 2.1 as 'operations sufficiently close to the ground or fixed objects on the ground, or near water and in the vicinity of ships, oil derricks, etc., that flying is primarily accomplished with reference to outside objects'. In near-earth operations, avoiding the ground and obstacles clearly dominates the pilot's attention and, in poor visibility, the pilot is forced to fly more slowly to maintain the same workload. During the formative years of ADS-33, it was recognised that the classification of the quality of the visual cues in terms of instrument or visual flight conditions was inadequate to describe the conditions in the NoE. To quote from Hoh (Ref. 2.4):

> *The most critical contributor to the total pilot workload appears to be the quality of the out-of-the-window cues for detecting aircraft attitudes, and, to a lesser extent, position, and velocity. Currently, these cues are categorized in a very gross way by designating the environment as either VMC (visual meteorological conditions) or IMC (instrument meteorological conditions). A more discriminating approach is to classify visibility in terms of the detailed attitude and position cues available during the experiment or proposed mission and to associate handling qualities requirements with these finer grained classifications.*

The concept of the outside visual cues (OVCs) was introduced, along with an OVC pilot rating that provided a subjective measure of the visual cue quality. The stimulus for the development of this concept was the recognition that handling qualities are particularly affected by the visual cues in the NoE, yet there was no process or methodology to quantify this contribution. One problem is that the cue is a dynamic variable and can be judged only when used in its intended role. Eventually, out of the confusion surrounding this subject emerged the usable cue environment (UCE), which was to become established as one of the key innovations of ADS-33. In its developed form, the UCE embraces not only the OVC but also any artificial vision aids provided to the pilot, and is determined from an aggregate of pilot visual cue ratings (VCRs) relating to the pilot's ability to perceive changes in, and adjust, aircraft attitude and velocity. Handling qualities in degraded visual conditions, the OVC and the UCE will be discussed in more detail in Chapter 7.

The MTE and the UCE are two important building blocks in the new language of flying qualities; a third relates to the aircraft's response characteristics and provides a vital link between the MTE and UCE.

2.2.3 The Vehicle Configuration, Dynamics, and Flight Envelope

The helicopter, or tiltrotor, is required to perform as a dynamic system within the user-defined operational flight envelope (OFE), or that combination of airspeed, altitude, rate of climb/descent, sideslip, turn rate, load factor, and other limiting parameters that bound the vehicle dynamics, required to fulfil the user's function. Beyond this lies the manufacturer-defined safe flight envelope (SFE), which sets the limits to safe flight, normally in terms of the same parameters as the OFE, but represents the physical limits of structural, aerodynamic, powerplant, transmission, or flight control capabilities. The margin between the OFE and the SFE needs to be large enough so that inadvertent transient excursions beyond the OFE are tolerable. Within the OFE, the flight mechanics of a rotorcraft can be discussed in terms of three characteristics – *trim, stability,* and *response* – a classification covered in more detail in Chapters 4 and 5 and later in Chapter 10 for tiltrotors.

Trim is concerned with the ability to maintain flight equilibrium with controls fixed; the most general trim condition is a turning (about the vertical axis), descending or climbing (assuming constant air density and temperature), sideslipping manoeuvre at constant speed. More conventional flight conditions such as hover, cruise, autorotation, or sustained turns are also trims, of course, but the general case is distinguished by the four 'outer' flight-path states, and this is simply a consequence of having four independent helicopter controls – three for the main rotor and one for the tail rotor. The rotorspeed is not normally controllable by the pilot, but is set to lie within the automatically governed range. For a helicopter, the so-called inner states – the fuselage attitudes and rates – are uniquely defined by the flight path states in a trim condition. For tilt rotors and other compound rotorcraft, the additional controls provide more flexibility in trim; the former will be examined in Chapter 10.

Stability is concerned with the behaviour of the aircraft when disturbed from its trim condition; will it return or will it depart from its equilibrium point? The initial tendency has been called the static stability, while the longer-term characteristics, the dynamic stability. These are useful physical concepts, though rather crude, but the keys to developing a deeper understanding and quantification of rotorcraft stability comes from theoretical modelling of the interacting forces and moments. From there come the concepts of small perturbation theory and linearization, of stability and control derivatives and the natural modes of motion and their stability characteristics. The insight value gained from theoretical modelling is particularly high when considering the *response* to pilot controls and external disturbances. Typically, a helicopter responds to a single-axis control input with multi-axis behaviour; cross-coupling is almost synonymous with helicopters. In this book, we shall be dealing with direct and coupled responses, sometimes described as on-axis and off-axis responses. On-axis responses will be discussed within a framework of response types – rate, attitude, and translational-rate responses will feature as types that characterise the initial response following a step control input. Further discussion is deferred until the modelling section within this Tour and later in Chapters 3–5. Some qualitative appreciation of vehicle dynamics can be gained, however, without recourse to detailed modelling.

Rotor Controls

Figure 2.5 illustrates the conventional main rotor collective and cyclic controls applied through a swash plate. Collective applies the same pitch angle to all blades and is the primary mechanism for direct lift or thrust control on the rotor. Cyclic is more complicated and can be fully appreciated only when the rotor is rotating. The cyclic operates through a swash plate or similar device (see Figure 2.5), which has nonrotating and rotating halves, the latter attached to the blades with pitch link rods, and the former to the control actuators. Tilting the swash plate gives rise to a one-per-rev sinusoidal variation in blade pitch with the maximum/minimum

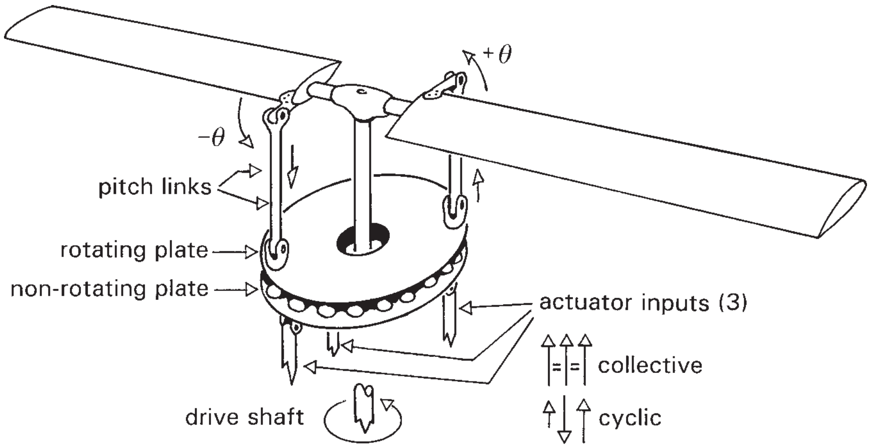

Fig. 2.5 Rotor control through a swash plate

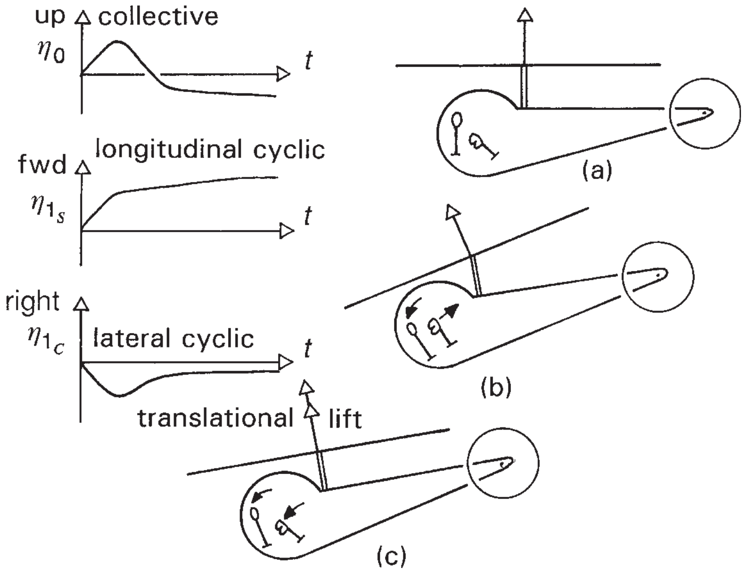

Fig. 2.6 Control actions as helicopter transitions into forward flight: (a) hover; (b) forward acceleration; (c) translational lift

axis normal to the tilt direction. The rotor responds to collective and cyclic inputs by flapping as a disc, in coning, and tilting modes. In hover the responses are uncoupled with collective pitch resulting in coning and cyclic pitch resulting in rotor disc tilting. The concept of the rotor as a coning and tilting disc (defined by the rotor blade tip path plane) will be further developed in the modelling chapters. The sequence of sketches in Figure 2.6 illustrates how the pilot would need to apply cockpit main rotor controls to transition into forward flight from an out-of-ground-effect (oge) hover. Points of interest in this sequence are:

(1) Forward cyclic (η_{1s}) tilts the rotor disc forward through the application of cyclic pitch with a maximum/minimum axis laterally – pitching the blade down on the advancing side and pitching up on the retreating side of the disc; this 90° phase shift between pitch and flap is the most fundamental facet of rotor behaviour and will be revisited later on this Tour and in the modelling chapters;

(2) Forward tilt of the rotor directs the thrust vector forward and applies a pitching moment to the helicopter fuselage, hence tilting the thrust vector further forward and accelerating the aircraft into forward flight;
(3) As the helicopter accelerates, the pilot first raises his collective (η_c) to maintain height, then lowers it as the rotor thrust increases through 'translational lift' – the dynamic pressure increasing more rapidly on the advancing side of the disc than it decreases on the retreating side; cyclic needs to be moved increasingly forward and to the left (η_{1c}) (for anticlockwise rotors) as forward speed is increased. The cyclic requirements are determined by the asymmetric fore–aft and lateral aerodynamic loadings induced in the rotor by forward flight.

The main rotor combines the primary mechanisms for propulsive force and control, aspects that are clearly demonstrated in the simple manoeuvre described above. Typical control ranges for main rotor controls are 15° for collective, more than 20° for longitudinal cyclic and 15° for lateral cyclic, which requires that each individual blade has a pitch range of more than 30°. At the same time, the tail rotor provides the anti-torque reaction (due to the powerplant) in hover and forward flight, while serving as a yaw control device in manoeuvres. Tail rotors, or other such controllers on single main rotor helicopters, e.g. Fenestron/fantail or Notar (Refs. 2.5, 2.6), are normally fitted only with collective control applied through the pilot's pedals on the cockpit floor, often with a range of more than 40°; such a large range is required to counteract the negative pitch applied by the built-in pitch/flap coupling normally found on tail rotors to alleviate transient flapping.

Two Distinct Flight Regimes

It is convenient for descriptive purposes to consider the flight of the helicopter in two distinct regimes – hover/low speed (up to about 45 knots), including vertical manoeuvring, and mid/high speed flight (up to V_{ne} – never-exceed velocity). The low-speed regime is very much unique to the helicopter as an operationally useful regime; no other flight vehicles are so flexible and efficient at manoeuvring slowly, close to the ground and obstacles, with the pilot able to manoeuvre the aircraft almost with disregard for flight direction. The pilot has direct control of thrust with collective and the response is fairly immediate (time constant to maximum acceleration $O(0.1\ \text{s})$); the vertical rate time constant is much greater, $O(3\ \text{s})$, giving the pilot the impression of an acceleration command response type (see Section 2.3). Typical hover thrust margins at operational weights are between 5% and 10% providing an initial horizontal acceleration capability of about 0.3–0.5g. This margin increases through the low-speed regime as the (induced rotor) power required reduces (see Chapter 3). Pitch and roll manoeuvring are accomplished through tilting the rotor disc and hence rotating the fuselage and rotor thrust (time constant for rate response types $O(0.5\ \text{s})$), yaw through tail rotor collective (yaw rate time constant $O(2\ \text{s})$), and vertical through collective, as described above. Flight in the low-speed regime can be gentle and docile or aggressive and agile, depending on aircraft performance and the urgency with which the pilot 'attacks' a particular manoeuvre. The pilot cannot adopt a carefree handling approach, however. Apart from the need to monitor and respect flight envelope limits, a pilot must be wary of several behavioural quirks of the conventional helicopter in its privileged low-speed regime. Many of these are not fully understood and similar physical mechanisms appear to lead to quite different handling behaviour depending on the aircraft configuration. A descriptive parlance has built up over the years, some of which has developed in an almost mythical fashion as pilots relate anecdotes of their experiences 'close to the edge'. These include ground horseshoe effect, pitch-up, vortex ring and power settling, fishtailing, and inflow roll. Later, in Chapter 3, some of these effects will be explained through modelling, but it is worth noting that such phenomena are difficult to model accurately, often being the result of strongly interacting, nonlinear, and time-dependent forces. A brief glimpse of just two will suffice for the moment.

Figure 2.7 illustrates the tail rotor control requirements for early Marks (Mks 1–5) of Lynx at high all-up-weight, in the low-speed regime corresponding to winds from different 'forward' azimuths (for pedal positions <40%). The asymmetry is striking, and the 'hole' in the envelope with winds from green 060–075 (green winds from starboard in directions between 60° and 75° from aircraft nose) is clearly shown. This has been attributed to main rotor wake/tail rotor interactions, which lead to a loss of tail rotor effectiveness when the main rotor wake becomes entrained in the tail rotor. The loss of control and high-power requirements threatening at this edge of the envelope provide for very little margin between the OFE and SFE.

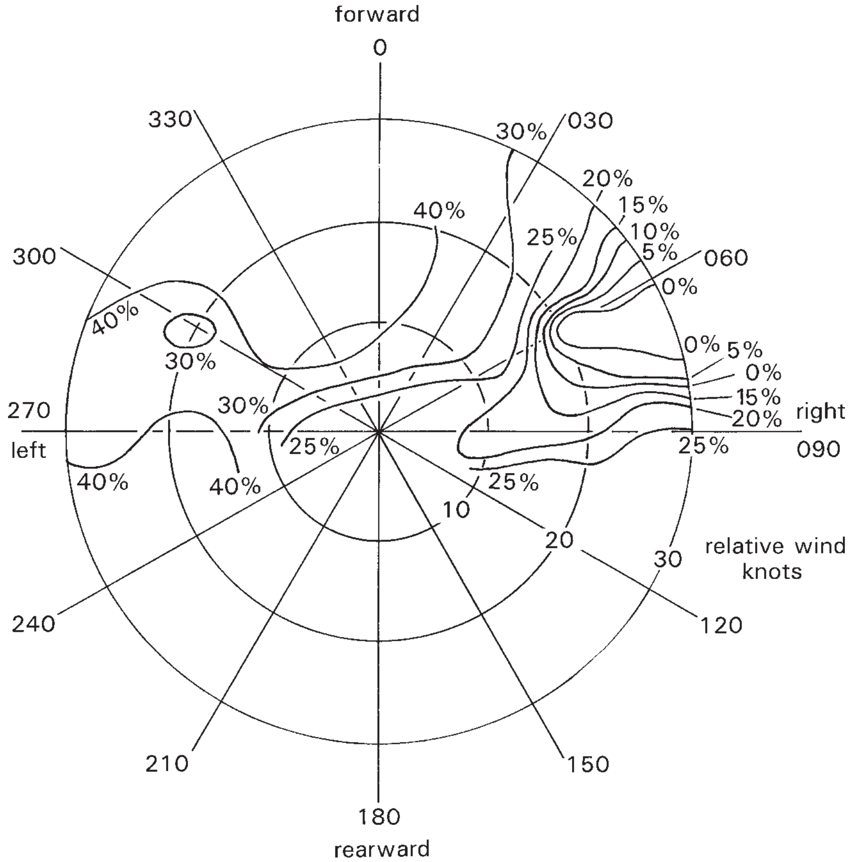

Fig. 2.7 Lynx Mk 5 tail rotor control limits in hover with winds from different directions

A second example is the so-called vortex-ring condition, which occurs in near-vertical descent conditions at moderate rates of descent (O(500–800 ft/min)) on the main rotor and corresponding conditions in sideways motion on the tail rotor. Figure 2.8, derived from Drees (Ref. 2.7), illustrates the flow patterns through a rotor operating in vertical flight. At the two extremes of helicopter (propeller) and windmill states, the flow is relatively uniform. Before the ideal autorotation condition is reached, where the induced downwash is equal and opposite to the upflow, a state of irregular and strong vorticity develops, where the upflow/downwash becomes entrained together in a doughnut-shaped vortex. The downwash increases as the vortex grows in strength, leading to large reductions in rotor blade incidences spanwise. Entering the vortex-ring state, the helicopter will increase its rate of descent very rapidly as the lift is lost; any further application of collective by the pilot will tend to reduce the rotor efficiency even further – rates of descent of more than 3000 ft/min can build up very rapidly. The consequences of entering a vortex ring when close to the ground are extremely hazardous. Chapter 10 discusses the peculiar characteristics of tiltrotors in vortex ring state, including so-called asymmetric vortex ring, where only one rotor enters the condition.

Rotor Stall Boundaries

While aeroplane stall boundaries in level flight can occur at low speed, helicopter stall boundaries typically occur at the high-speed end of the OFE. Figure 2.9 shows the aerodynamic mechanisms at work at the boundary. As the helicopter flies faster, forward cyclic is increased to counteract the lateral lift asymmetry due to cyclical dynamic pressure variations. Forward cyclic increases retreating blade pitch/incidence and reduces advancing blade pitch/incidence (α); at the same time, forward flight brings cyclical Mach number (M) variations and the α versus M locus takes the shape sketched in Figure 2.10. The stall boundary is also

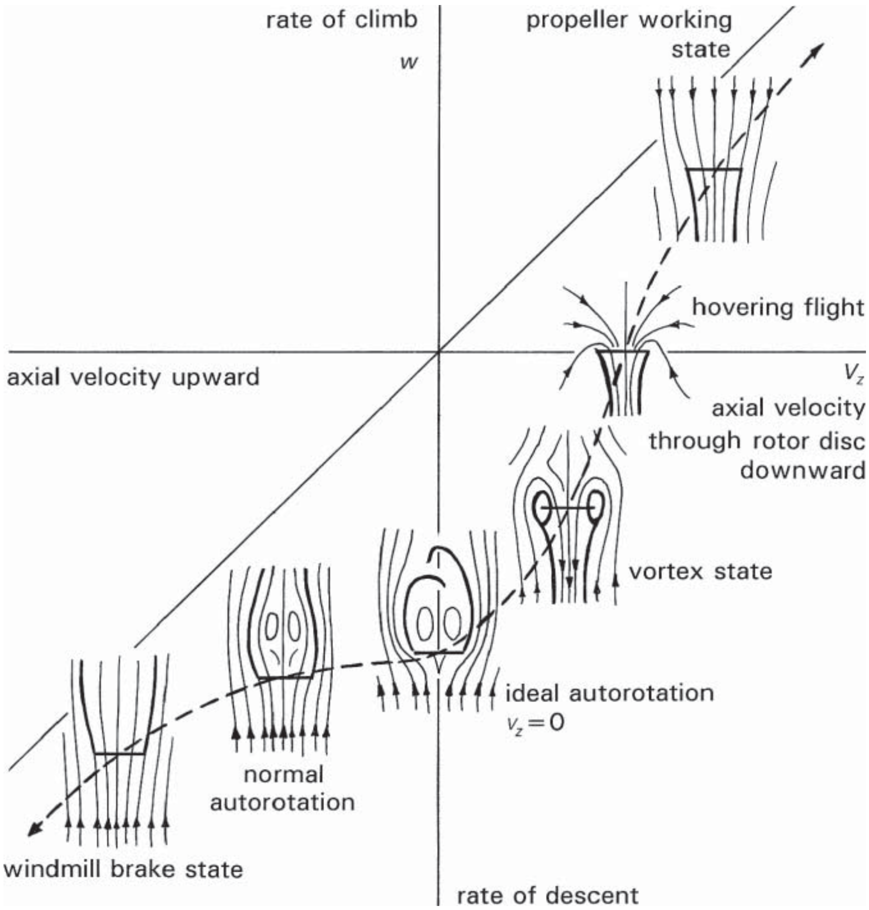

Fig. 2.8 Rotor flow states in axial flight

drawn, showing how both advancing and retreating blades are close to the limit at high speed. The low-speed, trailing edge-type, high incidence ($O(15°)$) stall on the retreating blade is usually triggered first, often by the sharp local incidence perturbations induced by the trailing tip vortex from previous blades. Shock-induced boundary layer separation will stall the advancing blade at very low incidence ($O(1–2°)$). Both retreating and advancing blade stall are initially local, transient effects, and self-limiting because of the decreasing incidence and increasing velocities in the fourth quadrant of the disc and the decreasing Mach number in the second quadrant. The overall effect on rotor lift will not be nearly as dramatic as when an aeroplane stalls at low speed. However, the rotor blade lift stall is usually accompanied by a large change in blade chordwise pitching moment, which in turn induces a strong, potentially more sustained, torsional oscillation and fluctuating stall, increasing vibration levels and inducing strong aircraft pitch and roll motions.

Rotor stall and the attendant increase in loads therefore determine the limits to forward speed for helicopters. This and other effects can be illustrated on a plot of rotor lift (or thrust T) limits against forward speed V. It is more general to normalise these quantities as thrust coefficient C_T and advance ratio μ, where

$$C_T = \frac{T}{\rho(\Omega R)^2 \pi R^2}, \quad \mu = \frac{V}{\Omega R}$$

where Ω is the rotorspeed, R the rotor radius, and ρ the air density. Figure 2.11 shows how the thrust limits vary with advance ratio and includes the sustained or power limit boundary, the retreating and advancing blade limit lines, the maximum thrust line and the structural boundary. The parameter s is the solidity defined as

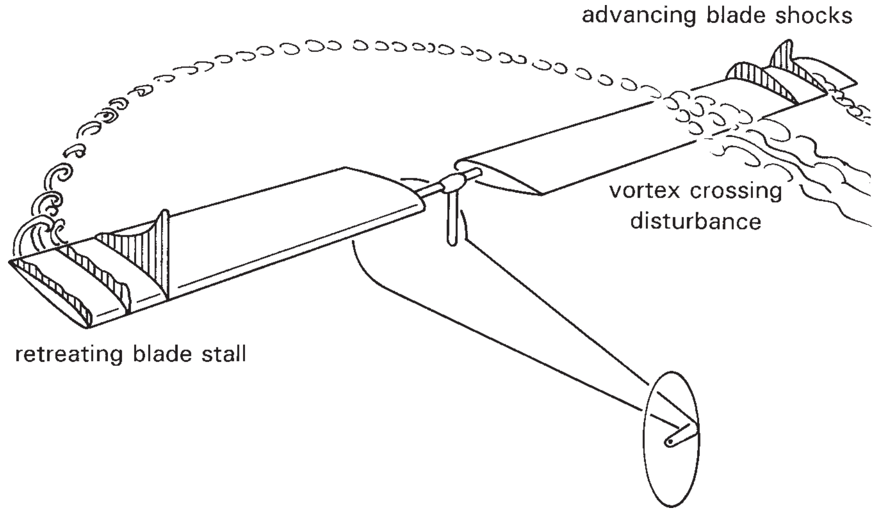

Fig. 2.9 Features limiting rotor performance in high-speed flight

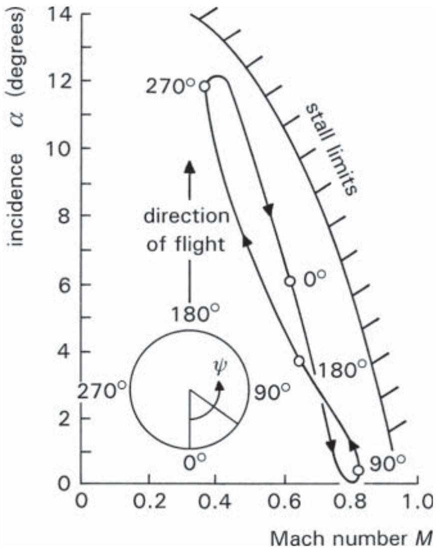

Fig. 2.10 Variation of incidence and Mach number encountered by the rotor blade tip in forward flight

the ratio of blade area to disc area. The retreating and advancing blade thrust lines in the figure correspond to both level and manoeuvring flight. At a given speed, the thrust coefficient can be increased in level flight, by increasing weight or height flown or by increasing the load factor in a manoeuvre. The manoeuvre can be sustained or transient and the limits will be different for the two cases, the loading peak moving inboard and ahead of the retreating side of the disc in the transient case. The retreating/advancing blade limits define the onset of increased vibration caused by local stall, and flight beyond these limits is accompanied by a marked increase in the fatigue life usage. These are soft limits, in that they are contained within the OFE and the pilot can fly through them. However, the usage spectrum for the aircraft will, in turn, define the amount of time the aircraft is likely (designed) to spend at different C_T or load factors, which, in turn, will define the service life of stressed components. The maximum thrust line defines the potential limit of the rotor, before local stall spreads so wide that the total lift reduces. The other imposed limits are defined by the capability

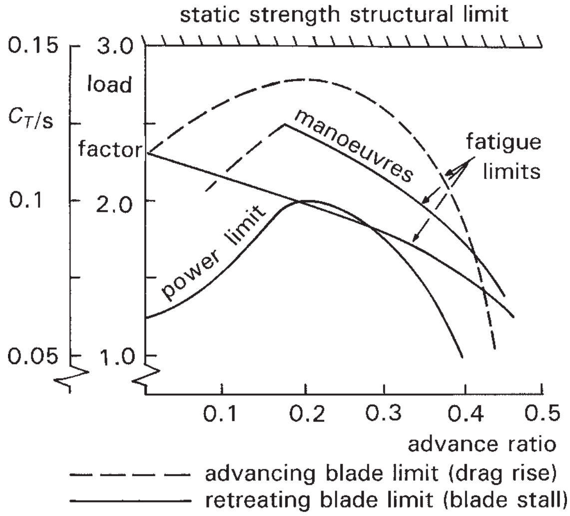

Fig. 2.11 Rotor thrust limits as a function of advance ratio

of the powerplant and structural strength of critical components in the rotor and fuselage. The latter is an SFE design limit, set well outside the OFE. However, rotors at high speed, just like the wings on fixed-wing aeroplanes, are sometimes aerodynamically capable of exceeding this.

Having dwelt on aspects of rotor physics and the importance of rotor thrust limits, it needs to be emphasised that the pilot does not normally know what the rotor thrust is; he or she can infer it from a load factor or *g* metre, and from a knowledge of take-off weight and fuel burn, but the rotor limits of more immediate and critical interest to the pilot will be torque (more correctly a coupled rotor/transmission limit) and rotorspeed. Rotorspeed is automatically governed on turbine-powered helicopters, and controlled to remain within a narrow range, dropping only about 5% between autorotation and full power climb, for example. Overtorquing and overspeeding are potential hazards for the rotor at the two extremes and are particularly dangerous when the pilot tries to demand full performance in emergency situations, e.g. evasive hard turn or pop-up to avoid an obstacle.

Rotor limits – whether thrust, torque, or rotorspeed in nature – play a major role in the flight dynamics of helicopters, in the changing aeroelastic behaviour through to the handling qualities experienced by the pilot. Understanding the mechanisms at work near the flight envelope boundary is important in the provision of carefree handling, a subject we shall return to in Chapter 7.

2.2.4 The Pilot and Pilot–Vehicle Interface

This aspect of the subject draws its conceptual and application boundaries from the engineering and psychological facets of the human factors discipline. We are concerned in this book with the piloting task and hence with only that function in the crew station; the crew have other, perhaps more important, mission-related duties, but the degree of spare capacity that the pilot has available to devote to these will depend critically on his flying workload. The flying task can be visualised as a closed-loop feedback system with the pilot as the key sensor and motivator (Figure 2.12).

The elements of Figure 2.12 form this fourth reference point. The pilot will be well trained and highly adaptive (this is particularly true of helicopter pilots), and ultimately his or her skills and experience will determine how well a mission is performed. Pilots gather information visually from the outside world and instrument displays, from motion cues and tactile sensory organs. They continuously make judgements of the quality of their flight path management and apply any required corrections through their controllers. The pilot's acceptance of any new function or new method of achieving an existing function that assists the piloting task is so important that it is vital that prototypes are evaluated with test pilots prior to delivery into service.

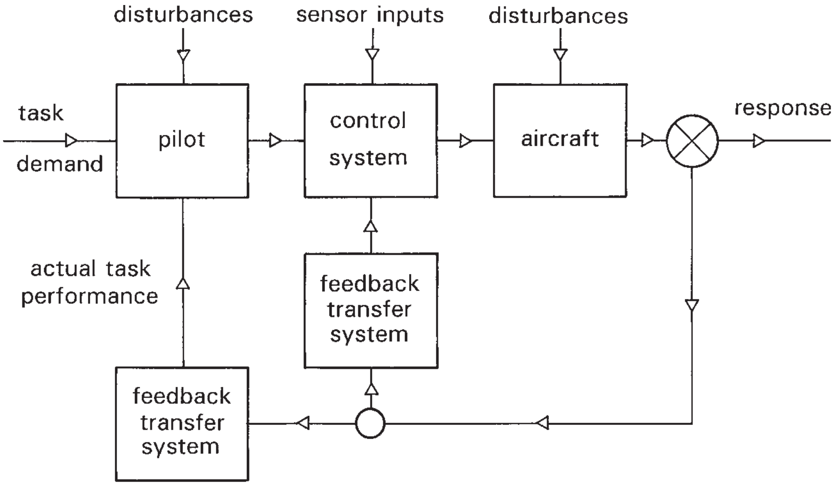

Fig. 2.12 The pilot as sensor and motivator in the feedback loop

This is emphasised because of its profound impact on the flying qualities *process,* e.g. the development of new handling criteria, new helmet-mounted display formats or multi-axis sidesticks. Pilot-subjective opinion of quality, its measurement, interpretation, and correlation with objective measures, underpins all substantiated data and hence needs to be central to all new developments. Here lies a small catch; most pilots learn to live with and love their aircraft and to compensate for deficiencies. They will almost certainly have invested some of their ego in their high level of skill and ability to perform well in difficult situations. Any developments that call for changes in the way they fly can be met by resistance. To a large extent, this reflects a natural caution and needs to be heeded; test pilots are trained to be critical and to challenge the engineer's assumptions because ultimately, they will have to work with the new developments.

Later in this book, in Chapter 6 and, more particularly, Chapter 7, the key role that test pilots have played in the development of flying qualities and flight control technology over many decades will be addressed. In Chapter 8 the treatment of the topic of degraded handling qualities will expose some of the dangerous conditions that pilots can experience. Lessons learnt through the author's personal experience of working with test pilots will be covered.

2.2.5 Résumé of the Four Reference Points

Figure 2.13 illustrates in composite form the interactional nature of the flight dynamics process as reflected by the four reference points. The figure, drawing from the parlance of ADS-33, tells us that to achieve Level 1 handling qualities in a UCE of 1, a rate response type is adequate; to achieve the same in UCEs of 2 and 3 require AC (attitude command) or TRC (translational rate command) response types, respectively. This classification represents a fundamental development in helicopter handling qualities that lifts the veil off a very complex and confused matter. The figure also shows that if the UCE can be upgraded from a 3 to a 2, then reduced augmentation will be required. A major trade-off between the quality of the visual cues and the quality of the control augmentation emerges. This will be a focus of attention in later chapters. Figure 2.13 also reflects the requirement that the optimum vehicle dynamic characteristics may need to change for different MTEs and at the edges of the OFE; terminology borrowed from fixed-wing parlance serves to describe these features – task-tailored or mission-oriented flying qualities and carefree handling. Above all else, the quality requirements for flying are driven by the performance and piloting workload demands in the MTEs, which are themselves regularly changing user-defined requirements. The whole subject is thus evolving from the four reference points – the mission, the environment, the vehicle, and the pilot; they support the flight dynamics discipline and provide an application framework for understanding and interpreting the modelling

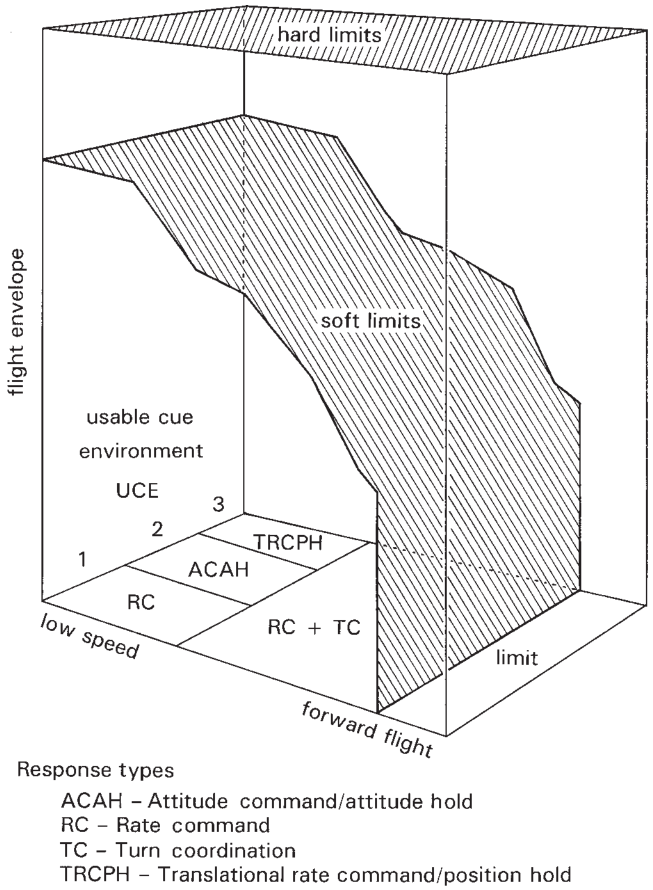

Fig. 2.13 Response types required to achieve Level 1 handing qualities in different UCEs

and criteria of task-oriented flying qualities. Continuing the Tour, we address the first of three key technical areas with stronger analytical content – theoretical modelling.

2.3 Modelling Helicopter/Tiltrotor Flight Dynamics

A mathematical description or simulation of a helicopter's or tilt rotor's flight dynamics needs to embody the important aerodynamic, structural, and other internal dynamic effects (e.g. engine, actuation) that combine to influence the response of the aircraft to pilot's controls (handling qualities) and external atmospheric disturbances (ride qualities). The problem is highly complex and the dynamic behaviour of the rotorcraft is often limited by local effects that rapidly grow in their influence to inhibit larger or faster motion, e.g. blade stall. The helicopter behaviour is naturally dominated by the main and tail rotors, and these will receive primary attention in this stage of the Tour; we need a framework to place the modelling in context.

2.3.1 The Problem Domain

A convenient and intuitive framework for introducing this important topic is illustrated in Figure 2.14, where the natural modelling dimensions of frequency and amplitude are used to characterise the range of problems within the OFE. The three fundamentals of flight dynamics – trim, stability, and response – can be seen

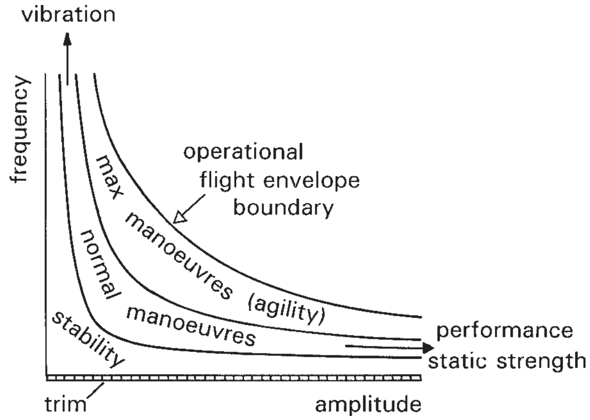

Fig. 2.14 Frequency and amplitude – the natural modelling dimensions for flight mechanics

delineated, with the latter expressed in terms of the manoeuvre envelope from normal to maximum at the OFE boundary. The figure also serves as a guide to the scope of flight dynamics as covered in this book. At small amplitudes and high frequency, the problem domain merges with that of the loads and vibration engineer. The separating frequency is not distinct. The flight dynamicist is principally interested in the loads that can displace the aircraft's flight path, and over which the human or automatic pilot has some direct control. On the rotor, these reduce to the zeroth and first harmonic motions and loads – all higher harmonics transmit zero mean vibrations to the fuselage; so, the distinction would appear deceptively simple. The first harmonic loads will be transmitted through the various load paths to the fuselage at a frequency depending on the number of blades. Perhaps the only general statement that can be made regarding the extent of the flight dynamicist's domain is that they must be cognisant of all loads and motions that are of primary (generally, controlled) and secondary (generally, uncontrolled) interest in the achievement of good flying qualities. So, for example, the forced response of the first elastic torsion mode of the rotor blades (natural frequency O(20 Hz)) at one-per-rev could be critical to modelling the rotor cyclic pitch requirements correctly (Ref. 2.8); including a model of the lead/lag blade dynamics could be critical to establishing the limits on rate stabilisation gain in an automatic flight control system (AFCS) (Ref. 2.9); modelling the fuselage bending frequencies and mode shapes could be critical to the flight control system sensor design and layout (Ref. 2.10).

At the other extreme, the discipline merges with that of the performance and structural engineers, although both will be generally concerned with behaviour across the OFE boundary. Power requirements and trim efficiency (range and payload issues) are part of the flight dynamicist's remit. The aircraft's static and dynamic (fatigue) structural strength present constraints on what can be achieved from the point of view of flight path control. These constraints need to be well understood by the flight dynamicist.

In summary, vibration, structural loads, and steady-state performance traditionally define the edges of the OFE within the framework of Figure 2.14. Good flying qualities then ensure that the OFE can be used safely, in particular that there will always be sufficient control margin to enable recovery in emergency situations. But control margin can be interpreted in a dynamic context, including concepts such as pilot-induced oscillations and agility. Just as with high-performance fixed-wing aircraft, the dynamic OFE can be limited, and hence defined, by flying qualities for rotorcraft. In practice, a balanced design will embrace these in harmony with the central flight dynamics issues, drawing on concurrent engineering techniques (Ref. 2.11) to quantify the trade-offs and to identify any critical conflicts.

2.3.2 Multiple Interacting Subsystems

The behaviour of a helicopter in flight can be modelled as the combination of many interacting subsystems. Figure 2.15 highlights the main rotor element, the fuselage, powerplant, flight control system, empennage and tail rotor elements and the resulting forces and moments. Shown in simplified form in Figure 2.16 is the

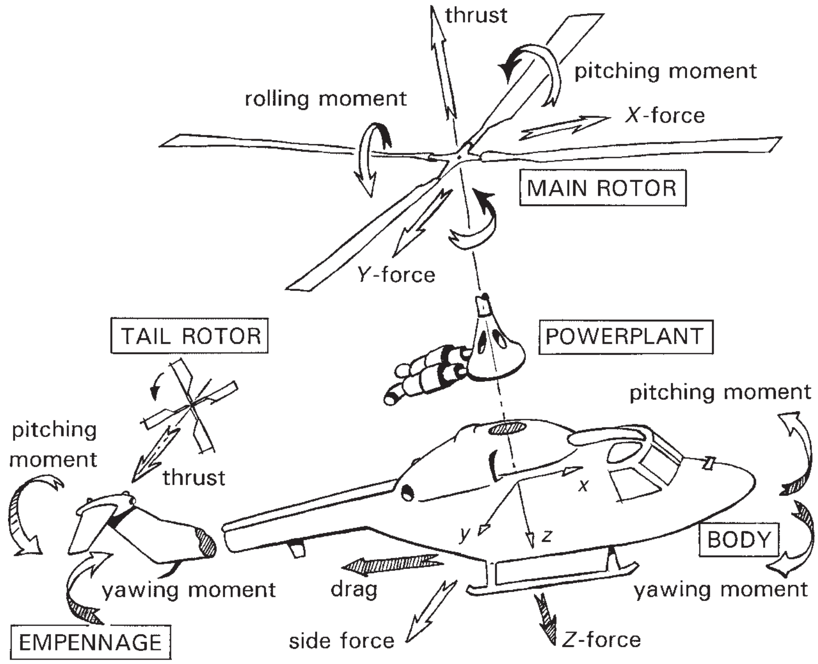

Fig. 2.15 The modelling components of a helicopter

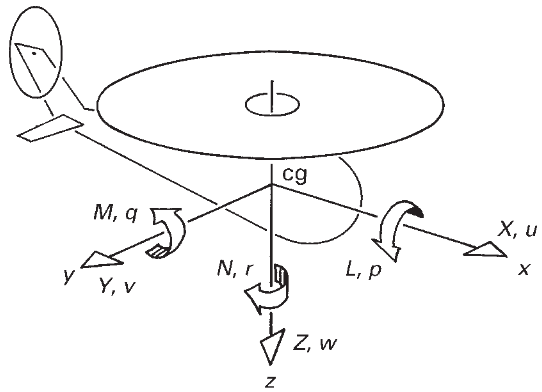

Fig. 2.16 The orthogonal axes system for helicopter flight dynamics

orthogonal body axes system, fixed at the centre of gravity/mass (cg/cm) of the whole aircraft, about which the aircraft dynamics are referred. Strictly speaking, the cg will move as the rotor blades flap, but we shall assume that the cg is located at the mean position, relative to a particular trim state. The equations governing the behaviour of these interactions are developed from the application of physical laws, e.g. conservation of energy and Newton's laws of motion, to the individual components, and commonly take the form of nonlinear differential equations written in the first-order vector form

$$\frac{d\mathbf{x}}{dt} = \mathbf{f}(\mathbf{x}, \mathbf{u}, t) \tag{2.1}$$

with initial conditions $\mathbf{x}(0) = \mathbf{x}_0$.

$\mathbf{x}$ (t) is the column vector of state variables; $\mathbf{u}$ (t) is the vector of control variables and $\mathbf{f}$ is a nonlinear function of the aircraft motion, control inputs and external disturbances. The reader is directed to Appendix 4A for a brief exposition on the matrix–vector theory used in this and later chapters. For the special case where only the six rigid-body degrees of freedom (DoFs) are considered, the state vector $\mathbf{x}$ comprises the three translational velocity components u, v, and w; the three rotational velocity components p, q, and r; and the Euler angles ϕ, θ, and ψ. The three Euler attitude angles augment the equations of motion through the kinematic relationship between the fuselage rates p, q, and r and the rates of change of the Euler angles. The velocities are referred to an axes system fixed at the cg as shown in Figure 2.16 and the Euler angles define the orientation of the fuselage with respect to an earth-fixed axes system.

The DoFs are usually arranged in the state vector as longitudinal and lateral motion subsets, as

$$\mathbf{x} = \{u, w, q, \theta, v, p, \phi, r, \psi\}$$

The function $\mathbf{f}$ then contains the applied forces and moments, again referred to the aircraft cg, from aerodynamic, structural, gravitational, and inertial sources. Strictly speaking, the inertial and gravitational forces are not 'applied', but it is convenient to label them so and place them on the right-hand side of the describing equation. The derivation of these equations from Newton's laws of motion will be carried out later in Chapter 3 and its appendix. It is important to note that this 6-DoF model, while itself complex and widely used, is still an approximation to the aircraft behaviour; all higher DoFs, associated with the rotors (including aeroelastic effects), powerplant/transmission, control system and the disturbed airflow, are embodied in a quasi-steady manner in the equations, having lost their own individual dynamics and independence as DoFs in the model reduction. This process of approximation is a common feature of flight dynamics, in the search for simplicity to enhance physical understanding and ease the computational burden, and will feature extensively throughout Chapters 4 and 5.

2.3.3 Trim, Stability, and Response

Continuing the discussion of the 6-DoF model, the solutions to the three fundamental problems of flight dynamics can be written as

$$\textit{Trim}: \quad \mathbf{f}(\mathbf{x}_e, \mathbf{u}_e) = \mathbf{0} \tag{2.2}$$

$$\textit{Stability}: \quad \det\left[\lambda \mathbf{I} - \left(\frac{\partial \mathbf{f}}{\partial \mathbf{x}}\right)_{\mathbf{x}_e}\right] = 0 \tag{2.3}$$

$$\textit{Response}: \quad \mathbf{x}(t) = \mathbf{x}(0) + \int_0^t \mathbf{f}(\mathbf{x}(\tau), \mathbf{u}(\tau), \tau)\mathrm{d}\tau \tag{2.4}$$

The *trim* solution is represented by the zero of a nonlinear algebraic function, where the controls $\mathbf{u}_e$ required to hold a defined state $\mathbf{x}_e$ (subscript e refers to equilibrium) are computed. With four controls, only four states can be prescribed in trim, the remaining set forming into the additional unknowns in Eq. (2.1). A trimmed flight condition is defined as one in which the rate of change (of magnitude) of the aircraft's state vector is zero and the resultant of the applied forces and moments is zero. In a trimmed manoeuvre, the aircraft will be accelerating under the action of nonzero resultant aerodynamic and gravitational forces and moments, but these will then be balanced by effects such as centrifugal (CF) and gyroscopic inertial forces and moments. The trim equations and associated problems, e.g. predicting performance and control margins, will be further developed in Chapter 4.

The solution of the *stability* problem is found by linearizing the equations about a trim condition and computing the eigenvalues of the aircraft system matrix, written in Eq. (2.3) as the partial derivative of the forcing vector with respect to the system states. After linearization of Eq. (2.1), the resulting first-order, constant coefficient differential equations have solutions of the form $e^{\lambda t}$, the stability of which is determined by the signs of the real parts of the eigenvalues λ. The stability thus found refers to small motions about the

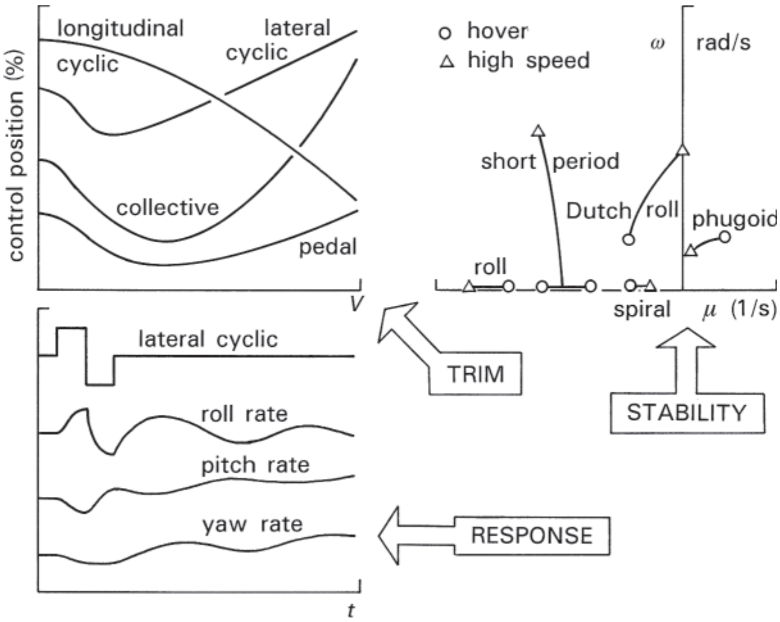

Fig. 2.17 Typical presentation of flight mechanics results for trim, stability, and response

trim point: will the aircraft return to – or depart from – the trim point if disturbed by, say, a gust? For larger motions, nonlinearities can alter the behaviour and recourse to the full equations is usually necessary.

The *response* solution given by Eq. (2.4) is found from the time integral of the forcing function and allows the evolution of the aircraft states, forces, and moments to be computed following disturbed initial conditions $\mathbf{x}(0)$, and/or prescribed control inputs and atmospheric disturbances. The nonlinear equations are usually solved numerically; analytical solutions generally do not exist. Sometimes, narrow-range approximate solutions can be found to describe special large-amplitude nonlinear motion, e.g. limit cycles, but these are exceptional and are usually developed to support the diagnosis of behaviour unaccounted for in the original design.

The sketches in Figure 2.17 illustrate typical ways in which trim, stability, and response results are presented; the key variable in the trim and stability sketches is the helicopter's forward speed. The trim control positions are shown with their characteristic shapes; the stability characteristics are shown as loci of eigenvalues plotted on the complex plane; the short-term responses to step inputs, or the step responses, are shown as a function of time. This form of presentation will be revisited later on this Tour and in later chapters.

The reader of this Tour may feel too quickly plunged into abstraction with the above equations and their descriptions; the intention is to give some exposure to mathematical concepts that are part of the toolkit of the flight dynamicist. Fluency in the parlance of this mathematics is essential for the serious practitioner. Perhaps even more essential is a thorough understanding of the fundamentals of rotor flapping behaviour, which is the next stop on this Tour; here we shall need to rely extensively on theoretical analysis. A full derivation of the results will be given later in Chapters 3–5.

2.3.4 The Flapping Rotor in a Vacuum

The equations of motion of a flapping articulated rotor will be developed in a series of steps (Figure 2.18a–e), designed to highlight several key features of rotor behaviour. Figure 2.18a shows a rotating blade (Ω, rad/s) free to flap (β, rad) about a hinge at the centre of rotation; to add some generality we shall add a flapping spring at the hinge (K_β, Nm/rad). The flapping angle β is referred to the rotor shaft; other reference systems, e.g. relative to the control axis, are discussed in Appendix 3A. It will be shown later in Chapter 3 that

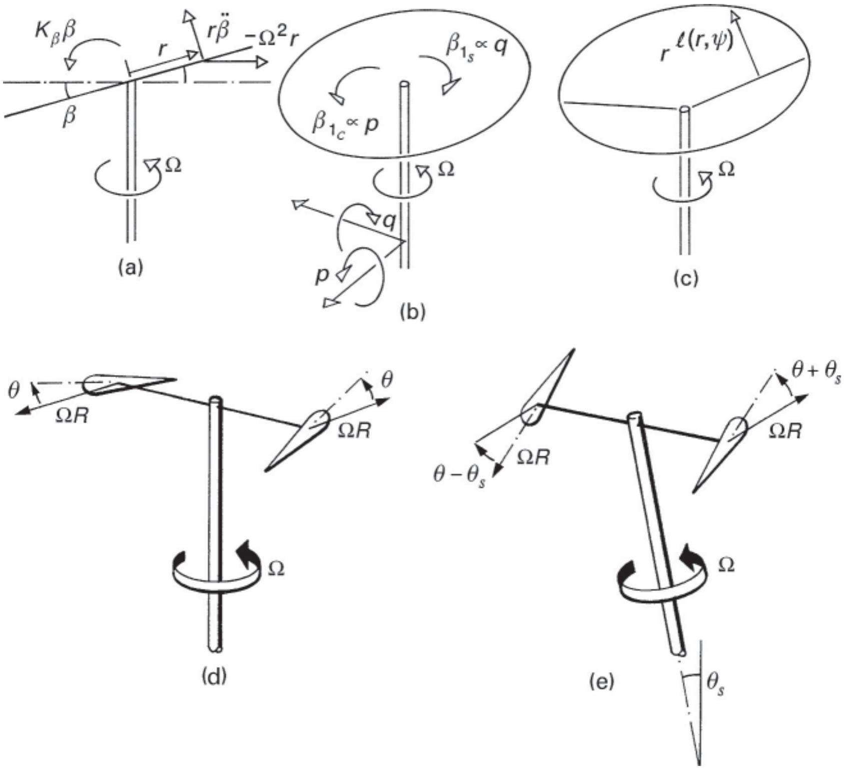

Fig. 2.18 Sketches of rotor flapping and pitch: (a) rotor flapping in vacuum; (b) gyroscopic moments in vacuum; (c) rotor coning in air; (d) before shaft tilt; (e) after shaft tilt showing effective cyclic path

this simple centre-spring representation is quite adequate for describing the flapping behaviour of teetering, articulated, and hingeless or bearingless rotors, under a wide range of conditions. Initially, we consider the case of flapping in a vacuum, i.e. no aerodynamics, and we neglect the effects of gravity. The first qualitative point to grasp concerns what happens to the rotor when the rotor shaft is suddenly tilted to a new angle. For the case of zero spring stiffness, the rotor disc will remain aligned in its original position, there being no mechanism to generate a turning moment on the blade. With a spring added, the blade will develop a persistent oscillation about the new shaft orientation, with the inertial moment due to out-of-plane flapping and the centrifugal moment continually in balance.

The dynamic equation of flapping can be derived by taking moments about the flap hinge during accelerated motion, so that the hinge moment $K_\beta\beta$ is balanced by the inertial moments, thus

$$K_\beta\beta = -\int_0^R rm(r)\{r\ddot{\beta} + r\Omega^2\beta\}\ \mathrm{d}r \tag{2.5}$$

where *m(r)* is the blade mass distribution (kg/m) and ($\dot{}$) indicates differentiation with respect to time t. Setting ($'$) as differentiation with respect to $\psi = \Omega t$, the blade azimuth angle, Eq. (2.5) can be rearranged and written as

$$\beta'' + \lambda_\beta^2\beta = 0 \tag{2.6}$$

where the flapping frequency ratio λ_β is given by the expression

$$\lambda_\beta^2 = 1 + \frac{K_\beta}{I_\beta\Omega^2} \tag{2.7}$$

and where the flap moment of inertia is

$$I_\beta = \int_0^R m(r)r^2 \, \mathrm{d}r \tag{2.8}$$

The two inertial terms in Eq. (2.5) represent the contributions from accelerated flapping out of the plane of rotation, $r\ddot{\beta}$, and the in-plane centrifugal acceleration arising from the blade displacement acting towards the centre of the axis of rotation, $r\Omega^2\beta$. Here, as will be the case throughout this book, we assume that β is small, so that $\sin\beta \sim \beta$ and $\cos\beta \sim 1$.

For the special case where $K_\beta = 0$, the solution to Eq. (2.6) is simple harmonic motion with a natural frequency of one-per-rev, i.e. $\lambda_\beta^2 = 1$. If the blade is disturbed in flap, the motion will take the form of a persistent, undamped, oscillation with frequency Ω; the disc cut by the blade in space will take up a new tilt angle equal to the angle of the initial disturbance. Again, with K_β set to zero, there will be no tendency for the shaft to tilt in response to the flapping, since no moments can be transmitted through the flapping hinge. For the case with nonzero K_β, the frequency ratio is greater than unity and the natural frequency of disturbed motion is faster than one-per-rev, disturbed flapping taking the form of a disc precessing against the rotor rotation, if the shaft is fixed. With the shaft free to rotate, the hub moment generated by the spring will cause the shaft to rotate into the direction normal to the disc. Typically, the stiffness of a hingeless rotor blade can be represented by a spring giving an equivalent λ_β^2 of between 1.1 and 1.3. The higher values are typical of the first generation of hingeless rotor helicopters, e.g. Lynx and Bo105, the lower more typical of modern bearingless designs. The overall stiffness is therefore dominated by the centrifugal force field.

Before including the effects of blade aerodynamics, we consider the case where the shaft is rotated in pitch and roll, p and q (see Figure 2.18b). The blade now experiences additional gyroscopic accelerations caused by mutually perpendicular angular velocities, p, q, and Ω. If we neglect the small effects of shaft angular accelerations, the equation of motion can be written as

$$\beta'' + \lambda_\beta^2\beta = \frac{2}{\Omega}(p\cos\psi - q\sin\psi) \tag{2.9}$$

The conventional zero reference for blade azimuth is at the rear of the disc and ψ is positive in the direction of rotor rotation; in Eq. (2.9) the rotor is rotating anticlockwise when viewed from above. For clockwise rotors, the roll rate term would be negative. The steady-state solution to the 'forced' motion takes the form

$$\beta = \beta_{1c}\cos\psi + \beta_{1s}\sin\psi \tag{2.10}$$

where

$$\beta_{1c} = \frac{2}{\Omega(\lambda_\beta^2 - 1)}p, \quad \beta_{1s} = \frac{-2}{\Omega(\lambda_\beta^2 - 1)}q \tag{2.11}$$

These solutions represent the classic gyroscopic motions experienced when any rotating mass is rotated out of plane; the resulting motion is orthogonal to the applied rotation. β_{1c} is a longitudinal disc tilt in response to a roll rate; β_{1s} a lateral tilt in response to a pitch rate. The moment transmitted by the single blade to the shaft, in the rotating axes system, is simply $K_\beta\ \beta$; in the nonrotating shaft axes, the moment can be written as pitch (positive nose up) and roll (positive to starboard) components:

$$M = -K_\beta\beta(\cos\psi) = -\frac{K_\beta}{2}(\beta_{1c}(1 + \cos 2\psi) + \beta_{1s}\sin 2\psi) \tag{2.12}$$

$$L = -K_\beta\beta(\sin\psi) = -\frac{K_\beta}{2}(\beta_{1s}(1 - \cos 2\psi) + \beta_{1c}\sin 2\psi) \tag{2.13}$$

Each component, therefore, has a steady value plus an equally large wobble at two-per-rev. For a rotor with N_b evenly spaced blades, it can be shown that the oscillatory moments cancel, leaving the steady values

$$M = -N_b\frac{K_\beta}{2}\beta_{1c} \tag{2.14}$$

$$L = -N_b \frac{K_\beta}{2} \beta_{1s} \tag{2.15}$$

This is a general result that will carry through to the situation when the rotor is working in air, i.e. the zeroth harmonic hub moments that displace the flight path of the aircraft are proportional to the tilt of the rotor disc. It is appropriate to highlight that we have neglected the moment of the in-plane rotor loads in forming these hub moment expressions. They are therefore strictly approximations to a more complex effect, which we shall discuss in more detail in Chapter 3. We shall see, however, that the aerodynamic loads are not only one-per-rev but also two-per-rev and higher, giving rise to vibratory moments.

Before considering the effects of aerodynamics, there are two points that need to be made about the solution given by Eq. (2.11). First, what happens when $\lambda_\beta^2 = 1$? This is the classic case of resonance, when according to theory, the response becomes infinite; clearly, the assumption of small flap angles would break down well before this and the nonlinearity in the centrifugal stiffening with amplitude would limit the motion. The second point is that the solution given by Eq. (2.11) is only part of the complete solution. Unless the initial conditions of the blade motion were very carefully set up, the response would actually be the sum of two undamped motions, one with the one-per-rev forcing frequency and the other with the natural frequency λ_β. A complex response would develop, with the combination of two close frequencies leading to a beating response or, in special cases, nonperiodic chaotic behaviour. Such situations are somewhat academic for the helicopter, as the aerodynamic forces distort the response described above in a dramatic way.

2.3.5 The Flapping Rotor in Air – Aerodynamic Damping

Figure 2.18c shows the blade in air, with the distributed aerodynamic lift $\ell(r, \psi)$ acting normal to the resultant velocity; we are neglecting the drag forces in this case. If the shaft is now tilted to a new reference position, the blades will realign with the shaft, even with zero spring stiffness. Figure 2.18d,e illustrates what happens. When the shaft is tilted, say, in pitch by angle θ_s, the blades experience an effective cyclic pitch change with maximum and minimum at the lateral positions ($\psi = 90°$ and $180°$). The blades will then flap to restore the zero hub moment condition.

For small flap angles, the equation of flap motion can now be written in the approximate form

$$\beta'' + \lambda_\beta^2 \beta = \frac{2}{\Omega}(p \cos\psi - q \sin\psi) + \frac{1}{I_\beta \Omega^2} \int_0^R \ell(r, \psi) r \mathrm{d}r \tag{2.16}$$

A simple expression for the aerodynamic loading can be formulated with reference to Figure 2.19, with the assumptions of two-dimensional, steady aerofoil theory, i.e.

$$\ell(r, \psi) = \frac{1}{2} \rho V^2 c a_0 \alpha \tag{2.17}$$

where V is the resultant velocity of the airflow, ρ the air density, and c the blade chord. The lift is assumed to be proportional to the incidence of the airflow to the chord line, α, up to stalling incidence, with lift curve slope a_0. In Figure 2.19 the incidence is shown to comprise two components, one from the applied blade pitch angle θ and one from the induced inflow ϕ, given by

$$\phi = \tan^{-1} \frac{\overline{U}_P}{\overline{U}_T} \approx \frac{\overline{U}_P}{\overline{U}_T} \tag{2.18}$$

where U_T and U_P are the in-plane and normal velocity components respectively (the bar signifies nondimensionalisation with ΩR). Using the simplification that $U_P \ll U_T$, Eq. 2.16 can be written as

$$\beta'' + \lambda_\beta^2 \beta = \frac{2}{\Omega}(p \cos\psi - q \sin\psi) + \frac{\gamma}{2} \int_0^1 (\overline{U}_T^2 \theta + \overline{U}_T \overline{U}_P) \, \overline{r} \, \mathrm{d}\overline{r} \tag{2.19}$$

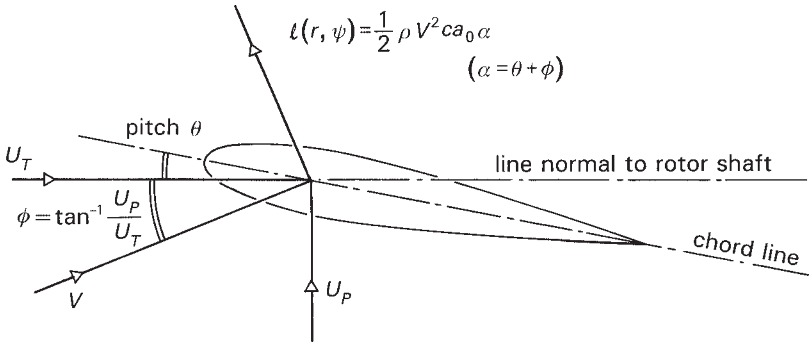

Fig. 2.19 Components of rotor blade incidence

where $\bar{r} = r/R$ and the Lock number, γ, is defined as (Ref. 2.12)

$$\gamma = \frac{\rho c a_0 R^4}{I_\beta} \tag{2.20}$$

The Lock number is an important nondimensional scaling coefficient, giving the ratio of aerodynamic to inertia forces acting on a rotor blade.

To develop the present analysis further, we consider the hovering rotor and a constant inflow velocity v_i over the rotor disc, so that the velocities at station r along the blade are given by

$$\overline{U}_T = \bar{r}, \quad \overline{U}_P = -\lambda_i + \frac{\bar{r}}{\Omega}(p\sin\psi + q\cos\psi) - \bar{r}\beta' \tag{2.21}$$

where

$$\lambda_i = \frac{v_i}{\Omega R}$$

We defer the discussion on rotor downwash until later in this chapter and Chapter 3; for the present purposes, we merely state that a uniform distribution over the disc is a reasonable approximation to support the arguments developed in this chapter.

Eq. (2.19) can then be expanded and rearranged as

$$\beta'' + \frac{\gamma}{8}\beta' + \lambda_\beta^2\beta = \frac{2}{\Omega}(p\cos\psi - q\sin\psi) + \frac{\gamma}{8}\left(\theta - \frac{4}{3}\lambda_i + \frac{p}{\Omega}\sin\psi + \frac{q}{\Omega}\cos\psi\right) \tag{2.22}$$

The flapping Eq. (2.22) can tell us a great deal about the behaviour of a rotor in response to aerodynamic loads; the presence of the flap damping β' alters the response characteristics significantly. We can write the applied blade pitch in the form (cf. Figure 2.5 and the early discussion on rotor controls)

$$\theta = \theta_0 + \theta_{1c}\cos\psi + \theta_{1s}\sin\psi \tag{2.23}$$

where θ_0 is the collective pitch and θ_{1s} and θ_{1c} the longitudinal and lateral cyclic pitch, respectively. The forcing function on the right-hand side of Eq. (2.22) is therefore made up of constant and first harmonic terms. In the general flight case, with the pilot active on his controls, the rotor controls θ_0, θ_{1c}, and θ_{1s} and the fuselage rates p and q will vary continuously with time. As a first approximation, we shall assume that these variations are slow compared with the rotor blade transient flapping. We can quantify this approximation by noting that the aerodynamic damping in Eq. (2.22), $\gamma/8$, varies between about 0.7 and 1.3. In terms of the

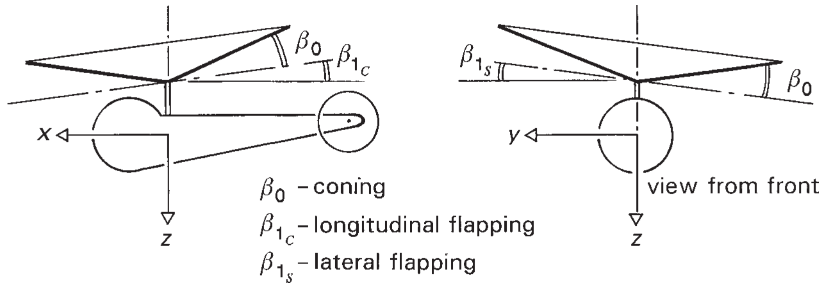

Fig. 2.20 The three rotor disc degrees of freedom

response to a step input, this corresponds to rise times (to 63% of steady-state flapping) between 60° and 112° azimuth ($\psi_{63\%} = 16\ \ln(2)/\gamma$). Rotorspeeds vary from about 27 rad/s on the AS330 Puma to about 44 rad/s on the Messerschmit–Bolkow–Blohm (MBB) Bo105, giving flap time constants between 0.02 and 0.07 s at the extremes. Provided that the time constants associated with the control activity and fuselage angular motion are an order of magnitude greater than this, the assumption of rotor quasi-steadiness during aircraft motions will be valid. We shall return to this assumption a little later on this Tour, but for now, we assume that the rotor flapping has time to achieve a new steady-state, one-per-rev motion following each incremental change in control and fuselage angular velocity. We write the rotor flapping motion in the quasi-steady-state form

$$\beta = \beta_0 + \beta_{1c}\cos\psi + \beta_{1s}\sin\psi \tag{2.24}$$

β_0 is the rotor coning and β_{1c} and β_{1s} the longitudinal and lateral flapping, respectively. The cyclic flapping can be interpreted as a tilt of the rotor disc in the longitudinal (forward) β_{1c} and lateral (port) β_{1s} planes. The coning has an obvious physical interpretation (see Figure 2.20).

The quasi-steady coning and first harmonic flapping solution to Eq. (2.22) can be obtained by substituting Eqs. (2.23) and (2.24) into Eq. (2.22) and equating constant and first harmonic coefficients. Collecting terms, we can write

$$\beta_0 = \frac{\gamma}{8\lambda_\beta^2}\left(\theta_0 - \frac{4}{3}\lambda_i\right) \tag{2.25}$$

$$\beta_{1c} = \frac{1}{1+S_\beta^2}\left\{S_\beta\theta_{1c} - \theta_{1s} + \left(S_\beta\frac{16}{\gamma} - 1\right)\bar{p} + \left(S_\beta + \frac{16}{\gamma}\right)\bar{q}\right\} \tag{2.26}$$

$$\beta_{1s} = \frac{1}{1+S_\beta^2}\left\{S_\beta\theta_{1s} + \theta_{1c} + \left(S_\beta + \frac{16}{\gamma}\right)\bar{p} - \left(S_\beta\frac{16}{\gamma} - 1\right)\bar{q}\right\} \tag{2.27}$$

where the stiffness number

$$S_\beta = \frac{8(\lambda_\beta^2 - 1)}{\gamma} \tag{2.28}$$

and

$$\bar{p} = \frac{p}{\Omega}, \quad \bar{q} = \frac{q}{\Omega}$$

The stiffness number S_β is a useful nondimensional parameter in that it provides a measure of the ratio of hub stiffness to aerodynamic moments.

2.3.6 Flapping Derivatives

The coefficients in Eqs. (2.26) and (2.27) can be interpreted as partial derivatives of flapping with respect to the controls and aircraft motion; hence, we can write

$$\frac{\partial \beta_{1c}}{\partial \theta_{1s}} = -\frac{\partial \beta_{1s}}{\partial \theta_{1c}} = -\frac{1}{1+S_\beta^2} \tag{2.29}$$

$$\frac{\partial \beta_{1c}}{\partial \theta_{1c}} = \frac{\partial \beta_{1s}}{\partial \theta_{1s}} = \frac{S_\beta}{1+S_\beta^2} \tag{2.30}$$

$$\frac{\partial \beta_{1c}}{\partial \overline{q}} = \frac{\partial \beta_{1s}}{\partial \overline{p}} = \frac{1}{1+S_\beta^2}\left(S_\beta + \frac{16}{\gamma}\right) \tag{2.31}$$

$$\frac{\partial \beta_{1c}}{\partial \overline{p}} = -\frac{\partial \beta_{1s}}{\partial \overline{q}} = \frac{1}{1+S_\beta^2}\left(S_\beta \frac{16}{\gamma} - 1\right) \tag{2.32}$$

The partial derivatives in Eqs. (2.29–2.32) represent the changes in flapping with changes in cyclic pitch and shaft rotation and are shown plotted against the stiffness number for different values of γ in Figure 2.21a–c. Although S_β is shown plotted up to unity, a maximum realistic value for current hingeless rotors with heavy blades (small value of γ) is about 0.5, with more typical values between 0.05 and 0.3. The control derivatives illustrated in Figure 2.21a show that the direct flapping response, $\partial\beta_{1c}/\partial\theta_{1s}$, is approximately unity up to typical maximum values of stiffness, i.e. a hingeless rotor blade flaps by about the same amount as a teetering or articulated rotor. However, the variation of the coupled flap response, $\partial\beta_{1c}/\partial\theta_{1c}$, is much more significant, being as much as 30% of the primary response at an S_β of 0.3. When this level of flap cross-coupling is transmitted through the hub to the fuselage, an even larger ratio of pitch/roll response coupling can result due the relative magnitudes of the aircraft inertias.

2.3.7 The Fundamental 90° Phase Shift

A fundamental result of rotor dynamics emerges from the above analysis, that the flapping response is approximately 90° out of phase with the applied cyclic pitch, i.e. θ_{1s} gives $-\beta_{1c}$, and θ_{1c} gives β_{1s}. For blades freely articulated at the centre of rotation, or teetering rotors, the response is lagged by exactly 90° in hover; for hingeless rotors, such as the Lynx and Bo105, the phase angle is about 75°–80°. The phase delay (approximately the ratio of the derivatives in Eq. (2.29) to Eq. (2.30)) is a result of the rotor being aerodynamically forced, through cyclic pitch, close to resonance, i.e. one-per-rev. The second-order character of Eq. (2.22) results in a low-frequency response in-phase with inputs and a high-frequency response with a 180° phase lag. The innovation of cyclic pitch, forcing the rotor close to its natural flapping frequency, is amazingly simple and effective – practically no energy is required and a degree of pitch results in a degree of flapping. A degree of flapping can generate between 0 (for teetering rotors), 500 (for articulated rotors) and greater than 2000 Nm (for hingeless rotors) of hub moment, depending on the rotor stiffness.

The flap-damping derivatives, given by Eqs. (2.31) and (2.32), are illustrated in Figure 2.21b, c. The direct flap damping, $\partial\beta_{1c}/\partial\overline{q}$, is practically independent of stiffness up to $S_\beta = 0.5$; the cross-damping, $\partial\beta_{1c}/\partial\overline{p}$, varies linearly with S_β and changes sign at high values of S_β. In contrast with the *in-vacuo* case, the direct flapping response now opposes the shaft motion. The disc follows the rotating shaft, lagged by an angle given by the ratio of the flap derivatives in the figures. For very heavy blades (e.g. $\gamma = 4$), the direct flap response is about four times the coupled motion; for very light blades, the disc tilt angles are more equal. This rather complex response stems from the two components on the right-hand side of the flapping equation, Eq. (2.22), one aerodynamic due to the distribution of airloads from the angular motion, the other from the gyroscopic flapping motion. The resultant effect of these competing forces on the helicopter motion is also complex and needs to be revisited for further discussion in Chapters 3 and 4. Nevertheless,

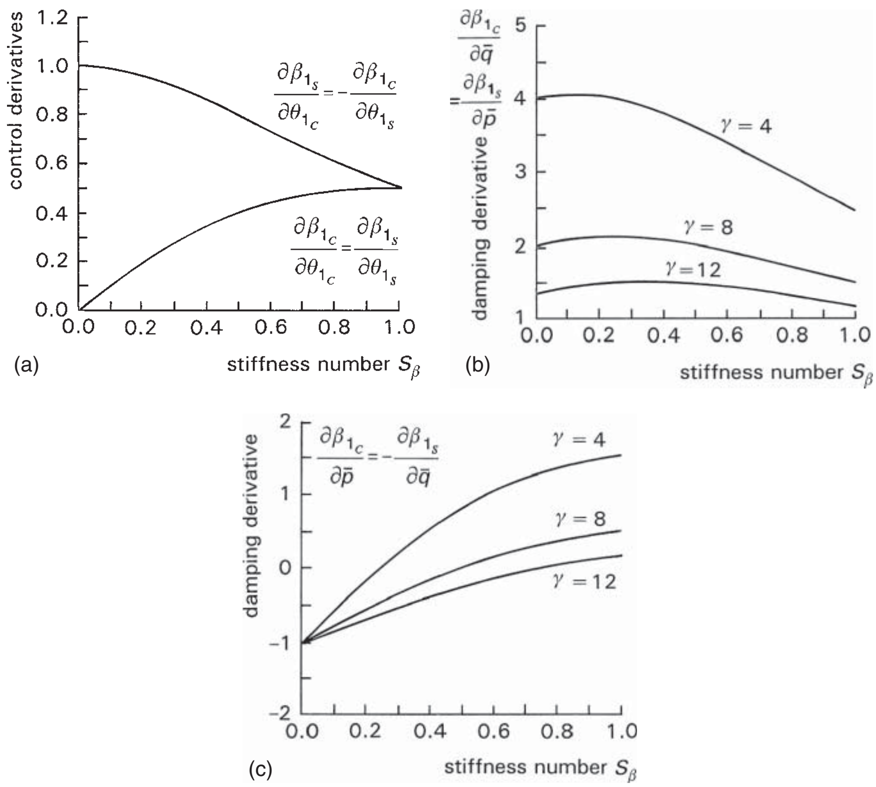

Fig. 2.21 Variation of flap derivatives with stiffness number in hover: (a) control; (b) damping; (c) cross-coupling

it should be clear to the reader that the calculation of the correct Lock number for a rotor is critical to the accurate prediction of both primary and coupled responses. Complicating factors are that most blades have strongly nonuniform mass distributions and aerodynamic loadings and any blade deformation will further affect the ratio of aerodynamic to inertia forces. The concept of the equivalent Lock number is often used in helicopter flight dynamics to encapsulate several of these effects. The degree to which this approach is valid will be discussed later in Chapter 3.

2.3.8 Hub Moments and Rotor/Fuselage Coupling

From the previous discussion, we can see the importance of the two key parameters, λ_β and γ, in determining the flapping behaviour and hence hub moment. The hub moments due to the out-of-plane rotor loads are proportional to the rotor stiffness, as given by Eqs. (2.14) and (2.15); these can be written in the form

$$\text{Pitch moment}: \quad M = -N_b \frac{K_\beta}{2} \beta_{1c} = -\frac{N_b}{2} \Omega^2 I_\beta (\lambda_\beta^2 - 1) \beta_{1c} \tag{2.33}$$

$$\text{Roll moment}: \quad L = -N_b \frac{K_\beta}{2} \beta_{1s} = -\frac{N_b}{2} \Omega^2 I_\beta (\lambda_\beta^2 - 1) \beta_{1s} \tag{2.34}$$

To this point in the analysis we have described rotor motions with fixed or prescribed shaft rotations to bring out the partial effects of control effectiveness and flap damping. We can now extend the analysis to shaft-free motion. To simplify the analysis, we consider only the roll motion and assume that the centre of mass of the rotor and shaft lies at the hub centre. The motion of the shaft is described by the simple equation relating the rate of change of angular momentum to the applied moment:

$$I_{xx}\dot{p} = L \tag{2.35}$$

where I_{xx} is the roll moment of inertia of the helicopter. By combining Eq. (2.27) with Eq. (2.34), the equation describing the one DoF roll motion of the helicopter, with quasi-steady rotor, can be written in the first-order differential form of a rate response type:

$$\dot{p} - L_p p = L_{\theta_{1c}}\theta_{1c} \tag{2.36}$$

where the rolling moment derivatives are given by

$$L_p \approx -\frac{N_b S_\beta I_\beta \Omega}{I_{xx}}, \quad L_{\theta_{1c}} \approx -\frac{N_b S_\beta \gamma I_\beta \Omega^2}{16\ I_{xx}} \tag{2.37}$$

where the approximation that $S_\beta^2 << 1$ has been made. Nondimensionalising by the roll moment of inertia I_{xx} transforms these into angular acceleration derivatives.

These are the most primitive forms of the roll damping and cyclic control derivatives for a helicopter, but they contain most of the first-order effects, as will be observed in Chapters 4 and 5. The solution to Eq. (2.36) is a simple exponential transient superimposed on the steady-state solution. For a simple step input in lateral cyclic, this takes the form

$$p = -(1 - e^{L_p t})\frac{L_{\theta_{1c}}}{L_p}\theta_{1c} \tag{2.38}$$

The time constant (time to reach 63% of steady state) of the motion, τ_p, is given by $-(1/L_p)$, the control sensitivity (initial acceleration) by $L_{\theta_{1c}}$, and the rate sensitivity (steady-state rate response per degree of cyclic) by

$$p_{ss}(\text{deg}/s.\,\text{deg}) = -\frac{L_{\theta_{1c}}}{L_p} = -\frac{\gamma\Omega}{16} \tag{2.39}$$

These are the three handling qualities parameters associated with the time response of Eq. (2.36), and Figure 2.22 illustrates the effects of the primary rotor parameters. The fixed parameters for this test case are $\Omega = 35$ rad/s, $N_b = 4$, $I_\beta/I_{xx} = 0.25$.

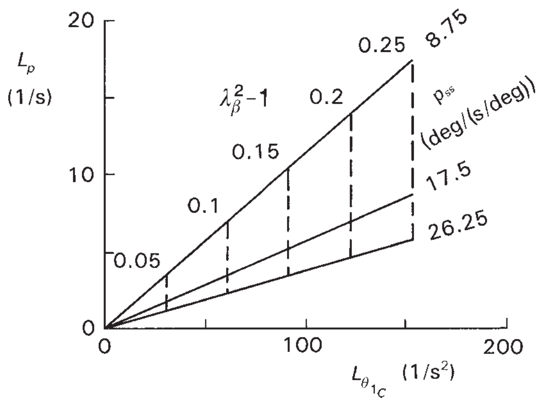

Fig. 2.22 Linear variation of rotor damping with control sensitivity in hover

Four points are worth highlighting:

(1) Contrary to popular understanding, the steady-state roll rate response to a step lateral cyclic is independent of rotor flapping stiffness; teetering and hingeless rotors have effectively the same rate sensitivity.
(2) Rate sensitivity varies linearly with Lock number.
(3) Both control sensitivity and damping increase linearly with rotor stiffness.
(4) The response time constant is inversely proportional to rotor stiffness.

These points are further brought out in the generalised sketches in Figure 2.23a, b, illustrating the first-order time response in roll rate from a step lateral cyclic input. These time response characteristics were used to describe short-term handling qualities until the early 1980s when the revision to Mil Spec 8501A (Ref. 2.2) introduced the frequency domain as a more meaningful format, at least for nonclassical short-term response. One of the reasons for this is that the approximation of quasi-steady flapping motion begins to break down when the separation between the frequency of rotor flap modes and fuselage attitude modes decreases. The full derivation of the equations of flap motion will be covered in Chapter 3, but to complete this analysis of rotor/fuselage coupling in hover, we shall briefly examine the next, improved, level of approximation. Eqs. (2.40) and (2.41) describe the coupled motion when only first-order lateral flapping (the so-called flap regressive mode) and fuselage roll are considered. The other rotor modes – the coning and advancing flap modes – and coupling into pitch, are neglected at this stage.

$$\dot{\beta}_{1s} + \frac{\beta_{1s}}{\tau_{\beta_{1s}}} = p + \frac{\theta_{1c}}{\tau_{\beta_{1s}}} \tag{2.40}$$

$$\dot{p} - L_{\beta_{1s}}\beta_{1s} = 0 \tag{2.41}$$

where

$$L_{\beta_{1s}} = L_{\theta_{1c}} = -\frac{N_b}{2}\Omega^2\frac{I_\beta}{I_{xx}}(\lambda_\beta^2 - 1) = -\frac{1}{\tau_{\beta_{1s}}\tau_p} \tag{2.42}$$

and

$$\tau_{\beta_{1s}} = \frac{16}{\gamma\Omega}, \quad \tau_p = -\frac{1}{L_p} \tag{2.43}$$

The time constants $\tau_{\beta_{1s}}$ and τ_p are associated with the disc and fuselage (shaft) response, respectively. The modes of motion are now coupled roll/flap with eigenvalues given by the characteristic equation

$$\lambda^2 + \frac{1}{\tau_{\beta_{1s}}}\lambda + \frac{1}{\tau_{\beta_{1s}}\tau_p} = 0 \tag{2.44}$$

The roots of Eq. (2.44) can be approximated by the uncoupled values only for small values of stiffness and relatively high values of Lock number. Figure 2.24 shows the variation of the exact and uncoupled approximate roots with $(\lambda_B^2 - 1)$ for the case when $\gamma = 8$. The approximation of quasi-steady rotor behaviour

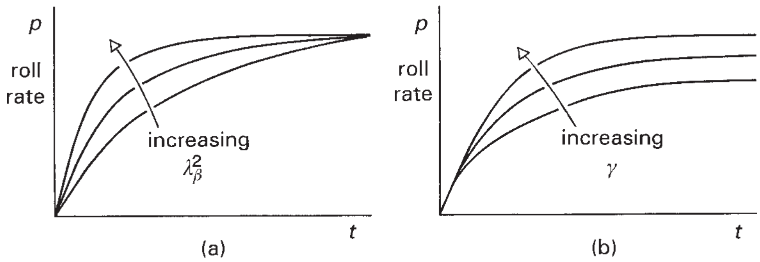

Fig. 2.23 Effects of rotor parameters on roll rate response: (a) rotor stiffness; (b) Lock number

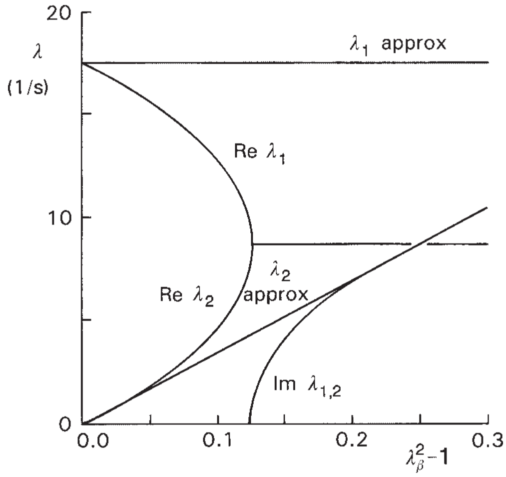

Fig. 2.24 Variation of roll/flap exact and approximate mode eigenvalues with rotor stiffness

will be valid for small offset articulated rotors and soft bearingless designs, but for hingeless rotors with λ_β^2 much above 1.1, the fuselage response is fast enough to be influenced by the rotor transient response, and the resultant motion is a coupled roll/flap oscillation. Note again that the rotor disc time constant is independent of stiffness and is a function only of rotorspeed and Lock number (Eq. (2.43)).

2.3.9 Linearization in General

The assumptions made to establish the above approximate results have not been discussed; we have neglected detailed blade aerodynamic and deformation effects and we have assumed the rotorspeed to be constant; these are important effects that will need to be considered later in Chapter 3, but would have detracted from the main points we have tried to establish in the foregoing analysis. One of these is the concept of the motion derivative, or partial change in the rotor forces and moments with rotor motion. If the rotor were an entirely linear system, then the total force and moment could be formulated as the sum of individual effects each written as a derivative times a motion.

This approach, which will normally be valid for small enough motion, has been established in both fixed- and rotary-wing flight dynamics since the early days of flying (Ref. 2.13) and enables the stability characteristics of an aircraft to be determined. The assumption is made that the aerodynamic forces and moments can be expressed as a multidimensional analytic function of the motion of the aircraft about the trim condition; hence the rolling moment, for example, can be written as

$$L = L_{trim} + \frac{\partial L}{\partial u}u + \frac{\partial^2 L}{\partial u^2}u^2 + \cdots + \frac{\partial L}{\partial v}v + \cdots + \frac{\partial L}{\partial w}w + \cdots + \frac{\partial L}{\partial p}p + \cdots + \frac{\partial L}{\partial q}q$$
$$+ \text{ terms due to higher motion derivatives (e.g., } \dot{p}\text{) and controls} \tag{2.45}$$

For small motions, the linear terms will normally dominate and the approximation can be written in the form

$$L = L_{trim} + L_u u + L_v v + L_w w + L_p p + L_q q + L_r r$$
$$+ \text{ acceleration and control terms} \tag{2.46}$$

In this 6-DoF approximation, each component of the helicopter will contribute to each derivative; hence, for example, there will be an X_u and an N_p for the rotor, fuselage, empennage, and even the tail rotor, although many of these components, while dominating some derivatives, will have a negligible contribution to others.

Dynamic effects beyond the motion in the six rigid-body DoFs will be folded into the latter in quasi-steady form, e.g. rotor, air mass dynamics, and engine/transmission. For example, if the rotor DoFs were represented by the vector $\mathbf{x}_r$ and the fuselage by $\mathbf{x}_f$, then the linearised, coupled equations can be written in the form

$$\begin{bmatrix}\dot{\mathbf{x}}_f \\ \dot{\mathbf{x}}_r\end{bmatrix} - \begin{bmatrix}\mathbf{A}_{ff} & \mathbf{A}_{fr} \\ \mathbf{A}_{rf} & \mathbf{A}_{rr}\end{bmatrix}\begin{bmatrix}\mathbf{x}_f \\ \mathbf{x}_r\end{bmatrix} = \begin{bmatrix}\mathbf{B}_{ff} & \mathbf{B}_{fr} \\ \mathbf{B}_{rf} & \mathbf{B}_{rr}\end{bmatrix}\begin{bmatrix}\mathbf{u}_f \\ \mathbf{u}_r\end{bmatrix} \tag{2.47}$$

We have included, for completeness, fuselage, and rotor controls. Folding the rotor DoFs into the fuselage as quasi-steady motions will be valid if the characteristic frequencies of the two elements are widely separate and the resultant approximation for the fuselage motion can then be written as

$$\dot{\mathbf{x}}_f - [\mathbf{A}_{ff} - \mathbf{A}_{fr}\mathbf{A}_{rr}^{-1}\mathbf{A}_{rf}]\mathbf{x}_f = [\mathbf{B}_{ff} - \mathbf{A}_{fr}\mathbf{A}_{rr}^{-1}\mathbf{B}_{rf}]\mathbf{u}_f + [\mathbf{B}_{fr} - \mathbf{A}_{fr}\mathbf{A}_{rr}^{-1}\mathbf{B}_{rr}]\mathbf{u}_r \tag{2.48}$$

In the above, we have employed the weakly coupled approximation theory of Milne (Ref. 2.14), an approach used extensively in Chapters 4 and 5. The technique will serve us well in reducing and hence isolating the dynamics to single DoFs in some cases, thus maximizing the potential physical insight gained from such analysis. The real strength in linearization comes from the ability to derive stability properties of the dynamic motions.

2.3.10 Stability and Control Résumé

This Tour would be incomplete without a short discussion on stability and control derivatives and a description of typical helicopter stability characteristics. To do this, we need to introduce the helicopter model configurations we will be working with in this book and some basic principles of building the aircraft equations of motion. The three baseline simulation configurations are described in Appendix 4B and represent the Aerospatiale (Eurocopter France (ECF)) SA330 Puma, Westland Lynx, and MBB (Eurocopter Deutschland (ECD)) Bo105 helicopters. The Puma is a transport helicopter in the 6-ton class, the Lynx is a utility transport/anti-armour helicopter in the 4-ton class and the Bo105 is a light-utility/anti-armour helicopter in the 2.5-ton class. Both the Puma and Bo105 operate in civil and military variants throughout the world; the military Lynx operates with both land and sea forces throughout the world. All three helicopters were designed in the 1960s and have been continuously improved in a series of new Marks since that time. The Bo105 and Lynx were the first hingeless rotor helicopters to enter production and service. On these aircraft, both flap and lead–lag blade motion are achieved through elastic bending, with blade pitch varied through rotations at a bearing near the blade root. On the Puma, the blade flap and lead–lag motions largely occur through articulation with the hinges close to the hub centre. The distance of the hinges from the hub centre is a critical parameter in determining the magnitude of the hub moment induced by blade flapping and lagging; the moments are approximately proportional to the hinge offset, up to values of about 10% of the blade radius. Typical values of the flap hinge offset are found between 3% and 5% of the blade radius. Hingeless rotors are often quoted as having an effective hinge offset, to describe their moment-producing capability, compared with articulated rotor helicopters. The Puma has a flap hinge offset of 3.8%, while the Lynx and Bo105 have effective offsets of about 12.5% and 14%, respectively. We can expect the moment capability of the two hingeless rotor aircraft to be about three times that of the Puma. This translates into higher values of λ_β and S_β, and hence, higher rotor moment derivatives with respect to all variables, not only rates and controls as described in the above analysis.

The simulation model of the three aircraft will be described in Chapter 3 and is based on the Royal Aircraft Establishment (RAE) *Helisim* model (Ref. 2.15). The model is generic in form, with two input files, one describing the aircraft configuration data (e.g. geometry, mass properties, aerodynamic and structural characteristics, control system parameters), the other the flight condition parameters (e.g. airspeed, climb/descent rate, sideslip, and turn rate), and atmospheric conditions. The datasets for the three Helisim aircraft are in Chapter 4, Section 4B.1, while Section 4B.2 contains charts of the stability and control derivatives. The derivatives are computed using a numerical perturbation technique applied to the full nonlinear equations of motion and are not generally derived in explicit analytic form. Chapters 3 and 4 will include some analytic formulations to illustrate the physics at work; it should be possible to gain insight into the primary aerodynamic effects for all the important derivatives in this way. The static stability derivative M_w is a good example and allows us to highlight some of the differences between fixed- and rotary-wing aircraft.

2.3.11 The Static Stability Derivative M_w

In simple physical terms, the derivative M_w represents the change in pitching moment about the aircraft's centre of mass when the aircraft is subjected to a perturbation in normal velocity w or, effectively, incidence. If the perturbation leads to a positive, pitch-up, moment, then M_w is positive and the aircraft is said to be statically unstable in pitch; if M_w is negative then the aircraft is statically stable. Static stability refers to the initial tendency only and the M_w effect is analogous to the spring in a simple spring/mass/damper dynamic system. In fixed-wing aircraft flight dynamics, the derivative is proportional to the distance between the aircraft's centre of mass and the overall aerodynamic centre, i.e. the point about which the resultant lift force acts when the incidence is changed. This distance metric, in normalised form, referred to as the static margin, does not carry directly across to helicopters, because as the incidence changes, not only does the aerodynamic lift on the rotor change, but it also rotates (as the rotor disc tilts). So, while we can consider an effective static margin for helicopters, this is not commonly used because the parameter is very configuration dependent and is also a function of perturbation amplitude. There is another reason why the static margin concept has not been adopted in helicopter flight dynamics. Prior to the deliberate design of fixed-wing aircraft with negative static margins to improve performance, fundamental configuration, and layout parameters were defined to achieve a positive static margin. Most helicopters are inherently unstable in pitch, and very little can be achieved with layout and configuration parameters to change this, other than through the stabilizing effect of a large tailplane at high speed (e.g. UH-60). When the rotor is subjected to a positive incidence change in forward flight, the advancing blade experiences a greater lift increment than does the retreating blade (see Figure 2.25). The 90° phase shift in response means that the rotor disc flaps back and cones up and hence applies a positive pitching moment to the aircraft. The rotor contribution to M_w will tend to increase with forward speed; the contributions from the fuselage and horizontal stabiliser will also increase with airspeed but tend to cancel each other, leaving the rotor contribution as the primary contribution. Figure 2.26 illustrates the variation in M_w for the three baseline aircraft in forward flight. The effect of the hingeless rotors on M_w is quite striking, leading to large destabilizing moments at high speed. It is interesting to consider the effect of this static instability on the dynamic, or longer term, stability of the aircraft.

A standard approximation to the short-term dynamic response of a fixed-wing aircraft can be derived by considering the coupled pitch/heave motions, if the airspeed is constant. This is a gross approximation for helicopters but can be used to approximate high-speed flight in certain circumstances (Ref. 2.16). Figure 2.27

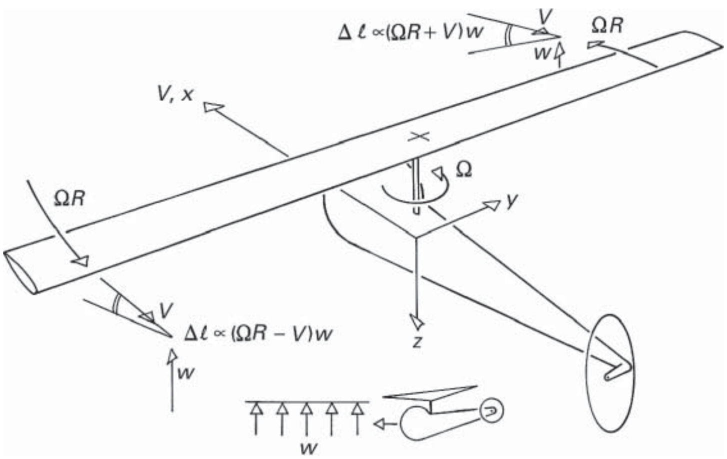

Fig. 2.25 Incidence perturbation on advancing and retreating blades during encounter with vertical gust

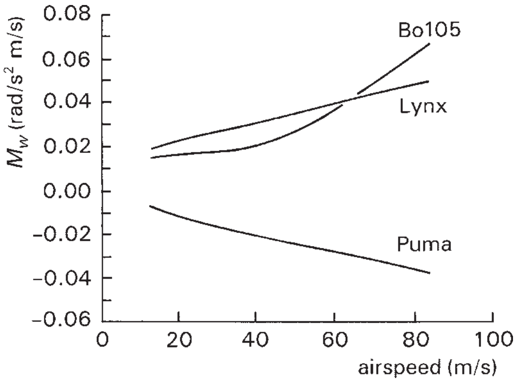

Fig. 2.26 Variation of static stability derivative, M_w, with forward speed for Bo105, Lynx, and Puma

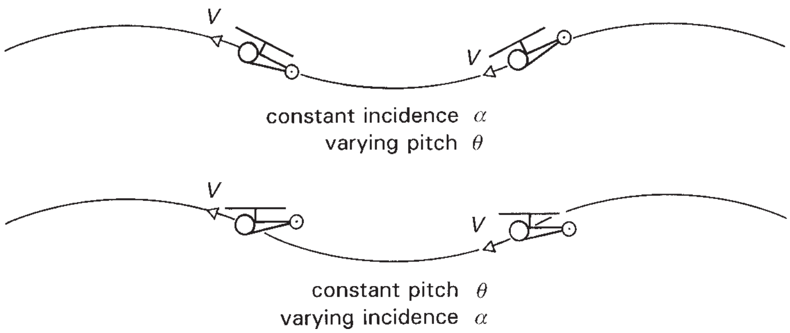

Fig. 2.27 Constant pitch and heave motions

illustrates generalised longitudinal motion, distinguishing between pitch and incidence. For the present, we postulate that the assumption of constant speed applies, and that the perturbations in heave velocity, w, and pitch rate, q, can be described by the linearised equations:

$$I_{yy}\dot{q} = \delta M$$
$$M_a\dot{w} = M_a U_e q + \delta Z \tag{2.49}$$

where I_{yy} is the pitch moment of inertia of the helicopter about the reference axes and M_a is the mass. U_e is the trim or equilibrium forward velocity and δZ and δM are the perturbation Z force and pitching moment. Expanding the perturbed force and moment into derivative form, we can write the perturbation equations of motion in matrix form:

$$\frac{\mathrm{d}}{\mathrm{d}t}\begin{bmatrix} w \\ q \end{bmatrix} - \begin{bmatrix} Z_w & Z_q + U_e \\ M_w & M_q \end{bmatrix}\begin{bmatrix} w \\ q \end{bmatrix} = \begin{bmatrix} Z_{\theta 1s} & Z_{\theta 0} \\ M_{\theta 1s} & M_{\theta 0} \end{bmatrix}\begin{bmatrix} \theta_{1s} \\ \theta_0 \end{bmatrix} \tag{2.50}$$

The derivatives Z_w, M_q, etc., correspond to the linear terms in the expansion of the normal force and pitch moment, as described in Eq. (2.45). It is more convenient to discuss these derivatives in semi-normalised form, and we therefore write these in Eq. (2.50), and throughout the book, without any distinguishing dressings, as

$$M_w \equiv \frac{M_w}{I_{yy}}, \quad Z_w \equiv \frac{Z_w}{M_a}, \quad \text{etc.} \tag{2.51}$$

The solution to Eq. (2.50) is given by a combination of transient and steady-state components, the former having an exponential character, with the exponents, the stability discriminants, as the solutions to the characteristic equation

$$\lambda^2 - (Z_w + M_q)\lambda + Z_w M_q - M_w(Z_q + U_e) = 0 \tag{2.52}$$

According to Eq. (2.52), when the static stability derivative M_w is zero, then the pitch and heave motions are uncoupled, giving two first-order transients (decay rates given by Z_w and M_q). As M_w becomes increasingly positive, the aircraft will not experience dynamic instability until the manoeuvre margin, the stiffness term in Eq. (2.52), becomes zero. Long before this, however, the above approximation breaks down.

One of the chief reasons why this short period approximation has a limited application range with helicopters is the strong coupling with speed variations, reflected in the speed derivatives, particularly M_u. This speed-stability derivative is normally zero for fixed-wing aircraft at subsonic speeds, because the moments from all aerodynamic surfaces are proportional to dynamic pressure and hence perturbations tend to cancel one another. For the helicopter, the derivative M_u is significant even in the hover, again caused by differential effects on advancing and retreating blades leading to flapback; so, while this positive derivative can be described as statically stable, it contributes to the dynamic instability of the pitch phugoid. This effect will be further explored in Chapter 4, along with the second reason why low-order approximations are less widely applicable for helicopters, namely cross-coupling. Practically all helicopter motions are coupled, but some couplings are more significant than others, in terms of their effect on the direct response on the one hand, and the degree of pilot off-axis compensation required, on the other.

Alongside the fundamentals of flapping, the rotor thrust, and torque response to normal velocity changes are key rotor aeromechanics effects that need some attention on this Tour.

2.3.12 Rotor Thrust, Inflow, Z_w, and Vertical Gust Response in Hover

The rotor thrust T in hover can be determined from the integration of the lift forces on the blades

$$T = \sum_{i=1}^{N_b} \int_0^R \ell(\psi, r)\ \mathrm{d}r \tag{2.53}$$

Using Eq. (2.17)–(2.21), the thrust coefficient in hover and vertical flight can be written as

$$C_T = \frac{a_0 s}{2}\left(\frac{\theta_0}{3} + \frac{\mu_z - \lambda_i}{2}\right) \tag{2.54}$$

Again, we have assumed that the induced downwash λ_i is constant over the rotor disc; μ_z is the normal velocity of the rotor, positive down, and approximates to the aircraft velocity component w. Before we can calculate the vertical damping derivative Z_w, we need an expression for the uniform downwash. The induced rotor downwash is one of the most important individual components of helicopter flight dynamics; it can also be the most complex. The downwash, representing the discharged energy from the lifting rotor, takes the form of a spiralling vortex wake with velocities that vary in space and time. We shall give a more comprehensive treatment in Chapter 3, but in this introduction to the topic we make some major simplifications. We assume that the rotor takes the form of an actuator disc (Ref. 2.17) supporting a pressure change and accelerating the air mass, so that the induced velocity can be derived by equating the work done by the integrated pressures with the change in air-mass momentum. In hover, the downwash over the rotor disc can then be written as

$$v_{i_{hover}} = \sqrt{\frac{T}{2\rho A_d}} \tag{2.55}$$

where A_d is the rotor disc area and ρ is the air density.

Or, in normalised form

$$\lambda_i = \frac{v_i}{\Omega R} = \sqrt{\left(\frac{C_T}{2}\right)} \tag{2.56}$$

The rotor thrust coefficient C_T will typically vary between 0.005 and 0.01 for helicopters in 1g flight, depending on the tip speed, density altitude and aircraft weight. Hover downwash λ_i then varies between 0.05 and 0.07. The physical downwash is proportional to the square root of the rotor disc loading, L_d, and at sea level is given by

$$v_{i_{hover}} = 14.5\sqrt{L_d} \tag{2.57}$$

For low disc loading rotors (L_d = 6 lbf/ft^2, 280 N/m^2), the downwash is about 35 ft/s (10 m/s); for high disc loading rotors (L_d = 12 lb/ft^2, 560 N/m^2), the downwash rises to over 50 ft/s (15 m/s).

The simple momentum considerations that led to Eq. (2.55) can be extended to the energy and hence power required in the hover

$$P_i = Tv_i = \frac{T^{3/2}}{\sqrt{(2\rho A_d)}} \tag{2.58}$$

The subscript i refers to the induced power, which accounts for about 70% of the power required in hover; for a 10 000 lb (4540 kg) helicopter developing a downwash of 40 ft/s (typical of a Lynx), the induced power comes to nearly 730 horsepower (HP) (545 kW).

Equations (2.54) and (2.56) can be used to derive the heave damping derivative

$$Z_w = -\frac{\rho(\Omega R)\pi R^2}{M_a}\frac{\partial C_T}{\partial \mu_z} \tag{2.59}$$

where

$$\frac{\partial C_T}{\partial \mu_z} = \frac{2a_0 s\lambda_i}{16\lambda_i + a_0 s} \tag{2.60}$$

and hence

$$Z_w = -\frac{2a_0 A_b \rho(\Omega R)\lambda_i}{(16\lambda_i + a_0 s)M_a} \tag{2.61}$$

where A_b is the blade area and s the solidity, or ratio of blade area to disc area. For our reference Helisim Lynx configuration, the value of Z_w is about −0.33 s^{-1} in hover, giving a heave motion time constant of about 3 s (rise time to 63% of steady state). This is typical of heave time constants for most helicopters in hover. With such a long time constant, the vertical response would seem more like an acceleration than a velocity type to the pilot. The response to vertical gusts, w_g, can be derived from the first-order approximation to the heave dynamics

$$\frac{\mathrm{d}w}{\mathrm{d}t} - Z_w w = Z_w w_g \tag{2.62}$$

The initial acceleration response to a sharp-edge vertical gust provides a useful measure of the ride qualities of the helicopter, in terms of vertical bumpiness

$$\frac{\mathrm{d}w}{\mathrm{d}t}_{t=0} = Z_w w_g \tag{2.63}$$

A gust of magnitude 30 ft/s (10 m/s) would therefore produce an acceleration bump in Helisim Lynx of about 0.3 g. Additional effects such as the blade flapping, downwash lag, and rotor penetration will modify the response. Vertical gusts of this magnitude are rare in the hovering regime close to the ground, and the low values of Z_w and the typical gust strengths make the vertical gust response in hovering flight benign. There are some important exceptions to this general result, e.g. helicopters operating close to structures or obstacles with large downdrafts (e.g. approaching oil rigs) or encountering the wakes of other aircraft (see Chapter 8) that make the vertical performance and handling qualities, such as power margin and heave sensitivity, particularly critical. We shall return to gust response as a special topic in Chapter 5.

2.3.13 Gust Response in Forward Flight

A similar analysis can be conducted for the rotor in forward flight, leading to the following set of approximate equations for the induced downwash and heave damping; V is the flight speed and V' is the total velocity at the disc

$$v_{i_\mu} = \frac{T}{2\rho A_d V'} \tag{2.64}$$

$$\frac{\partial C_T}{\partial \mu_z} = \frac{2a_0 s\mu}{8\mu + a_0 s} \tag{2.65}$$

$$\mu = \frac{V}{\Omega R} \tag{2.66}$$

$$Z_w = -\frac{\rho a_0 V A_b}{2M_a}\left(\frac{4}{8\mu + a_0 s}\right) \tag{2.67}$$

The coefficient outside the parenthesis in Eq. (2.67) is the expression for the corresponding value of heave damping for a fixed-wing aircraft with wing area A_w.

$$Z_{w_{FW}} = -\frac{\rho a_0 V A_w}{2M_a} \tag{2.68}$$

The key parameter is again blade/wing loading. The factor in parenthesis in Eq. (2.67) indicates that the helicopter heave damping or gust response parameter flattens off at high-speed while the fixed-wing gust sensitivity continues to increase linearly. At lower speeds, the rotary-wing factor in Eq. (2.67) increases to greater than one. Typical values of lift curve slope for a helicopter blade can be as much as 50% higher than a moderate aspect-ratio aeroplane wing. It would seem therefore that all else being equal, the helicopter will be more sensitive to gusts at low-speed. However, typical blade loadings are considerably higher than wing loadings for the same aircraft weight; values of 100 lb/ft^2 (4800 N/m^2) are typical for helicopters, while fixed-wing executive transports have wing loadings around 40 lb/ft^2 (1900 N/m^2). Military jets have higher wing loadings, up to 70 lb/ft^2 (3350 N/m^2) for an aircraft like the Harrier, but this is still quite a bit lower than typical blade loadings. Figure 2.28 shows a comparison of heave damping for our Helisim Puma helicopter ($a_0 = 6$, blade area = 144 ft^2 (13.4 m^2)) with a similar class of fixed-wing transport ($a_0 = 4$, wing area = 350 ft^2 (32.6 m^2)), both weighing in at 13 500 lb (6130 kg). Only the curve for the rotary-wing aircraft has been extended to zero speed, the Puma point corresponding to the value of Z_w given by Eq. (2.61). The helicopter is seen to be more sensitive to gusts below about 50 m/s (150 ft/s); above this speed,

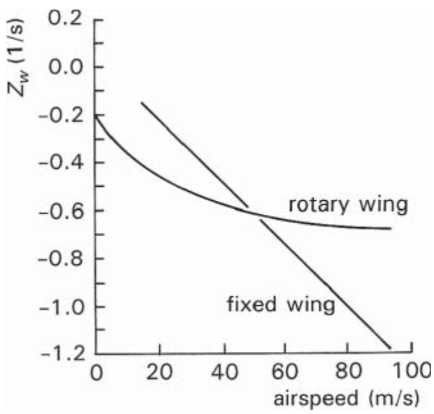

Fig. 2.28 Variation of heave damping, Z_w, with airspeed for rotary- and fixed-wing aircraft

the helicopter value remains constant, while the aeroplane response continues to increase. Three points are worth developing about this result for the helicopter:

(1) The alleviation due to blade flapping is often cited as a major cause of the lower gust sensitivity of helicopters. In fact, this effect is fairly small as far as the vertical gust response is concerned. The rotor coning response, which determines the way that the vertical load is transmitted to the fuselage, reaches its steady state very quickly, typically in about 100 ms. While this delay will take the edge off a truly sharp gust, the gust front is usually of ramp form, extending over several of the blade response time constants.

(2) The Z_w derivative reflects the initial response only; a full assessment of ride qualities will need to consider the short-term transient response of the helicopter and, of course, the shape of the gust. We shall see later in Chapter 5 that there is a key relationship between gust shape and aircraft short-term response that leads to the concept of the worst-case gust, when there is tuning or resonance between the aircraft response and the gust scale/amplitude.

(3) The third point concerns the insensitivity of the response with speed for the helicopter at higher speeds. It is not obvious why this should be the case, but the result is clearly connected with the rotation of the rotor. To explore this point further, it will help to revisit the thrust equation; thus, exploiting the modelling approach to the full:

$$T = \sum_{i=1}^{N_b} \int_0^R \ell(\psi, r)\ \mathrm{d}r$$

or

$$\frac{2C_T}{a_0 s} = \int_0^1 (\overline{U}_T^2 \theta + \overline{U}_P \overline{U}_T)\ \mathrm{d}\bar{r} \tag{2.69}$$

where

$$\overline{U}_T \approx \bar{r} + \mu \sin\psi, \quad \overline{U}_P = \mu_z - \lambda_i - \mu\beta\cos\psi - \bar{r}\beta' \tag{2.70}$$

The vertical gust response stems from the product of velocities $\overline{U}_P\overline{U}_T$ in Eq. (2.69). It can be seen from Eq. (2.70) that the forward velocity term in $\overline{U}_T$ varies one-per-rev, therefore contributing nothing to the quasi-steady hub loading. The most significant contribution to the gust response in the fuselage comes through as an N_b-per-rev vibration superimposed on the steady component represented by the derivative Z_w. The ride bumpiness of a helicopter, therefore, has quite a different character from that of a fixed-wing aircraft where the lift component proportional to velocity dominates the response.

2.3.14 Vector-Differential Form of Equations of Motion

Returning now to the general linear problem, we shall find it convenient to use the vector–matrix shorthand form of the equations of motion, written in the form

$$\frac{\mathrm{d}\mathbf{x}}{\mathrm{d}t} - \mathbf{A}\mathbf{x} = \mathbf{B}\mathbf{u} + \mathbf{f}(t) \tag{2.71}$$

where

$$\mathbf{x} = \{u, w, q, \theta, v, p, \phi, r, \psi\}$$

A and **B** are the matrices of stability and control derivatives, and we have included a forcing function $\mathbf{f}(t)$ to represent external disturbances, e.g. gusts. Eq. (2.71) is a linear differential equation with constant coefficients